DIATOMS:
SIZE AND METABOLIC PROCESSES

By

Zoe Vanessa Finkel

SUBMITTED IN PARTIAL FULFILLMENT OF THE
REQUIREMENTS FOR THE DEGREE OF
MASTER OF SCIENCE
AT
DALHOUSIE UNIVERSITY
HALIFAX, NOVA SCOTIA
MARCH 1998

DALHOUSIE UNIVERSITY
DEPARTMENT OF
BIOLOGY

The undersigned hereby certify that they have read and recommend to the Faculty of Graduate Studies for acceptance a thesis entitled "**Diatoms: Size and Metabolic Processes**" by **Zoe Vanessa Finkel** in partial fulfillment of the requirements for the degree of **Master of Science**.

Dated: March 1998

Supervisor: _____
Trevor C. Platt

Readers: _____
W. K. W. Li

_____
Ian A. McLaren

_____
David C. Patriquin

DALHOUSIE UNIVERSITY

Date: **March 1998**

Author: **Zoe Vanessa Finkel**

Title: **Diatoms: Size and Metabolic Processes**

Department: **Biology**

Degree: **M.Sc.** Convocation: **May** Year: **1998**

Signature of Author

To my family.

Contents

List of Tables

List of Figures

List of Symbols

Symbol	Description
$\log a$	The intercept associated with the allometric equation for metabolic rates.
$a(\lambda)$	Absorption coefficient of phytoplankton at wavelength λ [m^{-1}].
$\bar{a}$	Spectrally-averaged, unweighted mean of $a(\lambda)$ [m^{-1}].
a^*_λ	Chlorophyll-*a*-specific absorption coefficient of phytoplankton at λ [m^2 mg^{-1}].
a^{cell}_λ	Cell-specific absorption coefficient of phytoplankton at λ [m^2 mg^{-1}].
$\bar{a}^*$	Spectrally-averaged mean value of $a^*(\lambda)$ [m^2 mg chlorophyll a^{-1}].
$\bar{a}^C$	Spectrally-averaged mean value of $a^*(\lambda)$ [m^2 mg C^{-1}].
b	The slope associated with the allometric equation for metabolic rates.
B	An estimate of cellular biomass.
$\log c$	The intercept associated with the allometric equation for biomass.
C	Intracellular carbon content [μg].
c_i	Intracellular chlorophyll *a* concentration [mg chlorophyll *a* m^{-3}].
d	The slope associated with the allometric equation for biomass.
D	Diameter [μm].
E	Rate of exudation.
E^C	Rate of exudation normalized to phytoplankton biomass [mg C (mg C)$^{-1}$ h^{-1}].
E^{cell}	Rate of exudation normalized to phytoplankton cell number [mg C (cell)$^{-1}$ h^{-1}].
E^{chl}	Rate of exudation normalized to phytoplankton biomass [mg C (mg chl-*a*)$^{-1}$ h^{-1}].
F	Fraction of net as a function of gross photosynthesis [dimensionless].

Symbol	Description
F_0	Minimum rate of fluorescence [relative units].
F_m	Maximum rate of fluorescence [relative units].
k	Specific growth rate determined using log base two [h^{-1}].
k_e	Specific growth rate determined using log base e [h^{-1}].
k_s	Specific growth rate [s^{-1}].
I	Available irradiance [μmol m^{-2} s^{-1}].
I_g	Incident irradiance in the growth chamber [μmol m^{-2} s^{-1}].
l	Length of the cells [μm].
n	Number of data points.
M	Metabolic rate.
N	Intracellular nitrogen content [μg]
O	Optical density of materials on the filter [dimensionless].
P^C	Photosynthetic rate normalized to carbon [h−1].
P_g	Gross photosynthesis.
P_g^C	Gross photosynthesis normalized to carbon [h^{-1}].
P_k	Rate of photosynthesis at growth irradiance.
P_k^C	Rate of photosynthesis at growth irradiance, normalized to phytoplankton biomass [mg C (mg C)$^{-1}$ h^{-1}].
P_m^C	Rate of photosynthesis at saturating irradiance, normalized to phytoplankton biomass [mg C (mg C)$^{-1}$ h^{-1}].
$P_{\max}^{\text{cell}}$	Rate of photosynthesis at saturating irradiance, normalized to phytoplankton cell number [mg C (cell)$^{-1}$ h^{-1}].
$P_{\max}^{\text{chl}}$	Rate of photosynthesis at saturating irradiance, normalized to phytoplankton biomass [mg C (mg chl-a)$^{-1}$ h^{-1}].
P_n	Net photosynthesis.
PER	Percent extracellular release of dissolved organic carbon [percentage]
R	Rate of respiration.
${}^{14C}R$	Rate of respiration derived from the PI curve.
${}^{O(h)}R$	Rate of respiration derived from oxygen electrode measurements in an h hour incubation.
R^C	Rate of respiration normalized to phytoplankton biomass [mg C (mg C)$^{-1}$ h^{-1}].
R^{cell}	Rate of respiration normalized to phytoplankton cell number [mg C (cell)$^{-1}$ h^{-1}].

Symbol	Description
R^{chl}	Rate of respiration normalized to phytoplankton biomass [mg C (mg chl-a)$^{-1}$ h^{-1}].
R_t	Total respiratory rate, including the maintenance and the biosynthetic respiratory rate [h^{-1}].
r_k	Respiratory rate associated with biosynthetic processes [dimensionless].
r_0	Respiratory rate associated with maintenance processes [h^{-1}].
r	The radius of the cell [μm].
S	The surface area of the cell [μm^2].
t	Time [hours].
V	Cell volume [μm^3].
X	Number of cells per milliliter [cells ml^{-1}].
α^C	Carbon-specific rate of photosynthesis at low irradiance [mg C (mg C)$^{-1}$ h^{-1} (W m^{-2})$^{-1}$].
α^{cell}	Cell-specific rate of photosynthesis at low irradiance [mg C (cell)$^{-1}$ h^{-1} (W m^{-2})$^{-1}$].
α^{chl}	Chlorophyll a-specific rate of photosynthesis at low irradiance [mg C (mg chl-a)$^{-1}$ h^{-1} (W m^{-2})$^{-1}$].
β-factor	Pathlength amplification factor, defined as the ratio of optical to geometrical pathlength [dimensionless].
λ	Wavelength [nm].
θ	The carbon-to-chlorophyll-a ratio [wt:wt].
ϕ_c	Maximum quantum yield of carbon assimilation [mol C (mol photons)$^{-1}$].
ϕ_D	Maximum quantum yield of photochemistry [dimensionless].
ϕ_k	Maximum quantum yield of growth [mol C (mol photons)$^{-1}$].

Acknowledgements

I want to thank my supervisor Trevor Platt, and all the people in the Biological Oceanography Section at BIO for all the support they provided.

Specifically, I want to thank Jay Bugden and Paul Kepkay for all their assistance, especially with the oxygen electrodes and the DOC analysis. I want to thank Brian Irwin for his instruction on the ^{14}C photosynthesis-irradiance experiments, and Venetia Stuart for her help with the spectrophotometric analysis. I want to thank Vivian Lutz for the HPLC analysis and the countless references and useful discussions, Rob Campbell for the CHN analysis, and Heidi Bishop for help with the slides. I also want to thank Bill Li, Erica Head, Shubha Sathyendranath, Glen Harrison, Heidi Maass, Carla Caverhill and Paul Dickie for their recommendations and useful scientific discussions.

There are also a number of people at Dalhousie University and the NRC who have been extremely helpful. Thanks to Jim Craigie, Dave Patriquin, and Hal Whitehead whose support meant a great deal to me.

I want to thank my friends and family. Heather Bouman, Cat Stevens, Heidi Bishop, Jay Bugden, Kevin MacIssac, Alan and Jaqueline Jean-Joyce; thank you for making my time here as enjoyable as it was, and I thank my family, who have given me the strength and support to pursue my goals.

Thank you Andrew, I couldn't have done this without you.

Abstract

The light-limited size-dependence of photosynthesis, light absorption, quantum yield, respiration, exudation, and growth was quantified for eight species of centric marine diatoms: *Chaetoceros calcitrans* (Paulsen), *Thalassiosira pseudonana* ((Hustedt) Hasle et Heimdal), *Chaetoceros* sp., *Thalassiosira weissflogii* ((Grunow) Fryxell et Hasle), *Hyalodiscus* sp., *Planktoniella sol*, *Coscinodiscus* sp. (Ehr. (1839)), and *Coscinodiscus* sp.. The size scaling exponent associated with the photosynthetic rate is significantly smaller than the commonly reported exponent of $-1/4$. In contrast, carbon-specific respiratory loss and the specific growth rate have size scaling exponents close to $-1/4$. Exudation does not have a statistically significant relationship with cell size. In contrast to growth and photosynthetic processes, growth and photosynthetic efficiencies are independent of cell size. The size-dependence of light absorptive properties can provide a mechanism to explain the anomalous size scaling exponents associated with anabolic rates. The robust statistically significant relationships between cell size and photosynthesis, respiration, and growth was confirmed, but the magnitude of the size scaling exponent associated with light-limited anabolic processes indicates that the allometric power law with an exponent of $3/4$ does not apply to photosynthetic organisms under all environmental conditions.

Chapter 1

General Introduction – Size-dependence of phytoplankton metabolism

Algal growth can be related to the anabolic and catabolic processes using a simplified form of the balanced growth equation (Peters, 1983),

$$P_g = k + R + E, \tag{1.1}$$

where P_g refers to gross photosynthesis, k refers to growth or net photosynthesis (P_n), R refers to respiration, and E refers to exudation. The variables in the balanced growth equation are most commonly expressed in carbon or energy units. Measurement of all of the variables in Equation 1.1 would be expensive and time consuming. It would be advantageous to be able to predict the metabolic variables in the balanced growth equation from one easily measured variable.

All of the variables in the balanced growth equation (Eq. 1.1) are metabolic rates. According to Kleiber (1961), scientists have noted a quantitative, predictive relationship between body size and metabolic rates since the late 1800s. Measurements of particle sizes in the field have become easier and more common since the introduction of image analysis systems (Joint, 1991), coulter counters and flow cytometers. The ability to predict the metabolic rates in the balanced growth equation from cell size would be very useful. The size-dependent relationship of a metabolic rate is commonly described by the following equation:

$$M = aV^b, \tag{1.2}$$

where a is the constant and b an exponent of the relationship between the metabolic rate (M) and the size of the organism (V) (Peters, 1983). Since M and V are often plotted on logarithmic scales, a is often referred to as the intercept and b the slope. The intercept a is quite variable, although related organisms often have similar values (Fenchel, 1974; Chisholm, 1992). The exponent b is commonly around 3/4, and when the metabolic rate is normalized to cell mass the exponent becomes $-1/4$ (Kleiber, 1961).

Among the oldest and best accepted explanation for the relationship between metabolic rate and body size is the surface rule. The surface rule suggests that as the surface area to volume (S/V) ratio decreases with increasing cell volume there will be a corresponding decrease in nutrient and gas diffusion per unit volume through the surface of the organism. A geometrical analysis of the surface rule suggests a size scaling exponent of 2/3. Kleiber (1947) was one of the first to note that the majority of allometric studies of metabolic rates support an allometric slope of 3/4, somewhat larger than the slope suggested by the surface rule. Kleiber (1961) and Peters (1983) have summarized a number of proposed explanations for the relation between body size and metabolic rate. Many of the explanations invoke morphological features or physiological processes not available to unicellular photoautotrophs, but size-dependent metabolic rates have been reported in unicellular algae (Banse, 1976; Taguchi, 1976; Blasco et al., 1982; Chisholm, 1992; Tang, 1995; Tang and Peters, 1995).

Photoautotrophs differ from other groups of organisms because they absorb and transform light energy into biomass. The absorption of light by single-celled organisms is size-dependent (Morel and Bricaud, 1981; Agustí, 1991; Kirk, 1994). If the processes underlying the size-dependence of metabolic rates in heterotrophs also occur in autotrophs, the size-dependence of phytoplankton photosynthesis and growth may be fundamentally different from that in heterotrophs due to the additional size-dependence of light absorption. Thus the theories and equations describing the allometric relationship of metabolic rate to cell size in heterotrophs may be inadequate

to describe the allometric relationship between anabolic rates and cell size in algae.

The large size range of phytoplankton cells, and the variability associated with measured metabolic rates in the field suggests that size scaling could be useful in phytoplankton physiological ecology. The diameters of diatom cells encompass an approximate size range from a few microns to over a millimeter, making them ideal experimental organisms for allometric studies. Assuming that an allometric equation with a 3/4 or 2/3 exponent applies to the above mentioned size range, 18- to 46-fold variation in the biomass-specific rates of photosynthesis, respiration, exudation, and growth can be ascribed to cell size.

The relationships between phytoplankton anabolic and catabolic processes and growth to biological and environmental variables, are important for understanding trophic structure, the flow of energy in the food web, and the estimation of biogeochemical fluxes in aquatic ecosystems. More specifically, photosynthetic parameters from field measurements are the basis of most primary production models and must often be extrapolated over large spatial and temporal scales. As a result, variability in the photosynthetic parameters in time and space may result in large errors in the estimates of global primary production (Sathyendranath et al., 1995). Given this variability, it is important to measure key parameters of phytoplankton physiology under controlled environmental conditions in the laboratory.

Size-dependent growth relationships reported in the literature have been used to successfully estimate *in situ* rates of primary production from the size and taxonomic affiliation of the species making up the biomass profile (Joint and Pomroy, 1988; Joint, 1991). Since most of the size scaling exponents in the literature represent ideal growth conditions, more experimental work is required to determine the size scaling exponents associated with the sub-optimal growth conditions that the phytoplankton are likely to encounter in nature. The most important sub-optimal growth condition that limits phytoplankton growth in the ocean is the availability of light.

In this thesis, the size-dependence of light limited diatom metabolism is examined in the context of the balanced growth equation. All of the metabolic rates in the

balanced growth equation are quantified for eight diatom clones that cover a size range from 9.5 to 370000 μm^3. In Chapter 2, the size-dependence of the light absorptive properties and photosynthetic parameters are reported and discussed. In Chapter 3, the catabolic processes of respiration and exudation are examined. In Chapter 4, the size-dependence of growth is discussed in relation to the size-dependence of the other variables in the balanced growth equation, and in Chapter 5, the major results are summarized along with recommendations for future research.

Chapter 2

Size-dependence of photosynthetic processes

2.1 Introduction

2.1.1 Parameterization of phytoplankton photosynthesis

Photosynthesis is measured at a range of irradiances to derive a photosynthesis-irradiance (PI) curve. In the absence of photoinhibitory processes, the photosynthetic response to increasing light intensity can be described by a two-parameter hyperbolic tangent or exponential curve (Platt and Jassby, 1976). The two photosynthetic parameters are the initial slope at low irradiance, α, referred to as the photosynthetic efficiency, and the horizontal asymptote, $P_{\max}$, alternatively called the maximum rate of photosynthesis, or the photosynthetic capacity. The photosynthetic parameters, α and $P_{\max}$, are used to calculate primary production and to compare photosynthetic performance in response to different environmental and biological variables.

Variability in α is in part due to the use of available irradiance in estimating this parameter. Photosynthetic efficiency is a measure of the efficiency of conversion of incident light energy into carbon biomass at low irradiance. A more physiologically reasonable estimate of the efficiency of photosynthesis uses photosynthesis at low irradiance as a function of absorbed quanta (ϕ). Cell structure, pigment composition, and cell size will all affect the efficiency with which the cell is able to absorb light (Johnsen, 1994). Photosynthetic efficiency, calculated as the moles of inorganic carbon fixed or oxygen evolved divided by the moles of quanta absorbed is termed the

maximum quantum yield (Platt and Jassby, 1976). In contrast to α, the maximum quantum yield provides a measure of the efficiency of energy transfer from light absorption to organic products. As incident irradiance increases, the effectiveness with which the cells use light energy decreases, and the maximum photosynthetic rate known as the photosynthetic capacity is reached. The maximum photosynthetic rate often co-varies with α, but is considered to be a reflection of the enzymatic reactions of photosynthesis.

2.1.2 Variability in the PI parameters

It has been well documented that photosynthetic efficiency (α) and capacity ($P_{\max}$) vary temporally and spatially (Steemann Nielsen and Hansen, 1959; Jassby and Platt, 1976; Côté and Platt, 1983; Kirk, 1994). A number of environmental factors have been correlated with the major spatial and temporal differences in the photosynthetic parameters (Sathyendranath et al., 1995). Light intensity and quality, temperature, and nutrient concentration have all been correlated with changes in photosynthetic efficiency and capacity (Côté and Platt, 1983; Davison, 1991; Falkowski and LaRoche, 1991; Geider and Osborne, 1992; Kroon et al., 1993). Similar changes have been attributed to species-specific, class-specific, and size-specific biological factors (Taguchi, 1976; Côté and Platt, 1983; Geider and Osborne, 1992; Sathyendranath et al., 1996). In contrast, the maximum quantum yield of photosynthesis has often been assumed to be constant (Geider and Osborne, 1992), although it appears to be species-specific and variable with light quality (Kroon et al., 1993), light history (Gerath and Chisholm, 1989), nutrient concentration (Greene et al., 1994), temperature (Sosik and Mitchell, 1994), and life cycle (Senger and Bishop, 1967). A number of studies suggest cell size may be responsible for some of the variation associated with the photosynthetic parameters (Banse, 1976; Taguchi, 1976; Sathyendranath et al., 1996; Stuart et al., 1997). An understanding of metabolic and physiological processes associated with cell size will provide a basis for resolving patterns of variability in growth and photosynthesis in nature.

2.1.3 Size-dependence of the photosynthetic parameters

Most of the allometric studies of phytoplankton have examined respiration or growth (Peters, 1983). According to Geider et al. (1986), there are few laboratory studies on the size-dependence of diatom photosynthesis and absorption. Taguchi (1976) documented size-dependence in $P_{\max}$ and α, but only recently has photosynthesis been routinely examined as a function of absorbed, not incident, photon flux density. The absorptive properties and the quantum yield of photosynthesis may both have important roles in the size-dependence of photosynthesis (Stuart et al., 1997).

Theoretically, the ratio of light absorbed to light incident through an infinitesimally thin layer will be affected by cell size (Morel and Bricaud, 1981; Geider et al., 1986; Kirk, 1994). The relationship between cell size and specific absorption will affect the size-dependence of the photosynthetic parameters. Variability in the maximum quantum yield of photosynthesis could account for variability in growth rates and photosynthetic parameters, but the size-dependence of quantum yield has not been established in the laboratory (Geider et al., 1986). There are two major objectives in Chapter 2. The first is to examine the variation of PI parameters, the maximum quantum yield of photosynthesis, and the absorption coefficient with cell size. The maximum quantum yield of photosynthesis occurs only under conditions of light-limited photosynthesis, therefore for comparison all metabolic and physiological parameters were measured under one subsaturating light intensity. This evaluation of the size-dependence of photosynthesis under a subsaturating light intensity is ecologically relevant since light is the primary factor limiting production in the oceans. The second objective is to evaluate the utility of size as a scaling factor in studies of diatom photosynthesis and absorption.

2.2 Materials and methods

2.2.1 Phytoplankton cultures and growth conditions

Eight different species of diatoms were chosen to represent a wide spectrum of cell sizes (Table 2.1). All species were centric with numerous discoid chloroplasts, except for the *Chaetoceros* spp. which have one or more sheet-like plastids (Round et al., 1990). All cultures were obtained from the Provasoli-Guillard National Center for the Culture of Marine Phytoplankton (CCMP) with the exception of *Chaetoceros* sp., which was isolated by J. M. Martin from the Huntsman Marine Science Center in St. Andrews, New Brunswick. For more detailed information on the diatom clones see Appendix A.

Cultures were grown at in 2.8 litre glass Fernbach flasks at 20°C in $f/2$ enriched, 0.45 μm filtered Bedford Basin seawater (Guillard and Ryther, 1962). The cultures were exposed to a continuous photon flux density of 25 ± 0.5 μE m^{-2} s^{-1}, and were manually agitated approximately once per day. Semi-continuous culture technique was used to keep the cultures in exponential growth for a minimum of three generations prior to the photosynthetic experiments.

2.2.2 Estimates of phytoplankton biomass

2.2.2.1 Cell density

Levy Improved Neubauer and American Optical Brightline haemacytometers (both 0.2 mm deep) were used to determine the number of cells per unit volume for the five smallest diatoms. A Sedwick-Rafter chamber was used to determine the cell density of the three larger clones. When practically possible, enough cells were counted to keep the coefficient of variation of the mean population estimate below 20%. In general, four slides, or eight fields were measured for the five smallest diatoms. The Sedwick-Rafter chamber was divided into 11 fields of view. Two to four slides were employed, and approximately 20-40 fields of view were examined. More detail on the

Table 2.1: Morphological characteristics of diatom cultures.

Taxon	CCMP ID	Shape	Plastid type	Diameter	cv	Length	cv	Volume	S	S/V	ESR
				μm	%	μm	%	μm^3	μm^2	μm^{-1}	μm
Chaetoceros calcitrans	1315	elliptical	sheet	1.80	27	3.71	16	$9.44 \cdot 10^0$	$2.61 \cdot 10^1$	2.76	1.31
Cyclotella nana	1335	cylindrical	discoid	4.05	13	4.74	15	$6.12 \cdot 10^1$	$8.62 \cdot 10^1$	1.41	2.45
Chaetoceros sp.	na	elliptical	sheet	4.49	11	9.02	16	$1.43 \cdot 10^2$	$1.59 \cdot 10^2$	1.11	3.24
Thalassiosira weissflogii	1336	cylindrical	discoid	12.8	13	16.0	14	$2.06 \cdot 10^3$	$9.00 \cdot 10^2$	0.44	7.89
Hyalodiscus sp.	1679	cylindrical in pairs	discoid	18.7	9	24.6	8	$6.76 \cdot 10^3$	$2.00 \cdot 10^3$	0.30	11.8
Planktoniella sol	1608	discoid	discoid	36.3	3	23.5	13	$2.43 \cdot 10^4$	$4.75 \cdot 10^3$	0.20	18.0
Coscinodiscus 312	312	discoid	discoid	61.4	5	44.9	15	$1.33 \cdot 10^5$	$1.46 \cdot 10^4$	0.11	31.7
Coscinodiscus 1583	1583	discoid	discoid	84	16	42.8	9	$2.37 \cdot 10^5$	$2.24 \cdot 10^4$	0.09	38.4

maintenance and determination of the exponential growth rate appears in Chapter 4.

2.2.2.2 Chlorophyll *a* concentrations

Chlorophyll *a* concentrations were determined fluorometrically, in triplicate, from samples concentrated on filters and then extracted for 24 or more hours in ice-cold 90% acetone (Holm-Hansen et al., 1965). In addition, High Performance Liquid Chromatographic (HPLC) analysis was used to determine the concentration of all pigments in a subset of the samples. Samples were run on a Beckman C18, reversed-phase, 3 mm Ultrasphere column using the solvent gradient system of Head and Horne (1993). Fluorometer estimates of chlorophyll *a* were calibrated to the HPLC determinations of chlorophyll *a*.

2.2.2.3 Carbon, hydrogen and nitrogen determinations

Phytoplankton were filtered onto pre-combusted GF/F filters and placed in the freezer or desiccator until analysis. A Perken-Elmer 2400 CHN Elemental Analyzer was used to measure the carbon, hydrogen, and nitrogen content of the phytoplankton cells.

2.2.2.4 Volume estimates

The diameter (D) and length (l) of the diatoms were measured under the microscope with an ocular ruler that was calibrated with a micrometer. All diatoms were assumed to be cylinders. The cell volume (V), surface area (S), and equivalent spherical radius (ESR) were calculated by the following formulae:

$$V = \pi r^2 l \tag{2.1}$$

$$S = 2\pi r^2 + 2\pi r l \tag{2.2}$$

$$ESR = \left(\frac{3r^2 l}{4}\right)^{\frac{1}{3}} \tag{2.3}$$

where r is the radius in microns (Table 2.1). For each culture, approximately 80-100 measurements were made in each dimension. Length and diameter measurements

were taken once during the determination of the specific growth rate (k), the absorptive properties, the photosynthesis-irradiance experiments and the metabolic loss experiments. The cell volume of the four smallest clones was relatively stable compared with the volume of the four larger clones.

2.2.3 The photosynthetic parameters

2.2.3.1 Photosynthesis-irradiance (PI) experiments

Photosynthetic rate was estimated from the uptake of radioactive carbon in the form of $NaH^{14}CO_3$, following the procedures of Irwin et al. (1986). Some details and modifications are briefly mentioned below. For each experimental organism, from ten to twelve litres of culture were maintained in exponential growth for a minimum of three generations prior to the PI experiment. Each experiment employed 30 light bottles and 3 dark bottles. The light bottles were placed in a light gradient that ranged from 1 to 1300 $\mu\text{Em}^{-2}\text{s}^{-1}$. The bottle contents were filtered after a one-hour incubation at the experimental irradiance. Inorganic radioactive carbon was removed by placing the filters over concentrated HCl for 20-30 minutes prior to placement in scintillation fluid. Disintegrations per minute, measured by a Beckman LS 5000 CE liquid scintillation counter, were converted to photosynthetic rates as described in Geider and Osborne (1992). The dark bottles were subtracted from the light bottles. A three-parameter hyperbolic tangent function was fitted to the PI data:

$$P(I) = P_{\max} \tanh(\alpha I / P_{\max}) - {}^{14C}R \tag{2.4}$$

where I is the irradiance in $\mu\text{Em}^{-2}\text{s}^{-1}$, $P_{\max}$ is the photosynthetic capacity in mg C h^{-1}, α is the photosynthetic efficiency in mg C h^{-1} $\mu\text{Em}^{-2}\text{s}^{-1}$, and ${}^{14C}R$ represents the dark respiratory rate in mg C h^{-1} (Platt and Jassby, 1976). Photosynthetic efficiency is reported in mg C $(Wm^2)^{-1}$ h^{-1} for comparison to literature values. Photosynthetic efficiency was converted from mg C h^{-1} $\mu\text{Em}^{-2}\text{s}^{-1}$ to mg C $(Wm^2)^{-1}$ h^{-1} using a multiplicative factor of 4.16 that converts micromoles of quanta to watts based on the average wavelength of light from the tungsten-halogen lamp. For the calculation of

quantum yield, photosynthetic efficiency was corrected for variations in the spectrum of the tungsten lamp according to Dubinsky et al. (1986) and Kyewalyanga (1997).

2.2.4 Phytoplankton absorption measurements

The ratio of incident irradiance to that of transmitted irradiance, the optical density (O), was obtained from a Shimadzu UV-2101 PC spectrophotometer equipped with an integrating sphere. Phytoplankton culture was filtered under low pressure onto GF/F filters. The same volume of GF/F filtrate was filtered under low pressure onto a second GF/F filter. The two filters were placed in the spectrophotometer in special filter holders, with the filtrate collected on a second filter serving as a blank. The absorption of the phytoplankton culture and detritus was estimated using the methods described in Hoepffner and Sathyendranath (1993) and references therein.

The filter paper will scatter light, increasing the measured absorption of the particles on the filter. A path-length amplification factor was determined experimentally to convert the absorption values distorted by the filter into corresponding values of absorption in suspension (Kiefer and SooHoo, 1982; Mitchell, 1990; Kirk, 1994). A two-parameter quadratic function, termed a β-factor, was fitted to the optical density data as described by Mitchell (1990); Hoepffner and Sathyendranath (1993); Cleveland and Weidemann (1993). The β-factor was used to convert absorption on the filter to absorption in suspension.

A single average value for absorption ($\bar{a}$) was calculated by integrating the absorption over all measured wavelengths and dividing by the number of wavelengths measured

$$\bar{a} = \frac{\int_{400}^{700} a(\lambda)\ d\lambda}{\int_{400}^{700} d\lambda}. \tag{2.5}$$

The spectrally-averaged absorption ($\bar{a}$), normalized to chlorophyll a, concentration is termed the specific absorption coefficient or the chlorophyll-specific absorption cross-section ($\bar{a}^*$). The spectrally-averaged absorption ($\bar{a}$) normalized to C content is referred to as $\bar{a}^C$, the carbon-specific absorption coefficient, or the carbon-specific

absorption cross-section. When normalized to cell number, absorption is termed $\bar{a}^{\text{cell}}$ or the cellular absorption cross-section.

2.2.5 Quantum yield

2.2.5.1 Quantum yield of carbon fixation

Quantum yield of carbon fixation (ϕ_c) is the amount of energy, in terms of the moles of photons required to fix a mole of carbon (C). Quantum yield is calculated by

$$\phi_c = 0.231\alpha/a, \tag{2.6}$$

where 0.231 converts mg C to moles, hours to seconds, and μmol to moles photons (Platt and Jassby, 1976).

2.2.5.2 The maximum quantum yield of photochemistry

The maximum quantum yield of photochemistry (ϕ_D) was estimated from the measurement of *in vivo* dark-adapted fluorescence (F_0) and 3-[3,4-dichlorophenyl]-1,1-dimethyl urea (DCMU) enhanced fluorescence (F_m). The ϕ_D was estimated using the method of Olson et al. (1996). DCMU fluorescence, or maximum fluorescence (F_m), provides an estimate of the incident energy that would enter the photochemical apparatus if DCMU did not effectively close all the phototraps. Fluorescence measured after the cells are acclimated to the dark provides an estimate of the minimum fluorescence (F_0), which occurs when the maximum amount of absorbed light goes toward photosynthetic processes. The quantum yield of photochemistry is then calculated as

$$\phi_D = \frac{F_m - F_0}{F_m}, \tag{2.7}$$

where the difference between F_m and F_0 provides an estimate of energy going into photosynthesis, and F_m is an approximation of the light energy absorbed by the photochemical apparatus.

2.2.6 Regression analysis and the determination of size scaling exponents

According to the allometric power law, metabolic rates can be described by an expression relating cell size to a common exponent. All rates were measured per cell, per unit of chlorophyll *a*, and per unit of carbon. Cell volume and cell carbon were used as estimates for cell size. The size-dependence of the cell-specific metabolic rates and physiological properties were determined by fitting the following equation to the data:

$$\log M = a + b \log V, \tag{2.8}$$

where M, is the metabolic rate or physiological parameter, V is cell volume, a is the intercept and b is the size scaling exponent. Log refers in all cases to log base ten unless otherwise noted. To determine the size-dependence of the mass-specific metabolic rates and physiological properties of the diatoms, equation 2.8 is divided by the representation of biomass of interest, in this thesis that representation is chlorophyll *a* or carbon content. Biomass can be expressed as a power law of cell volume:

$$\log B = c + d \log V, \tag{2.9}$$

where c is the intercept and d is the size scaling exponent of the biomass to cell volume relationship. The size-dependence of B will affect the size-dependence of the biomass normalized metabolic rates. When the metabolic rate is normalized to biomass, the allometric equation becomes:

$$M/B = \frac{a}{c} V^{b-d}. \tag{2.10}$$

In diatoms, biomass is often not linearly proportional to volume (Strathmann, 1967). Assuming the 3/4 allometric rule applies, if d is less than one, $b - d$ will tend to be more positive than the proposed -0.25. Note that an exponent of -0.25 is not expected for parameters that are not metabolic rates.

Metabolic rates and cell size are often reported in carbon units. This representation can be obtained from equation 2.10 if the relationship between B and V is known (Eq. 2.9). When rearranged and solved for V, Equation 2.9 can be substituted into equation 2.10 to obtain the size scaling exponent and intercept of the carbon-specific metabolic rate as a function of cell carbon:

$$M/B = wB^{b/d-1}, \tag{2.11}$$

where w is equal to $a/c^{\frac{b}{d}}$, and is a constant.

Least squares regression analysis was performed to determine the coefficients of the exponential equations (Banse, 1976; Taguchi, 1976; Ikeda and Mitchell, 1982; Agustí, 1991; Tang, 1995; Tang and Peters, 1995). According to Ricker (1973) and LaBarbera (1989) model II regression is preferred, although results will converge as the goodness of fit increases. Regression coefficients will be referred to as statistically significant at the 95% significance level unless otherwise noted. In addition, means are reported with their standard errors unless otherwise noted. Ordinary least squares regression was used for comparison with the majority of studies in the literature and because in most cases r^2 was close to 1.

2.3 Results and discussion

2.3.1 Cell size and cellular composition

A single taxonomic group of phytoplankton, the Bacillariophyceae, was selected in an attempt to eliminate the effect of pigment composition on the metabolic rates. Total intracellular pigment content has a 3000-fold range from 0.187 to 564 pg pigment. The relative pigment composition of the eight clones is similar. Chlorophyll *a* and fucoxanthin together represent 70-89% of the total cellular pigment content. Chlorophyll *c*, β-carotene, and diadinoxanthin account for the majority of the remaining pigment fraction (Table 2.3.1). Diatoms were chosen because they are an important component of almost all major aquatic ecosystems, and as a taxonomic group they cover one of the largest size ranges of all the phytoplankton. The eight clones in this study span a 50,000-fold size range, from about 10 to 500 000 μm^3. All cells were solitary except *Hyalodiscus* sp. which occurred in doublets. In the calculations, each doublet was treated as a single cell. The carbon content (C) of the phytoplankton cells ranges from $2.26 \cdot 10^{-6}$ to $5.40 \cdot 10^{-2}$ μg C, and cellular nitrogen content (N) ranges from $4.89 \cdot 10^{-7}$ to $1.46 \cdot 10^{-3}$ μg N, an almost 24000- and 3000-fold difference between the smallest and largest cells, respectively. All the measured cellular components are highly correlated with cell volume.

There is presently no consensus on the relationship between cellular composition and cell size (Banse, 1976; Jassby and Platt, 1976; Taguchi, 1976; Geider and Osborne, 1992). The linear regression coefficients of the log of the cellular components as a function of log cell volume are listed in Table 2.3. The relationship between log C, N, total pigment, chlorophyll *a*, and carotenoids with log cell volume (V in μm^3) indicate that there is an orderly change in cellular composition with increasing cell size. The slope of the relationship between the total pigment content (total pigment, chlorophyll *a*, chlorophyll *c*, carotenoids, fucoxanthin, β-carotene, and diadinoxanthin) and cell volume is approximately 3/4 (Figure 2.1a). In contrast, intracellular

Table 2.2: Cellular composition of the diatom clones. Tot. Car. is total carotenoid content, diadino. is diadinoxanthin content, and θ is the C to chlorophyll ratio [wt:wt].

Taxa	Total pigments	Total chl-a	Chl-a	Chl-c	Tot.Car.	Fucoxanthin	Diadino.	β-carotene
Chaetoceros calcitrans	$1.87{\cdot}10^{-1}$	$1.12{\cdot}10^{-1}$	$1.11{\cdot}10^{-1}$	$1.32{\cdot}10^{-2}$	$6.19{\cdot}10^{-2}$	$5.29{\cdot}10^{-2}$	$6.26{\cdot}10^{-3}$	$2.78{\cdot}10^{-3}$
Cyclotella pseudonana	$5.84{\cdot}10^{-1}$	$3.37{\cdot}10^{-1}$	$3.27{\cdot}10^{-1}$	$4.90{\cdot}10^{-2}$	$1.98{\cdot}10^{-1}$	$1.73{\cdot}10^{-1}$	$1.92{\cdot}10^{-2}$	$6.66{\cdot}10^{-3}$
Chaetoceros sp.	$8.05{\cdot}10^{-1}$	$4.44{\cdot}10^{-1}$	$4.11{\cdot}10^{-1}$	$8.62{\cdot}10^{-2}$	$2.74{\cdot}10^{-1}$	$2.37{\cdot}10^{-1}$	$2.06{\cdot}10^{-2}$	$9.79{\cdot}10^{-3}$
Thalassiosira weissflogii	$1.22{\cdot}10^{1}$	$7.40{\cdot}10^{0}$	$7.07{\cdot}10^{0}$	$9.45{\cdot}10^{-1}$	$3.85{\cdot}10^{0}$	$3.23{\cdot}10^{0}$	$4.47{\cdot}10^{-1}$	$1.67{\cdot}10^{-1}$
Hyalodiscus sp.	$1.32{\cdot}10^{1}$	$7.27{\cdot}10^{0}$	$5.94{\cdot}10^{0}$	$1.13{\cdot}10^{0}$	$4.78{\cdot}10^{0}$	$4.52{\cdot}10^{0}$	$1.50{\cdot}10^{-1}$	$1.07{\cdot}10^{-1}$
Planktoniella sol	$3.88{\cdot}10^{1}$	$1.68{\cdot}10^{1}$	$1.65{\cdot}10^{1}$	$4.11{\cdot}10^{0}$	$1.69{\cdot}10^{1}$	$1.05{\cdot}10^{1}$	$8.30{\cdot}10^{-1}$	$0.00{\cdot}10^{0}$
Coscinodiscus 312	$2.22{\cdot}10^{2}$	$1.22{\cdot}10^{2}$	$1.19{\cdot}10^{2}$	$1.93{\cdot}10^{1}$	$8.03{\cdot}10^{1}$	$6.84{\cdot}10^{1}$	$6.54{\cdot}10^{0}$	$2.64{\cdot}10^{0}$
Coscinodiscus 1583	$5.63{\cdot}10^{2}$	$2.61{\cdot}10^{2}$	$2.61{\cdot}10^{2}$	$5.49{\cdot}10^{1}$	$2.48{\cdot}10^{2}$	$1.37{\cdot}10^{2}$	$1.08{\cdot}10^{1}$	$0.00{\cdot}10^{0}$

(a) Phytoplankton pigments: cellular chlorophyll content in pg.

Taxa	Total chl-a	Chl-a	Chl-c	Tot.Car.	Fucoxanthin	Diadino.	β-carotene
Chaetoceros calcitrans	0.60	0.59	0.071	0.33	0.28	0.033	0.015
Cyclotella pseudonana	0.58	0.56	0.084	0.34	0.30	0.033	0.011
Chaetoceros sp.	0.55	0.51	0.107	0.34	0.29	0.026	0.012
Thalassiosira weissflogii	0.61	0.58	0.077	0.32	0.26	0.037	0.014
Hyalodiscus sp.	0.55	0.45	0.086	0.36	0.34	0.011	0.008
Planktoniella sol	0.43	0.43	0.106	0.44	0.27	0.021	0.000
Coscinodiscus 312	0.55	0.54	0.087	0.36	0.31	0.029	0.012
Coscinodiscus 1583	0.46	0.46	0.098	0.44	0.24	0.019	0.000

(b) Pigment composition as a fraction of total pigment.

Taxa	C	se	N	se	C/N	θ
Chaetoceros calcitrans	$2.26 \cdot 10^{-6}$	$2.83 \cdot 10^{-7}$	$4.89 \cdot 10^{-7}$	$4.37 \cdot 10^{-8}$	4.62	$2.00 \cdot 10^{1}$
Thalassiosira pseudonana	$8.50 \cdot 10^{-6}$	$8.01 \cdot 10^{-7}$	$1.64 \cdot 10^{-6}$	$1.50 \cdot 10^{-7}$	5.17	$2.94 \cdot 10^{1}$
Chaetoceros sp.	$1.18 \cdot 10^{-5}$	$1.16 \cdot 10^{-6}$	$2.34 \cdot 10^{-6}$	$2.23 \cdot 10^{-7}$	5.07	$3.33 \cdot 10^{1}$
Thalassiosira weissflogii	$2.11 \cdot 10^{-4}$	$2.89 \cdot 10^{-5}$	$3.62 \cdot 10^{-5}$	$1.63 \cdot 10^{-6}$	5.82	$2.94 \cdot 10^{1}$
Hyalodiscus sp.	$2.07 \cdot 10^{-4}$	$8.37 \cdot 10^{-6}$	$3.63 \cdot 10^{-5}$	$2.08 \cdot 10^{-6}$	5.71	$3.45 \cdot 10^{1}$
Planktoniella sol	$2.80 \cdot 10^{-3}$	$1.90 \cdot 10^{-4}$	$7.28 \cdot 10^{-4}$	$5.70 \cdot 10^{-5}$	3.84	$1.67 \cdot 10^{2}$
Coscinodiscus 312	$7.45 \cdot 10^{-3}$	$3.60 \cdot 10^{-4}$	$1.46 \cdot 10^{-3}$	$6.86 \cdot 10^{-5}$	5.11	$6.25 \cdot 10^{1}$
Coscinodiscus 1583	$5.40 \cdot 10^{-2}$	$5.18 \cdot 10^{-3}$	$8.61 \cdot 10^{-3}$	$5.30 \cdot 10^{-4}$	6.28	$2.07 \cdot 10^{2}$

(c) Carbon (C) and nitrogen (N) content per cell in μg.

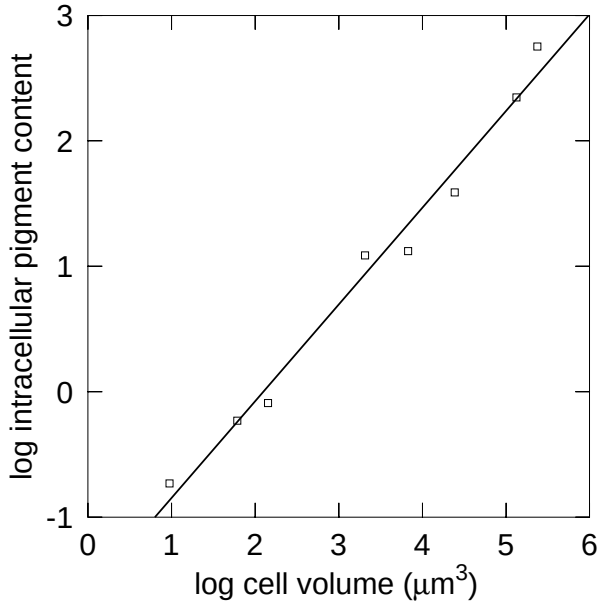

(a) Intracellular pigment content as a function of volume (pg chlorophyll a cell^{-1}).

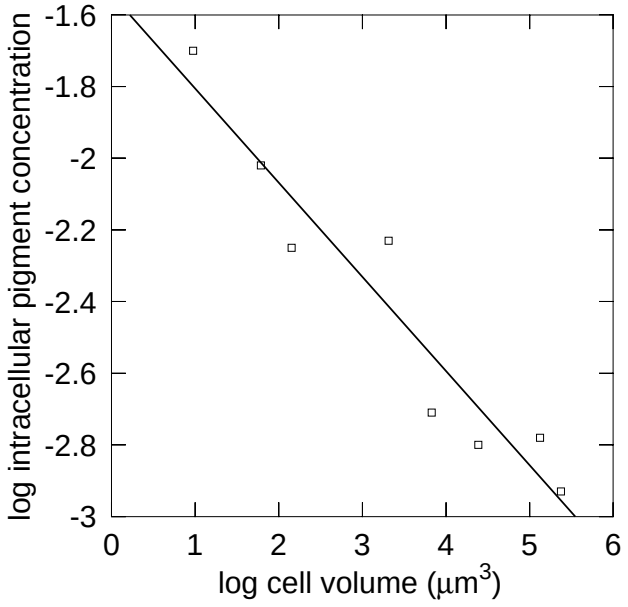

(b) Intracellular pigment concentration as a function of volume (pg chlorophyll a μm^{-3}).

Figure 2.1: Size-dependence of intracellular pigment content.

Table 2.3: Regression coefficients for the log of the cellular components vs. the log of the cell volume. TP is total pigment, Chl is chlorophyll a, Car is carotenoid, and θ is the carbon to chlorophyll a ratio [wt:wt].

Equation	n	Intercept ($\pm$se)	Slope ($\pm$se)	r^2
$\log TP = a + b \log V$	8	-1.62 ± 0.15	0.77 ± 0.04	0.98
$\log Chl = a + b \log V$	8	-1.84 ± 0.18	0.75 ± 0.05	0.97
$\log C = a + b \log V$	8	-6.81 ± 0.27	0.95 ± 0.07	0.97
$\log N = a + b \log V$	8	-7.49 ± 0.28	0.94 ± 0.08	0.96
$\log C/N = a + b \log V$	7	0.67 ± 0.02	0.02 ± 0.01	0.50
$\log \theta = a + b \log V$	7	1.09 ± 0.13	0.16 ± 0.03	0.69

pigment concentration per unit volume decreases with increasing cell volume (Figure 2.1b). The C/N (wt/wt) and the carbon to chlorophyll a (wt/wt) ratios (θ) increase with cell size, with a 1.63- and 8.3-fold range, respectively. Smaller cells have higher concentrations of proteins (inferred from nitrogen content) and pigments, compared with carbon, than the larger cells.

Gas vacuoles may distort any simple relationship between cell volume and cell carbon in diatoms (Strathmann, 1967; Tang, 1995). The slope, 0.94 ± 0.07, of the logarithmic relationship between cell carbon and cell volume was similar to that obtained in Taguchi's (1976) study of 7 species of marine diatoms, suggesting that carbon is almost linearly related to cell volume in low light adapted diatoms. Carbon content increases relative to pigment and nitrogen content with increasing cell size (Figure 2.2). The size-dependence of the C/N ratio is not statistically significant, in agreement with the results of Blasco et al. (1982) and Parsons et al. (1961). The size-dependence of θ is statistically significant, in agreement with the trend found by Banse (1976) and in contrast with the results found by Taguchi (1976), Blasco et al. (1982), and Parsons et al. (1961). *Planktoniella sol* was excluded from the regression analysis of the relationship between C/N and cell volume due to the presence of a mucilaginous wing, which may be responsible for *Planktoniella sol*'s relatively high C/N ratio compared with cells of similar size.

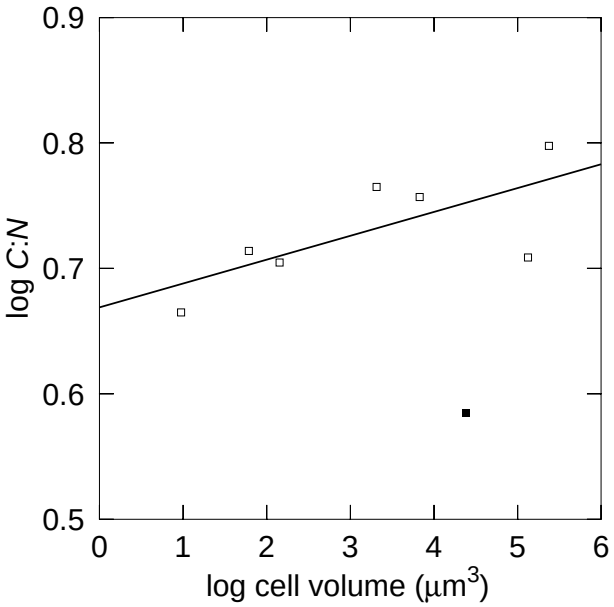

(a) Size-dependence of the C/N ratio.

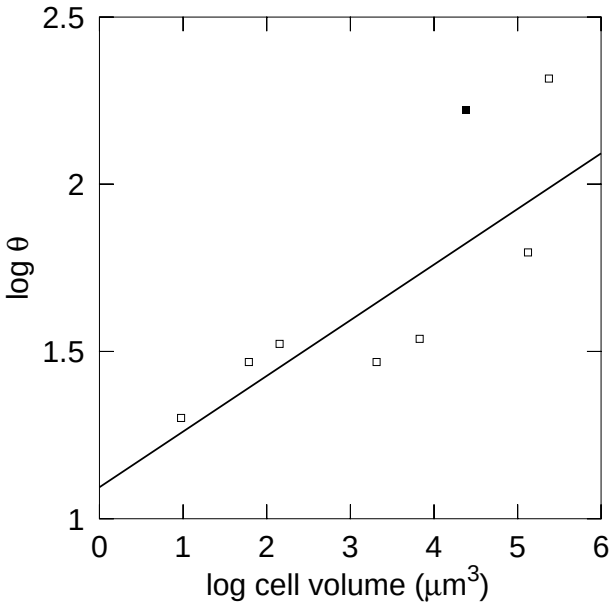

(b) Size-dependence of θ.

Figure 2.2: Relationship of the carbon to nitrogen (C/N) and the carbon-to-chlorophyll *a* ratio (θ) as a function of cell size. *Planktoniella sol* is an outlier, designated as a filled-in square.

In summary, carbon content appears to be almost linearly related to volume in the diatom cells. The relative pigment composition of the eight diatom clones is very similar, such that pigment composition will not be a major factor in the variation in metabolic and absorption parameters. Pigment content decreases relative to carbon content with increasing cell volume. The different relationships of cell carbon and chlorophyll with cell size have a impact on the chlorophyll *a*-, carbon- and cell-specific metabolic rates, which must be considered when examining the size-dependence of diatom metabolic processes.

2.3.2 Phytoplankton photosynthetic parameters

2.3.2.1 Photosynthetic capacity

The cell-specific PI curves are plotted in Figure 2.3. Photosynthesis requires the diffusion of carbon dioxide and nutrients through the cell membrane, suggesting that the size-dependence of photosynthetic rates, and specifically $P_{\max}$, may be a function of the cell surface area to volume relationship (Banse 1976). A 100% increase in the cell volume of a sphere is accompanied by a 59% increase in surface area. If the surface rule is a controlling factor behind size-dependent photosynthesis through the control of gas and nutrient exchange through the cell surface area, an allometric exponent of -0.33 (versus -0.25) will be expected for the biomass-specific $P_{\max}$ to V relationship (Banse 1976).

Table 2.4 lists all the photosynthetic parameters measured in this study. Cell-specific $P_{\max}$ has a 94-fold range (Figure 2.4a). Most of the variability in $P_{\max}^{\text{cell}}$ can be attributed to cell size. The allometric exponent of $P_{\max}^{\text{cell}}$ to V relationship, 0.502 ± 0.036, is in agreement with the slope obtained by Taguchi (1976). For comparison, Table 2.5 lists all regression coefficients from the PI parameters to cell volume relationship measured by Taguchi (1976) for a similar study. Larger cells have higher cellular photosynthetic capacity due to larger numbers of light harvesting components and photosynthetic reaction centers, which will be referred to as photosynthetic machinery. The increase in the quantity of photosynthetic machinery with cell size is

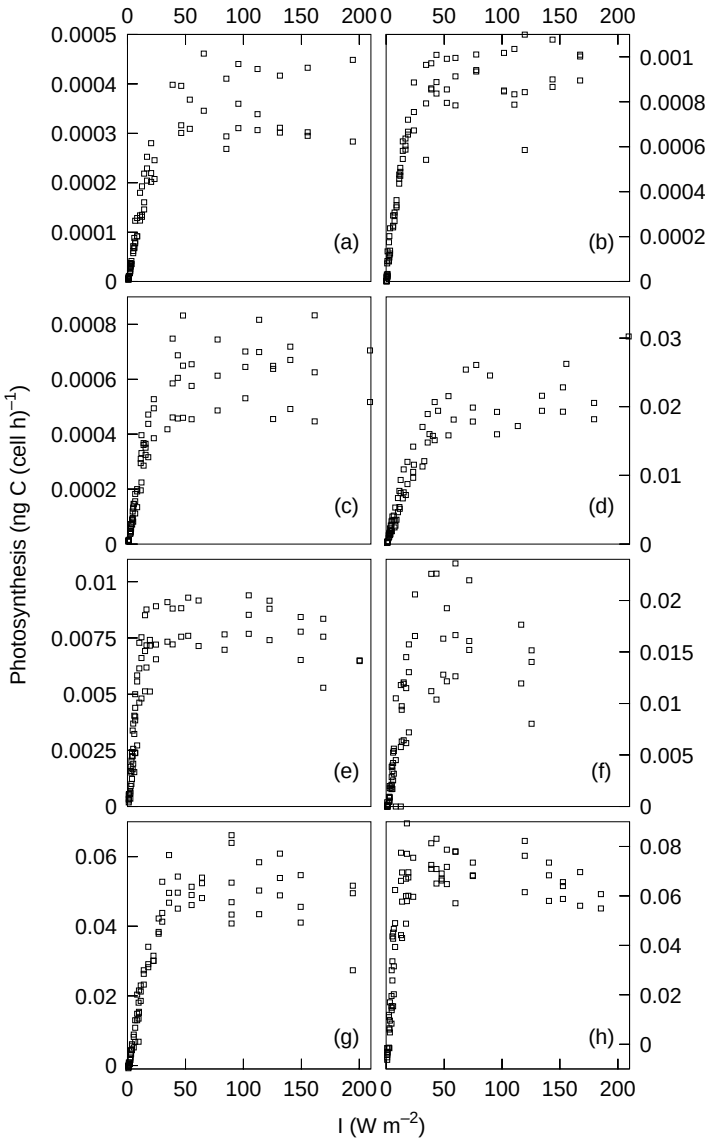

Figure 2.3: Replicate photosynthesis-irradiance data from ^{14}C incubations. Plots are labeled with a small letter: (a) *Chaetoceros calcitrans* (b) *Cyclotella nana*, (c) *Chaetoceros* sp., (d) *Thalassiosira weissflogii*, (e) *Hyalodiscus* sp., (f) *Planktoniella sol*, (g) *Coscinodiscus 312*, and (h) *Coscinodiscus 1583*.

Table 2.4: Photosynthetic parameters.

Taxa	$P_{\max}^{\text{cell}}$ $\frac{\text{mg C}}{\text{cell} \cdot \text{h}}$	se	$P_{\max}^{\text{chl}}$ $\frac{\text{mg C}}{\text{mg chl} - \text{a} \cdot \text{h}}$	se	$P_{\max}^{\text{C}}$ $\frac{\text{mg C}}{\text{mg C} \cdot \text{h}}$	se
Chaetoceros calcitrans	$3.60 \cdot 10^{-10}$	$8.05 \cdot 10^{-10}$	$3.19 \cdot 10^{0}$	$7.14 \cdot 10^{-2}$	$1.60 \cdot 10^{-1}$	$3.58 \cdot 10^{-3}$
Cyclotella nana	$9.12 \cdot 10^{-10}$	$2.41 \cdot 10^{-11}$	$3.15 \cdot 10^{0}$	$8.32 \cdot 10^{-2}$	$1.08 \cdot 10^{-1}$	$2.85 \cdot 10^{-3}$
Chaetoceros sp.	$6.50 \cdot 10^{-10}$	$1.64 \cdot 10^{-11}$	$1.84 \cdot 10^{0}$	$4.64 \cdot 10^{-2}$	$5.52 \cdot 10^{-2}$	$1.39 \cdot 10^{-3}$
Thalassiosira weissflogii	$2.06 \cdot 10^{-8}$	$3.57 \cdot 10^{-10}$	$2.87 \cdot 10^{0}$	$4.97 \cdot 10^{-2}$	$9.82 \cdot 10^{-2}$	$1.70 \cdot 10^{-3}$
Hyalodiscus sp.	$8.90 \cdot 10^{-9}$	$6.03 \cdot 10^{-10}$	$7.49 \cdot 10^{-1}$	$5.08 \cdot 10^{-2}$	$2.15 \cdot 10^{-2}$	$1.45 \cdot 10^{-3}$
Planktoniella sol	$1.53 \cdot 10^{-8}$	$1.87 \cdot 10^{-9}$	$9.00 \cdot 10^{-1}$	$1.10 \cdot 10^{-1}$	$5.48 \cdot 10^{-3}$	$6.71 \cdot 10^{-4}$
Coscinodiscus 312	$5.40 \cdot 10^{-8}$	$2.48 \cdot 10^{-9}$	$4.45 \cdot 10^{-1}$	$2.04 \cdot 10^{-2}$	$7.28 \cdot 10^{-3}$	$3.34 \cdot 10^{-4}$
Coscinodiscus 1583	$8.54 \cdot 10^{-8}$	$4.37 \cdot 10^{-9}$	$1.89 \cdot 10^{-1}$	$9.70 \cdot 10^{-3}$	$1.59 \cdot 10^{-3}$	$8.12 \cdot 10^{-5}$

(a) Photosynthetic capacity

Taxa	α^{cell} $\frac{\text{mg C}}{\text{cell} \cdot \text{h} \cdot \text{W} \cdot \text{m}^{-2}}$	se	α^{chl} $\frac{\text{mg C}}{\text{mg chl} - \text{a} \cdot \text{h} \cdot \text{W} \cdot \text{m}^{-2}}$	se	α^{C} $\frac{\text{mg C}}{\text{mg C} \cdot \text{h} \cdot \text{W} \cdot \text{m}^{-2}}$	se
Chaetoceros calcitrans	$1.50 \cdot 10^{-11}$	$9.31 \cdot 10^{-13}$	$1.33 \cdot 10^{-1}$	$8.26 \cdot 10^{-3}$	$6.64 \cdot 10^{-3}$	$4.14 \cdot 10^{-4}$
Cyclotella nana	$4.48 \cdot 10^{-11}$	$3.20 \cdot 10^{-12}$	$1.55 \cdot 10^{-1}$	$1.11 \cdot 10^{-2}$	$5.26 \cdot 10^{-3}$	$3.76 \cdot 10^{-4}$
Chaetoceros sp.	$2.83 \cdot 10^{-11}$	$1.97 \cdot 10^{-12}$	$8.01 \cdot 10^{-2}$	$5.56 \cdot 10^{-3}$	$2.40 \cdot 10^{-3}$	$1.67 \cdot 10^{-4}$
Thalassiosira weissflogii	$4.90 \cdot 10^{-10}$	$2.04 \cdot 10^{-11}$	$6.83 \cdot 10^{-2}$	$2.84 \cdot 10^{-3}$	$1.89 \cdot 10^{-3}$	$1.34 \cdot 10^{-4}$
Hyalodiscus sp.	$6.41 \cdot 10^{-10}$	$1.15 \cdot 10^{-10}$	$5.40 \cdot 10^{-2}$	$9.65 \cdot 10^{-3}$	$1.26 \cdot 10^{-3}$	$2.26 \cdot 10^{-4}$
Planktoniella sol	$9.25 \cdot 10^{-10}$	$3.27 \cdot 10^{-10}$	$5.46 \cdot 10^{-2}$	$1.93 \cdot 10^{-2}$	$3.27 \cdot 10^{-4}$	$1.17 \cdot 10^{-4}$
Coscinodiscus 312	$2.20 \cdot 10^{-9}$	$2.72 \cdot 10^{-10}$	$1.81 \cdot 10^{-2}$	$2.24 \cdot 10^{-3}$	$2.90 \cdot 10^{-4}$	$3.59 \cdot 10^{-5}$
Coscinodiscus 1583	$9.08 \cdot 10^{-9}$	$1.20 \cdot 10^{-9}$	$2.02 \cdot 10^{-2}$	$2.66 \cdot 10^{-3}$	$1.61 \cdot 10^{-4}$	$2.13 \cdot 10^{-5}$

(b) Photosynthetic efficiency

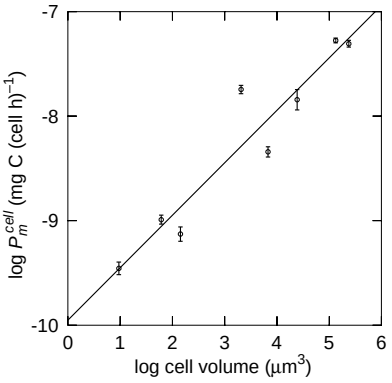

(a) Photosynthetic capacity per cell.

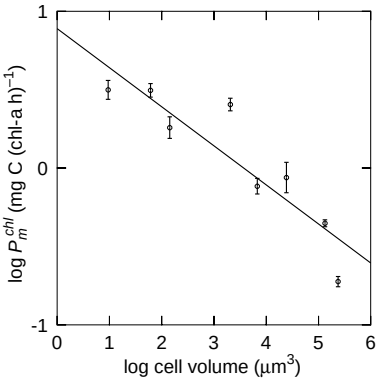

(b) Chlorophyll *a*-specific photosynthetic capacity.

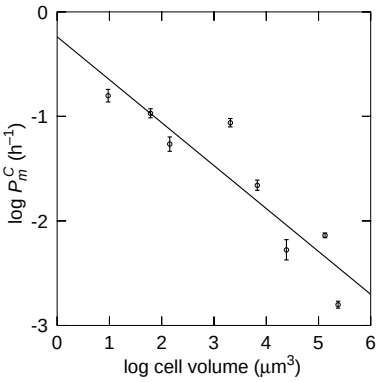

(c) Carbon-specific photosynthetic capacity.

Figure 2.4: The size-dependence of photosynthetic capacity.

Table 2.5: The regression coefficients for Taguchi's (1976) PI parameters.

Equation	n	Intercept	Slope	r^2
log $P^{\mathrm{C}}_{\mathrm{max}}$- log V	16	-0.2807 ± 0.2111	-0.2456 ± 0.0486	0.65
log $P^{\mathrm{chl}}_{\mathrm{max}}$- log V	16	0.8528 ± 0.2756	-0.1867 ± 0.06345	0.38
log α^C- log V	16	-1.701 ± 0.2175	-0.1893 ± 0.05007	0.51
log α^{chl}-log V	16	0.5670 ± 0.1749	-0.1304 ± 0.0403	0.42

reflected in the increase in intracellular pigment content with cell volume.

In contrast, smaller cells tend to have higher metabolic rates compared with larger cells when the photosynthetic parameters are normalized to cell mass (Figure 2.4). Chlorophyll *a*-specific P_{max} shows a 17-fold range, with a low of 0.18 for the largest cell, to a high of 3.19 mg C (mg chl-a)$^{-1}$ h^{-1} for the smallest cell. Much of the variability in $P^{\mathrm{chl}}_{\mathrm{max}}$ can be attributed to cell volume. The slope obtained for the $P^{\mathrm{chl}}_{\mathrm{max}}$ to V relationship, -0.245 ± 0.027, is in agreement with the value obtained by Taguchi (1976). As with the chlorophyll *a* normalized photosynthetic parameters, the carbon-specific parameter, $P^{\mathrm{C}}_{\mathrm{max}}$, tends to decrease with increasing cell volume (Figure 2.4c). The exponent of the $P^{\mathrm{C}}_{\mathrm{max}}$ to V relationship, -0.410 ± 0.039, is smaller than that measured by Taguchi (1976). The exponent of the $P^{\mathrm{C}}_{\mathrm{max}}$ to cell carbon relationship, -0.433, like the $P^{\mathrm{C}}_{\mathrm{max}}$ to V relationship, is somewhat smaller than expected if the 3/4 or surface rule described the size-dependence of the photosynthetic capacity of the diatom clones. The photosynthetic performance at the growth irradiance (P^C_k in mg C (mg C h)$^{-1}$) was calculated from the PI parameters. The size scaling exponent associated with the cell volume P^C_k relationship, -0.41 ± 0.06, is similar to the relationship between $P^{\mathrm{C}}_{\mathrm{max}}$and cell volume (Figure 2.5).

The results indicate a significant size-dependent relationship between P_{max}, P^C_k and cell size. The larger exponent associated with the $P^{\mathrm{C}}_{\mathrm{max}}$ to V compared with the $P^{\mathrm{chl}}_{\mathrm{max}}$ to V relationship is not supported by previous studies, and should be interpreted cautiously. Microscopic examination of the phytoplankton used in this study suggest that many of the larger cells produced large amounts of mucilaginous material. The

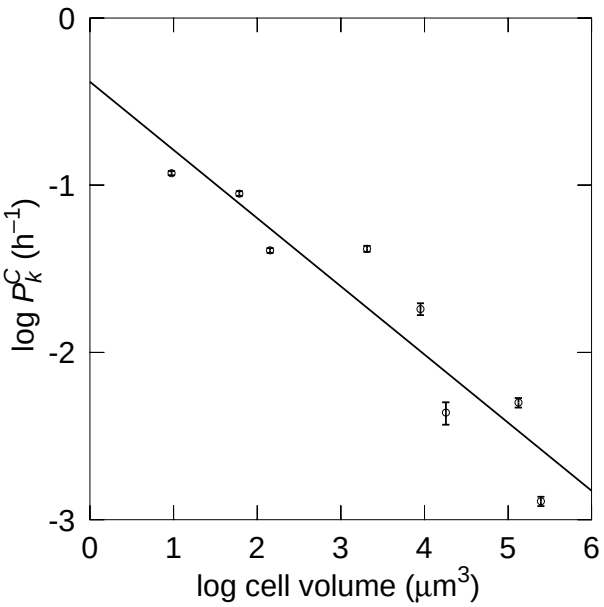

Figure 2.5: Size-dependence of photosynthetic performance (P_k^C).

mucilage may have been trapped on the filter and erroneously included in the carbon estimate. This mucilaginous component may be responsible for *Planktoniella sol*'s relatively high θ, and C/N ratio compared with cells of similar size.

2.3.2.2 Photosynthetic efficiency

Photosynthetic efficiency, like photosynthetic capacity was estimated from carbon fixation. Carbon fixation requires the diffusion of carbon dioxide and nutrients through the cell membrane, therefore α may also be subject to the surface rule. In addition, α is a function of light absorption and quantum yield. The relative size-dependence of these component processes will contribute to the size-dependence of the photosynthetic efficiency.

Photosynthetic efficiency per cell increases with cell volume, exhibiting a 605-fold range in values (Figure 2.6a). Most of the variation in α can be attributed to cell volume. The size scaling exponent of the α^{cell} to V relationship, 0.647 ± 0.031, is in good agreement with the exponent calculated by Taguchi (1976). Chlorophyll *a*- and carbon-specific α have an 8.5 and 664-fold range, respectively (Figure 2.6b&c).

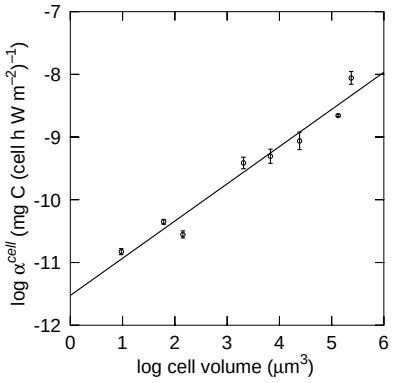

(a) Photosynthetic efficiency per cell.

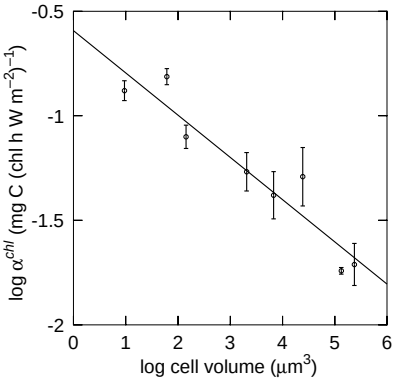

(b) Chlorophyll *a*-specific photosynthetic efficiency.

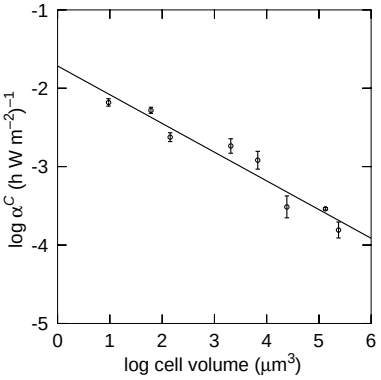

(c) Carbon-specific photosynthetic efficiency.

Figure 2.6: The size-dependence of photosynthetic efficiency.

Most of the variation in biomass normalized α can be attributed to cell volume. The exponent of the α^C to V relationship, -0.366 ± 0.025, is larger than the exponent of the α^{chl} to V relationship, -0.202 ± 0.020, but both slopes are statistically different from zero. In contrast to the slope obtained for α^{cell} as a function of V, the slope of the α^C and α^{chl} to V relationship is smaller than the exponent derived from data collected by Taguchi (1976). The slope of the α^C to C relationship, -0.386, is smaller than predicted by the 3/4 allometric rule but is similar to that predicted by the surface rule. Note that α^C is subject to the same errors mentioned for photosynthetic capacity (see Section 2.3.2.1 on page 21).

The size-dependent exponents of α^C to C and α^{chl} to V are lower than the exponents of the $P^{\text{C}}_{\text{max}}$ to C and $P^{\text{chl}}_{\text{max}}$ to V relationships. Variability in the photosynthetic efficiency is a function of variation in the fraction of incident light absorbed and the quantum yield of photosynthesis. To understand the size-dependence of α, light absorption and the quantum yield of photosynthesis were examined.

2.3.3 Phytoplankton absorption parameters

Interspecific variation in phytoplankton absorption parameters is a key component in the variation in the photosynthetic efficiency. The product of the absorption coefficient and the quantum yield of photosynthesis is α; therefore, by definition, absorption characteristics will have an impact on the photosynthetic efficiency. The size-dependence of phytoplankton absorption may shed light on the size-dependence of the photosynthetic parameters and growth. Cell volume and the absorptive properties of the diatom clones are listed in Table 2.6.

In this study, cellular absorption has a 550-fold range, from $2.45 \cdot 10^{-12}$ for the smallest cell to $1.35 \cdot 10^{-9}$ $\text{m}^2\text{cell}^{-1}$, for the largest cell (Figure 2.7). The regression equation of the logarithmic relationship of cellular absorption and cell volume,

$$\log \bar{a}^{\text{cell}} = 0.620 \pm 0.052 \log V - 12.3 \pm 0.20 \qquad r^2 = 0.96, \tag{2.12}$$

Table 2.6: Diatom absorption parameters.

Taxa	Volume	$\bar{a}^{\text{cell}}$	se	$\bar{a}^{*}$	se	$\bar{a}^{C}$	se	a_{676}^{cell}
	μm^3	m^2 cell^{-1}		$\text{m}^2(\text{mg chl-a})^{-1}$		$\text{m}^2(\text{mg C})^{-1}$		m^2 cell^{-1}
Chaetoceros calcitrans	$9.44 \cdot 10^{0}$	$2.45 \cdot 10^{-12}$	$5.92 \cdot 10^{-14}$	$2.16 \cdot 10^{-2}$	$5.23 \cdot 10^{-4}$	$1.88 \cdot 10^{-3}$	$4.53 \cdot 10^{-5}$	$3.15 \cdot 10^{-12}$
Cyclotella nana	$6.12 \cdot 10^{1}$	$5.43 \cdot 10^{-12}$	$1.91 \cdot 10^{-13}$	$1.87 \cdot 10^{-2}$	$6.56 \cdot 10^{-4}$	$7.04 \cdot 10^{-4}$	$2.47 \cdot 10^{-5}$	$7.19 \cdot 10^{-12}$
Chaetoceros sp.	$1.43 \cdot 10^{2}$	$7.54 \cdot 10^{-12}$	$2.65 \cdot 10^{-13}$	$2.13 \cdot 10^{-2}$	$7.46 \cdot 10^{-4}$	$4.37 \cdot 10^{-4}$	$1.53 \cdot 10^{-5}$	$9.44 \cdot 10^{-12}$
Thalassiosira weissflogii	$2.06 \cdot 10^{3}$	$9.44 \cdot 10^{-11}$	$1.02 \cdot 10^{-11}$	$1.31 \cdot 10^{-2}$	$1.41 \cdot 10^{-3}$	$4.33 \cdot 10^{-4}$	$4.66 \cdot 10^{-5}$	$1.24 \cdot 10^{-10}$
Hyalodiscus sp.	$8.97 \cdot 10^{3}$	$4.75 \cdot 10^{-11}$	$2.43 \cdot 10^{-12}$	$1.10 \cdot 10^{-2}$	$5.63 \cdot 10^{-4}$	$5.39 \cdot 10^{-5}$	$2.75 \cdot 10^{-6}$	$1.07 \cdot 10^{-10}$
Planktoniella sol	$1.80 \cdot 10^{4}$	$2.81 \cdot 10^{-10}$	$3.10 \cdot 10^{-11}$	$2.43 \cdot 10^{-2}$	$2.69 \cdot 10^{-3}$	$1.64 \cdot 10^{-4}$	$1.82 \cdot 10^{-5}$	$4.00 \cdot 10^{-10}$
Coscinodiscus 312	$3.72 \cdot 10^{5}$	$1.28 \cdot 10^{-9}$	$7.70 \cdot 10^{-11}$	$1.05 \cdot 10^{-2}$	$6.32 \cdot 10^{-4}$	$4.23 \cdot 10^{-5}$	$2.54 \cdot 10^{-6}$	$1.81 \cdot 10^{-9}$
Coscinodiscus 1583	$2.47 \cdot 10^{5}$	$1.35 \cdot 10^{-9}$	$8.14 \cdot 10^{-11}$	$1.12 \cdot 10^{-2}$	$6.76 \cdot 10^{-4}$	$6.57 \cdot 10^{-5}$	$3.96 \cdot 10^{-6}$	$1.86 \cdot 10^{-9}$

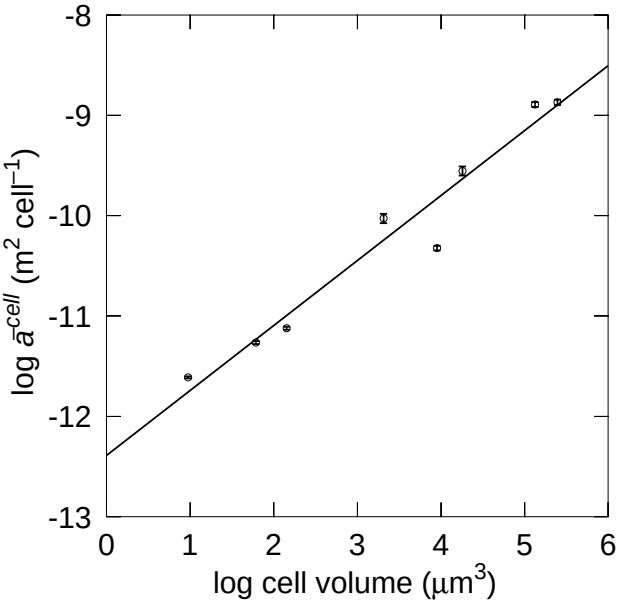

Figure 2.7: Size-dependence of the average cellular absorption cross-section.

suggests that cell size can account for a large fraction of the variation in light absorption by individual cells. For comparison with literature values, the logarithm of cellular absorption at the red peak (676 nm) was regressed against the logarithm of the equivalent spherical diameter (ESD) and the cellular chlorophyll content (Chl in pg chlorophyll a cell^{-1}):

$$\log a_{676}^{\text{cell}} = 1.91 \pm 0.12 \log ESD - 12.41 \pm 0.16 \qquad r^2 = 0.98 \qquad (2.13)$$

$$\log a_{676}^{\text{cell}} = 0.88 \pm 0.04 \log Chl - 4.68 \pm 0.05 \qquad r^2 = 0.99 \qquad (2.14)$$

The allometric slope of 1.91 ± 0.12 for the relationship between a_{676}^{cell} and the ESD is in agreement within two standard errors of the slope obtained by Agustí (1991), 2.32 ± 0.18 for a literature review of values that included a variety of taxonomic groups and growth conditions (Figure 2.8a&b). The slope of the a_{676}^{cell} to Chl relationship is in excellent agreement with the exponent calculated by Agustí (1991). Agustí (1991) suggests the relationship between cell size and intracellular pigment content may be an adaptation that facilitates efficient light absorption, where the relationship between the volume of the cells to their light absorptive properties is due to a coupling between

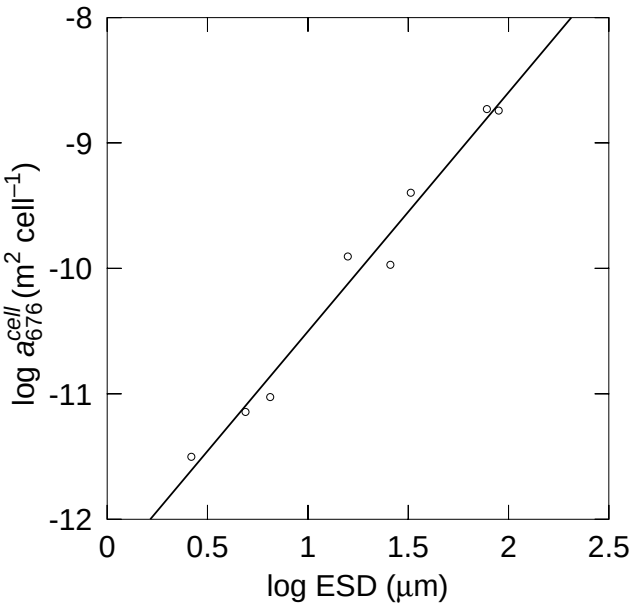

(a) Absorption per cell at 676 nm as a function of the ESD.

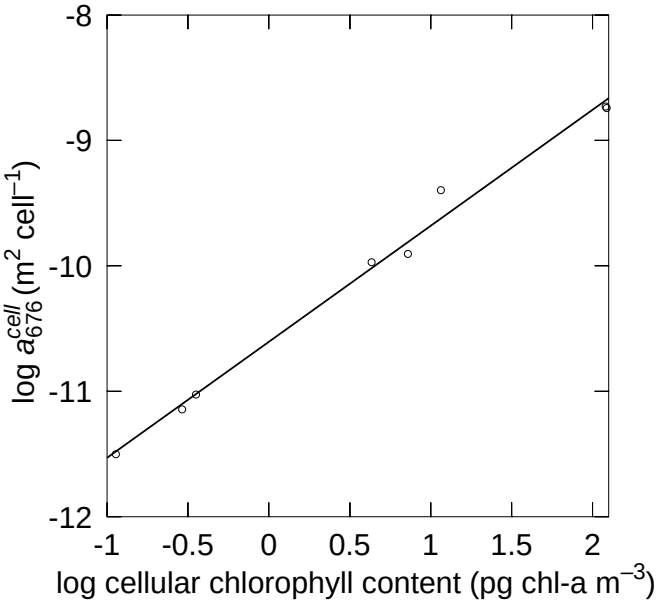

(b) Absorption per cell at 676 nm as a function of cellular chlorophyll a content.

Figure 2.8: Absorption per cell at 676 nm as a function of ESD and cellular chlorophyll a content.

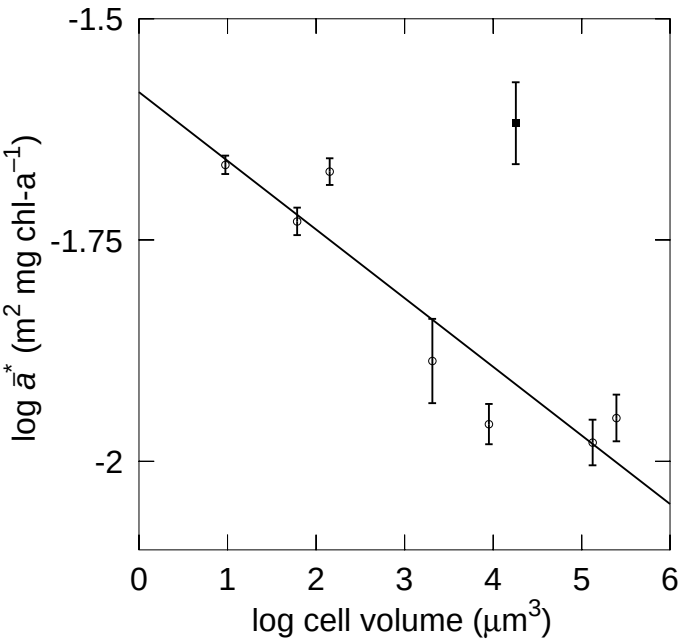

Figure 2.9: Size-dependence of specific absorption. *Planktoniella sol* is an outlier, designated as a filled-in circle.

the cellular chlorophyll *a* content and cell size. The ESD of the diatom clones is highly correlated to the cellular chlorophyll *a* content of the cells, with a slope that is in excellent agreement with that reported by Agustí (1991). The reciprocal relationship between V and ESD with the cellular chlorophyll *a* content results in a reduced variability in the specific absorption coefficient.

The specific absorption coefficient ($\bar{a}^*$) decreases with increasing cell size, from 0.022 to 0.011 m^2 (mg chl-a)$^{-1}$ (Figure 2.9). Chlorophyll *a*-specific absorption is a function of the concentration, arrangement, and type of pigments within the cell (Johnsen, 1994). The clones used in this study have similar ratios of pigments, therefore pigment composition is not a major factor associated with the two-fold variability in specific absorption. High concentrations of pigments in a cell, as well as a large cell volume, result in intracellular shading of the pigments and therefore a reduction in specific absorption.

The decrease in absorption due to the quantity and arrangement of pigment

molecules within the cell is termed the package effect (Duysens, 1956; Kirk, 1976, 1994). The package effect is a non-linear function of the intracellular pigment concentration and cell size where high values of absorption are more strongly damped than lower values of absorption. An increase in the pathlength required for the light to penetrate a larger cell volume results in a reduction of the light absorbed per unit volume. At any one intracellular chlorophyll *a* concentration, small cells are expected to have higher chlorophyll *a*-specific absorption coefficients than larger cells.

There is a statistically significant relationship between the average chlorophyll *a*-specific absorption coefficient and cell volume. The regression of the logarithm of $\bar{a}^*$ against $\log V$:

$$\log \bar{a}^* = -0.078 \log V - 1.583 \qquad r^2 = 0.83, \tag{2.15}$$

manifests a shallow size-dependent slope (Figure 2.9). The size-dependence of absorption caused by increased cell size is reduced by the decreased pigment packaging in the larger cells. Recall that the cellular pigment content per unit of volume decreases with cell volume. This results in a dilution of pigment within a larger volume, reducing self-shading associated with high cellular pigment content. The results of this study support the conclusions of Agustí (1991) that a reduction in pigment packaging moderates the lowering of specific absorption due to the longer pathlength the light must travel through the cells with larger volumes. It appears that the covariance in size and pigment concentration may be related to the maximization of absorptive efficiency over a large size range.

The highest absorption by phytoplankton occurs at the chlorophyll *a* peaks centered on 435 and 676 nm. Chlorophyll *a* absorption at the red peak is lower than at the blue; therefore it is expected that with an increase in the package effect there will be more reduction in absorption at the blue peak than in the red; this is termed the flattening effect. The flattening effect of the specific absorption spectrum is therefore expected with increases in cell volume due to an increase in the package effect (Kirk 1994).

The specific absorption spectra of the diatom clones cluster in two distinct groups

(Figure 2.10). *Chaetoceros calcitrans*, *Cyclotella nana*, and *Chaetoceros* sp., the three smallest clones examined, have high $\bar{a}^*$, and have high ratios of blue to red absorption. The four larger diatoms: *Cosinodiscus* 1583, *Cosinodiscus* 312, *Hyalodiscus* sp., and *Thalassiosira weissflogii* have lower values of $\bar{a}^*$ and have low ratios of blue to red absorption. As expected, the larger cells have relatively low values of $\bar{a}^*$ due to a larger package effect, which is reflected in their low values of blue to red absorption.

Planktoniella sol is an exception to the size-dependent absorption relationship. *Planktoniella sol* has high chlorophyll *a*-specific absorption compared with other diatoms of comparable size. The high $\bar{a}^*$ may be a function of unique morphological features. *P. sol* has a large mucilaginous wing that extends from the area around its girdle band which may contribute to absorption. The mathematical method of Hoepffner and Sathyendranath (1993) was used to estimate the detrital contribution to total absorption. The absorption by detritus represents absorption of light by components other than phytoplankton pigments. For a number of the larger diatom taxa, there was a persistent exponential increase in specific absorption of the phytoplankton in the blue portion of the spectra, characteristic of detrital material. This is not unexpected since this method uses an idealized phytoplankton absorption spectra with little flattening. *Planktoniella sol* had the most obvious and persistent increase in absorption in the blue part of the spectrum and was therefore excluded from the regression analysis of size and specific absorption.

The cell- and chlorophyll *a*-specific absorption coefficients are size-dependent. As expected, the size scaling exponents for the absorption to cell volume relationship did not agree with the 3/4 or 2/3 allometric rule for metabolic rates. The low size scaling exponent for $\bar{a}^*$ cannot explain most of the variability in the chlorophyll *a*-specific photosynthetic efficiency. This suggests that the quantum yield of photosynthesis could be size-dependent.

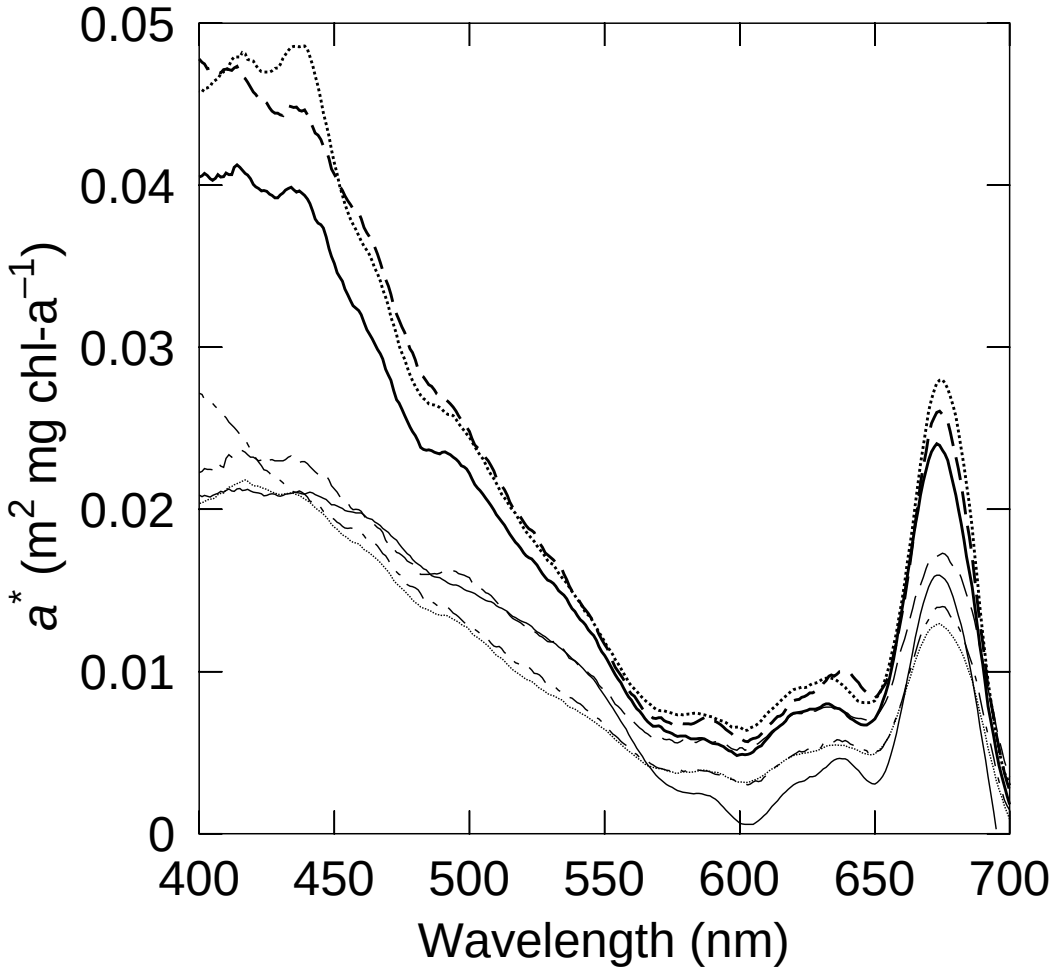

Figure 2.10: The chlorophyll *a*-specific absorption spectra of the diatom clones. The upper group of three heavy lines are *Chaetoceros calcitrans* (dotted, ···), *Cyclotella* (solid, –), and *Chaetoceros* sp. (dashed, --). The lower group of four thin lines are *Thalassiosira* (dashed, --), *Hyalodiscus* (solid, –), *Coscinodiscus* 312 (dotted, ···), and *Coscinodiscus* 1583 (dash-dotted, -·-·).

Table 2.7: Quantum yield of photosynthesis.

Taxa	ϕ_c	se	ϕ_D	se
Chaetoceros calcitrans	$5.18 \cdot 10^{-2}$	$6.78 \cdot 10^{-3}$	$6.78 \cdot 10^{-1}$	$1.73 \cdot 10^{-4}$
Cyclotella nana	$6.97 \cdot 10^{-2}$	$6.56 \cdot 10^{-3}$	$6.31 \cdot 10^{-1}$	$2.45 \cdot 10^{-2}$
Chaetoceros sp.	$3.21 \cdot 10^{-2}$	$3.61 \cdot 10^{-3}$	$6.85 \cdot 10^{-1}$	$3.79 \cdot 10^{-3}$
Thalassiosira weissflogii	$3.63 \cdot 10^{-2}$	$1.47 \cdot 10^{-3}$	$6.33 \cdot 10^{-1}$	$4.09 \cdot 10^{-3}$
Hyalodiscus sp.	$4.38 \cdot 10^{-2}$	$8.42 \cdot 10^{-3}$	$6.08 \cdot 10^{-1}$	$5.12 \cdot 10^{-2}$
Planktoniella sol	$1.83 \cdot 10^{-2}$	$3.96 \cdot 10^{-3}$	$5.23 \cdot 10^{-1}$	$1.41 \cdot 10^{-2}$
Coscinodiscus 312	$1.39 \cdot 10^{-2}$	$1.12 \cdot 10^{-3}$	$6.58 \cdot 10^{-1}$	$3.57 \cdot 10^{-2}$
Coscinodiscus 1583	$1.45 \cdot 10^{-2}$	$3.15 \cdot 10^{-3}$	$6.76 \cdot 10^{-1}$	$6.21 \cdot 10^{-3}$

2.3.4 Quantum yield

Theoretically, algae grown under low light and high nutrient concentrations should have a relatively constant maximum quantum yield between 0.1 to 0.125. In this study, there is 5-fold variation in ϕ_c, which ranges from 0.014 to 0.070 mole C/mole photons (Table 2.7). Quantum yield tends to decrease with increasing cell size. The regression equation for ϕ_c as a function of V is:

$$\log \phi_c = -0.141 \log V - 1.05, \qquad r^2 = 0.66. \tag{2.16}$$

The ϕ_c to V relationship is statistically significant at the 95% significance level (Figure 2.11). There is no previous evidence of size-dependent variation in the maximum quantum yield in diatoms (Geider et al. 1986). A decrease in the quantum efficiency of photosynthesis with increasing cell size suggests that there is a decrease in the efficiency with which carbon is incorporated into the cell with increasing cell size.

In contrast, there is no size-dependence in the DCMU-approximated quantum yield of photochemistry (ϕ_D) (Figure 2.12). The DCMU-approximated ϕ of the 8 diatom cultures range between 0.52 to 0.68, close to reported maximum values (Kolber and Falkowski, 1993). The size-dependence of ϕ_c, and the lack of size-dependence in ϕ_D, suggests that at the photochemical level, cells of all sizes have the same capacity

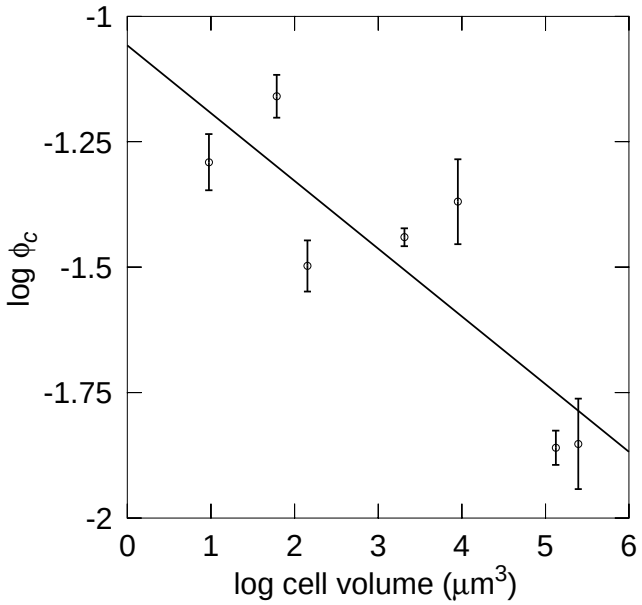

Figure 2.11: Size-dependence of the quantum yield of carbon assimilation.

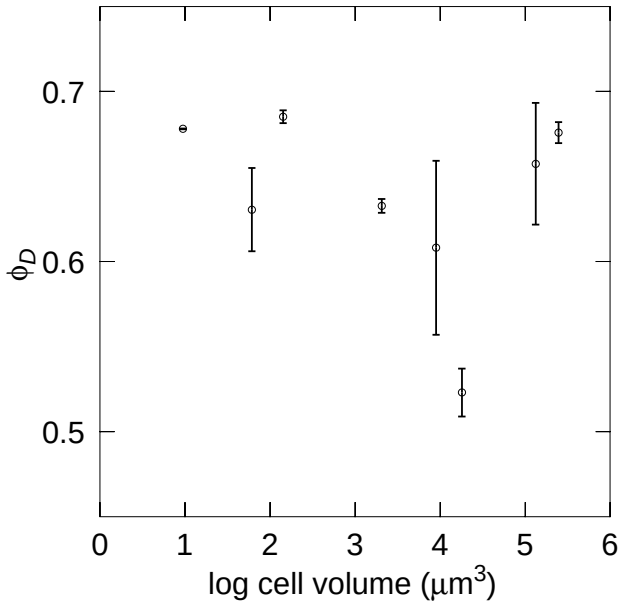

Figure 2.12: Quantum yield of photochemistry.

for the maximum quantum yield of photochemistry. There are many chemical reactions that occur between absorption and carbon fixation where size-dependent factors are of possible importance.

The low efficiency of specific absorption associated with increasing cell size indicates a decrease in the energy yield with equivalent amounts of photosynthetic pigments. Large cells capture fewer photons per unit of pigment than the smaller cells. The photosynthetic pigments within cells of every size have the same metabolic cost for maintenance and manufacture. The photosynthetic pigments in a large cell with a high package effect, capture less energy than pigments within a smaller cell with a lower package effect. Low absorption efficiency contributes to some of the decrease in ϕ_c with increasing cell size. In addition to lower absorption efficiency, large cells have a lower surface area to volume ratio than smaller cells. Cells with lower S/V ratios will have lower rates of passive nutrient diffusion per unit volume, therefore they require more metabolic energy expenditure for equivalent nutrient capture for their growth and photosynthetic processes. Furthermore any size-dependent funneling of reductant to reactions other than carbon fixation could be the cause of the size-dependence in ϕ_c.

The photosynthetic information provided by ϕ_c is very different from the information provided from ϕ_D. The difference between the two measurements is due in part to the different time-scales associated with the respective measurements. The quantum yield of carbon assimilation provides an estimate of the conversion efficiency of light into carbon products that is applicable to measurements associated with the flow of carbon in aquatic ecosystems. In contrast, the quantum yield derived from DCMU stimulated and dark-adapted fluorescence provides short-term estimates of physiological change in the efficiency of light transfer in the photochemical apparatus. As such, it is more applicable to measurements of stress and acclimation to short term changes in environmental conditions.

2.3.5 Cellular composition and the size-dependence of absorptive properties and photosynthetic parameters

The carbon-to-chlorophyll *a* ratio is significantly correlated with cell volume (Figure 2.2). The size-dependence of the carbon-to-chlorophyll *a* ratio can be perceived as a change in the proportion of structural (C) to photosynthetically functional (pigments, specifically c_i) content, which will increase with increasing cell volume. Differences between the size scaling exponents associated with the photosynthetic parameters normalized to carbon and the photosynthetic parameters normalized to chlorophyll *a* is a function of changes in the ratio of the cellular components (used as a proxy for biomass) associated with cell volume. The allometric relationships between carbon and chlorophyll content with volume are statistically significant, and less than one (Table 2.3). In contrast, Taguchi (1976) found no statistically significant relationship between cell volume and θ, accounting for the differences between our size scaling exponents for the C and chlorophyll *a*-specific PI parameters (Tables 2.4, 2.5).

Banse (1976) found 10-fold variation in θ with cell volume, in agreement with the results in the present study. When the allometric exponent of θ to V is less than one, the size scaling exponents associated with the carbon- and chlorophyll-specific photosynthetic parameters with volume will be lower than comparable exponents derived from studies where carbon is used as a proxy for biomass. Cell size is a good predictor of diatom photosynthesis and absorption. The relative size-dependence of cellular components provides a means for explaining the differences between the size scaling exponents derived from the normalization of metabolic rates to different representations of biomass.

2.4 Summary – Size as a scaling factor for phytoplankton absorption properties and photosynthetic parameters

Absorptive properties and photosynthetic parameters were measured for a large size range of diatoms to evaluate the importance of cell size as a scaling factor in photosynthetic studies in phytoplankton physiological ecology. Chlorophyll-specific absorption, photosynthetic efficiency, and capacity varied two-, 8.5-, and 18-fold, respectively. Cell volume can account for much of the variation in the photosynthetic parameters and absorptive properties of the marine diatoms. The following provides a summary of the main results that support the utility of size as a scaling factor for diatom photosynthetic parameters and absorptive properties.

The first objective of this chapter was to determine the size-dependence of the photosynthetic parameters and absorptive properties. The regression coefficients of many of the size-dependent parameters determined in this chapter are listed in Table 2.8. Photosynthetic capacity, photosynthetic efficiency, and its component processes, absorption and quantum yield were examined for size-dependence. Photosynthetic capacity represents the most important anabolic processes contributing to growth under conditions of saturating light. Larger cells possess larger quantities of functional and structural materials than smaller cells for an equivalent photosynthetic gain, contributing to lower carbon- compared to chlorophyll-specific photosynthetic rates. The agreement between the exponents of $P_{\max}^{\mathrm{cell}}$ and $P_{\max}^{\mathrm{chl}}$ to V relationships in this study with the slopes obtained from Taguchi (1976) indicates that the size-dependence of photosynthetic capacity with a uniform exponent is a general characteristic of marine diatoms.

Photosynthetic efficiency, which represents the most important anabolic processes contributing to growth under conditions of limiting light, also demonstrates marked size-dependence. Biomass-specific α decreases with increasing cell volume. The size-dependence of α obtained in this study is also in agreement with the values obtained

Table 2.8: Regression coefficients for the log of the photosynthetic capacity and efficiency, absorption, and quantum yield vs. the log of the cell volume.

Equation	n	Intercept	se	Slope	se	r^2
$\log P^{\text{cell}}_{\text{max}} = a + b \log V$	8	-9.95	0.133	0.502	0.036	0.90
$\log P^{\text{chla}}_{\text{max}} = a + b \log V$	8	0.889	0.098	-0.249	0.027	0.80
$\log P^{C}_{\text{max}} = a + b \log V$	8	-0.239	0.145	-0.410	0.039	0.83
$\log \alpha^{\text{cell}} = a + b \log V$	8	-11.53	0.11	0.593	0.030	0.95
$\log \alpha^{\text{chl}} = a + b \log V$	8	-0.593	0.074	-0.202	0.020	0.82
$\log \alpha^{C} = a + b \log V$	8	-1.72	0.091	-0.366	0.025	0.91
$\log a^{\text{cell}} = a + b \log V$	8	-12.4	0.114	0.647	0.031	0.95
$\log a^{*} = a + b \log V$	7	-1.58	0.029	-0.078	0.008	0.83
$\log \phi_c = a + b \log V$	7	-1.06	0.096	-0.135	0.027	0.72

by Taguchi (1976), indicating that the size-dependence of photosynthetic efficiency with a uniform exponent is also a robust physiological characteristic of marine diatoms.

Photosynthetic efficiency is a function of the quantum yield of photosynthesis and the specific absorption coefficient. Any factor that increases a^* or decreases ϕ will decrease the photosynthetic efficiency. The chlorophyll *a*specific absorption coefficient is size-dependent, decreasing 2-fold with increasing cell size, over the size range examined. The relationship between cellular absorption and cell volume is in agreement with values reported in the literature (Agustí, 1991), indicating that the size-dependence of absorption is a general characteristic of phytoplankton.

The 2-fold size-dependence of absorption cannot account for the 8.5-fold size-dependence of photosynthetic efficiency. This indicates size-dependence in the quantum yield of photosynthesis. The photosynthetic quantum yield demonstrates size-dependence when measured with the ^{14}C technique, but the quantum yield estimated from DCMU and dark-adapted fluorescence shows no size-dependence. The differences between the estimates of photosynthetic quantum yield highlight the relative strengths of the two methods, and pinpoint possible causes for the size-dependence

found in the quantum yield of carbon assimilation. Quantum yield derived from fluorescence provides an estimate of the efficiency of the initial photochemical reactions of photosynthesis but will not reflect energy lost in subsequent biochemical pathways. In contrast, quantum yield derived from ^{14}C estimates reflect the efficiency associated with both the biophysical and biochemical pathways associated with photosynthesis. The data indicate there is no size-dependence in the initial photochemical reactions of photosynthesis. The size-dependence of photosynthesis appears to be linked to later biochemical reactions.

It is often assumed that variability in physiological processes is in part a reflection of cellular composition (Eppley and Sloan, 1966). Systematic changes in photosynthetic and absorptive processes have been associated with cell size, and cellular composition has been associated with changes in size (Parsons et al., 1961; Eppley and Sloan, 1966; Banse, 1976; Taguchi, 1976; Chan, 1980; Blasco et al., 1982; Agustí, 1991). Cell size is a good predictor of both the absorptive properties and photosynthetic parameters of the diatom cells. Cellular composition provides complementary information of the size-dependence of the photosynthetic parameters. Changes in cellular composition associated with cell size can explain the variability in the size scaling exponent between different expressions of the biomass-specific metabolic rates.

Under the conditions of limiting light, photosynthesis is constrained by the efficiency of light absorption. Large cells can maximize specific absorption by decreasing the concentration of pigment within the cell (Kirk 1994). The acclimation to low light is reflected by the increasing θ with increasing cell size. This phenotypic adaptation results in a lowering of the size scaling exponent of the chlorophyll-specific rates of photosynthesis and an increase in the exponent of the carbon-specific rates of photosynthesis with cell volume. If θ is size-dependent and vulnerable to changes in environmental parameters, application of volume to carbon conversion factors from the literature should be used with caution.

The final objective of this chapter was to evaluate the utility of size as a scaling

factor for diatom absorptive properties and photosynthetic parameters. Diatom volumes vary over a large size range. If the empirical size-dependence (3/4 or 2/3) found for growth and respiration in heterotrophs applies to the photosynthetic parameters, 15- to 36-fold variation is expected over the size range measured. The size range examined reveals 17-, 8.5-, and 5-fold variation in $P_{\max}^{\mathrm{chl}}$, α^{chl}, and ϕ_c respectively. The variability in the photosynthetic parameters associated with size is of a similar magnitude to changes in environmental parameters such as nutrient concentration and temperature (Sosik and Mitchell, 1991, 1994; Cullen et al., 1992; Geider and Osborne, 1992), suggesting size could be an extremely useful scaling factor in studies of phytoplankton physiological ecology.

The size scaling exponents of the size-dependent absorptive properties and photosynthetic parameters differ from the common 3/4 slope. This suggests that the allometric relationships developed for non-photosynthetic organisms may be insufficient for phytoplankton. In addition, in field studies where the distribution of phytoplankton sizes is large, measurements of anabolic processes such as photosynthesis are community averages and do not represent the behaviour of individual species of phytoplankton. It is important to realize that community level changes in photosynthetic and absorptive parameters may be due to changes in the composition of the phytoplankton assemblage and not physiological changes associated with the individuals in the assemblage.

Chapter 3

Size-dependence of catabolic processes

3.1 Introduction

The metabolism of phytoplankton can be divided into anabolic and catabolic processes. Photosynthesis, the major anabolic process, results in the production and storage of reductant and organic carbon products from the biological conversion of light energy. Quantification of catabolic processes is important because they consume a significant fraction of gross photosynthate. The two most important catabolic processes that occur in phytoplankton cells are dark mitochondrial respiration, R, and the exudation of organic carbon, E. In this thesis, R describes the energy releasing reactions associated with the oxygenic combustion of carbon products, and E is the process that results in the release of dissolved organic material, as estimated from carbon, into the surrounding environment.

Quantification of respiratory and excretory losses enable the calculation of net photosynthesis from gross photosynthetic estimates. In the past, R was assumed to be approximately 10% of the maximum rate of photosynthesis (Parsons and Takahashi, 1973), but recent studies suggest that the 10% figure is often an underestimate of true respiratory losses (Geider and Osborne, 1989). In comparison to photosynthesis and respiration, there are few data on algal exudation in the literature. Estimates of algal exudation range from 5-95% of gross photosynthesis (Hellebust, 1965; Fogg, 1977; Sharp, 1977; Mague et al., 1980). Unlike respiration, little is known about the actual pathways leading to the excretion of dissolved organic carbon.

Mitochondrial respiration includes three major pathways: glycolysis, Krebs' citric acid cycle, and respiratory electron transport. Complete oxidation of glucose via glycolysis, the citric acid cycle and respiratory electron transport is a simplification of actual cellular processes, because most growing cells do not completely oxidize glucose to carbon dioxide. A variety of substrates are oxidized, and intermediate breakdown products are often used in the biosynthesis of needed cellular components (Geider and Osborne, 1989). The amount of catabolites produced depends on the pathway of breakdown and the efficiency of the respiratory processes. Differences in the organic carbon substrates respired, carbohydrate, protein, or lipid, and the respiratory pathway taken may be responsible for the variability in respiratory rates that have been correlated with species-specific, class-specific, size-specific, and environmental factors (Geider and Osborne, 1989; Geider, 1992). Respiratory processes, like photosynthetic and growth processes, have been correlated with changes in cell size (Banse, 1976; Taguchi, 1976; Tang and Peters, 1995).

In contrast to respiration, exuded organic carbon is not entirely lost to the food web. Exudation products include polysaccharides, carbohydrates, glycerol, glycollic acid, and small amounts of amino acids (Hellebust 1967). These substances provide a food source for heterotrophic bacteria (Pomeroy, 1974; Amon and Benner, 1996). Estimates of exudation are extremely variable (Fogg, 1977; Mague et al., 1980; Zlotnik and Dubinsky, 1989). The general consensus is that healthy cells tend to excrete 5-10% of gross photosynthate, but old and stressed cells may excrete much higher fractions of their gross photosynthate (Mague et al., 1980). Very little research has focused on the role of size on the exudation of dissolved organic material, although Malinsky-Rushansky and Legrand (1996) have tenatively suggested a correlation between the exudation of organic carbon and cell size. However, there are fewer hypotheses regarding the size-dependence of rates of exudation due to the lack of information on the actual mechanism and pathways of exudation (Chen and Wangersky, 1996). If the role of size-dependence in catabolic rates is not considered, patterns of respiration and excretion with other variables may be obscured.

This chapter examines respiratory and exudation rates associated with diatoms representing a large size range. The first objective of the chapter is to quantify the carbon lost through respiration and exudation, and the relationship of these catabolic rates to cell volume. The second objective is to examine the relationship of respiration and exudation to photosynthesis. The results will be evaluated to assess the usefulness of size as a scaling factor for R and E in phytoplankton physiological ecology.

3.2 Materials and methods

3.2.1 Culture conditions and estimates of biomass

The eight diatom clones were grown in two-litre batches. Detailed descriptions of the culture conditions and methods used to determine growth rates, cell volume and size, and chlorophyll *a* concentrations are described in Section 2.2.1, 2.2, and 4.2. Direct carbon and nitrogen determinations apply only to the respiratory measurements derived from the PI curve because the oxygen electrode and exudation experiments were done after the ^{14}C photosynthetic experiments. Carbon estimates for the oxygen electrode determinations of respiration and rates of dissolved organic carbon exudation were derived from the C to V relationship determined in Section 2.3.1, since the average cell volume of the diatom clones were slightly different in this second set of experiments (Tables 3.1 and 3.3).

3.2.2 Dark respiration

3.2.2.1 Indirect estimate of carbon dioxide liberation

Dark respiration was indirectly estimated as carbon dioxide liberation from the PI curve. A three-parameter hyperbolic tangent function was fitted to the PI data:

$$P(I) = P_{\max} \tanh(\alpha I / P_{\max}) - {}^{14C}R \tag{3.1}$$

where $P_{\max}$ and α are the photosynthetic capacity and photosynthetic efficiency, and ${}^{14C}R$ is the extrapolation of the initial PI slope to zero irradiance. The ${}^{14C}R$ estimate is interpreted as a representation of the dark respiratory rate (Jassby and Platt, 1976).

3.2.2.2 Oxygen consumption

Changes in oxygen concentrations in the dark provide another estimate of dark mitochondrial respiratory rates. Oxygen concentrations were determined by an ENDECO oxygen electrode system calibrated with a series of Winkler titrations using

the method of Levy et al. (1977). The procedures developed by Kepkay et al. (1997*a*) were used for the oxygen electrode estimation of respiration. Oxygen electrode measurements were made after a 45 minute equilibration period. The electrodes were pulsed every 5 minutes over a 24-30 hour period in a one liter jacketed glass vessel held at 20°C. The decimal counts obtained from the electrodes were converted to oxygen concentrations using a calibration. The calibration related decimal counts in 0.2μm filtered seawater that was sequentially sparged with three different analyzed gas mixtures of oxygen and nitrogen to Winkler titrations that were done on the gas sparged seawater. In addition, for one oxygen consumption experiment a number of discrete Winkler titrations were done in parallel. The two estimates of oxygen consumption were in good agreement, indicating that a blank as described by Kepkay et al. (1997*a*) for short term (one to two hour) experiments was not required for these day long experiments. The rate of oxygen consumption over the first hour and last 14 hours of the incubation were calculated as the difference in oxygen concentration over the difference in the incubation time. A multiplicative conversion factor of 499.17 was used to convert ml O_2 l^{-1} h^{-1} (μg C l^{-1})$^{-1}$ to moles O_2 h^{-1} (moles C)$^{-1}$. Assuming a respiratory quotient of one, moles O_2 h^{-1} (moles C)$^{-1}$ is equivalent to mg C (mg C h)$^{-1}$.

3.2.3 Exudation of dissolved organic carbon

Exudation of dissolved organic material from the phytoplankton cells was measured during exponential growth in the standard growth conditions described in Section 2.2. An initial 250 ml culture sample was filtered through an pre-acid washed swinette with a pre-combusted GF/F filter and placed in a 250 ml fluorinated polyethylene Nalgene bottle. A second sample was taken 24 or 48 hours later. The filtrate was frozen until analysis. Samples were analyzed within a few weeks of the collection date. The filtrate was thawed and three, five milliliter subsamples were analyzed to determine the average dissolved organic carbon in the sample. The filtrate was analyzed for dissolved organic carbon by high temperature catalytic oxidation with an

Ionics Model 1500 Carbon Analyzer using the method of Kepkay et al. (1997*b*). The concentration of dissolved organic carbon was determined from standard calibration curves generated by the daily analysis of known concentrations of glucose. There was no control associated with these experiments. The bacterial production of and possible consumption of dissolved organic material was assumed negligible because the cultures were continually diluted with bacteria-free nutrient media and aseptic techniques were used during sampling.

3.3 Results and discussion

3.3.1 Size-dependence of the dark respiratory rate

Respiration for many organisms can be related to cell mass by a power function with a common exponent (von Bertalanffy and Pirozynski, 1952; Fenchel, 1974). The most commonly reported mass-specific size scaling exponent is $-1/4$. Lewis (1989) argues that the size scaling exponent is absent in the carbon-specific respiratory rates of phytoplankton. Differences in the size scaling exponent are notable for two main reasons. First, if the the size scaling exponent differs between organisms, size scaling will have to be determined for every organism of interest, thereby reducing the predictive power of the allometric rule. Secondly, since respiration represents the energetic expenditure of the cell, different size scaling exponents associated with different organisms suggests that cells of similar sizes but representing different taxonomic groups have different energetic requirements. A fundamental difference between the respiratory costs of phytoplankton and other aquatic organisms of equivalent size would have implications on the competitive ability of cells and predator-prey interactions. Blasco et al. (1982), Lewis (1989) and Tang and Peters (1995) found that the size scaling exponent in the biomass specific respiratory rates of phytoplankton is larger than -0.25. Futhermore Blasco et al. (1982) showed that for diatoms, the size scaling exponent of the respiratory rate to cell volume relationship is higher than that for the respiratory rate to cell carbon relationship, indicating that caution should be used when applying conversion factors from the literature.

The size scaling exponent reported in the review of Tang and Peters (1995) depends on a variety of species grown under a variety of environmental conditions, using a variety of methods. The study by Blasco et al. (1982) utilized diatom cultures maintained in nutrient and probable light saturated conditions. In this study, the relationship of cell size to the respiratory rates associated with the light limited growth of diatoms was examined.

3.3.1.1 Dark respiratory rate – an indirect estimate of carbon dioxide liberation

The respiration data from the ^{14}C experiments are reported in Table 3.1. The estimation of dark respiration by this method is the intercept of the photosynthesis-irradiance curve at zero irradiance (Figure 3.1). Respiratory rates per cell span four orders of magnitude. Chlorophyll *a* and carbon-specific respiratory rates range 6.1 and 14-fold, respectively (Figure 3.2). Least-square regression analysis indicates that much of the variability in the cell- and carbon-specific respiratory rates can be attributed to cell size. Note that respiration by *Cyclotella nana* was negative and was therefore excluded from the analysis. The negative rate of respiration by *Cyclotelle nana* may be a function of the respiratory estimate and its associated error being at the detection limit the method.

Cell-, chlorophyll *a*-, and carbon-specific respiratory rates follow a different size-dependent exponent with cell volume (Figure 3.2). The exponent of the $^{14C}R^{\text{cell}}$ to V relationship, 0.717 ± 0.051, is statistically significant and much higher than the exponent found by Taguchi (1976), see Table 3.2. In contrast, the size scaling exponent of the chlorophyll *a*-specific respiration to cell volume relationship, with its large standard error, is not significantly different from zero. Lewis (1989), noted size independence in the biomass-specific respiratory rate, but due to a large error in the size scaling exponent it is difficult to determine if the lack of size-dependence is a reflection of the true physiology of the diatoms or due to variation associated with the measurement of respiration. In contrast, carbon-specific respiration, R^C, decreases with increasing cell volume with an statistically significant exponent of -0.242 ± 0.041, (Figure 3.2(c)). The exponent of the $^{14C}R^C$ to C relationship, -0.255, also indicates a size-dependent component in the biomass-specific respiratory rates of diatoms similar to that found for other marine organisms (Ikeda and Mitchell, 1982).

Even though the data from the PI curves indicate that carbon- and cell-specific respiration is size-dependent, the scatter in the ^{14C}R measurements within species casts doubt on the strength of this relationship. A one-way ANOVA demonstrated

Table 3.1: Dark respiratory rates determined from the PI curve.

Taxa	Volume	R^{cell}	se	R^{chl}	se	R^{C}	se
	μm^3	mg C/cell h		mg C/mg chl-a h		mg C/mg C h	
Chaetoceros calcitrans	$9.44 \cdot 10^{0}$	$8.96 \cdot 10^{-12}$	$6.40 \cdot 10^{-12}$	$7.95 \cdot 10^{-2}$	$5.67 \cdot 10^{-2}$	$3.98 \cdot 10^{-3}$	$2.84 \cdot 10^{-3}$
Cyclotella nana	$6.12 \cdot 10^{1}$	$-5.34 \cdot 10^{-13}$	$1.93 \cdot 10^{-11}$	$-1.84 \cdot 10^{-3}$	$6.67 \cdot 10^{-2}$	$-6.31 \cdot 10^{-5}$	$2.28 \cdot 10^{-3}$
Chaetoceros sp.	$1.43 \cdot 10^{2}$	$2.30 \cdot 10^{-11}$	$1.37 \cdot 10^{-11}$	$6.52 \cdot 10^{-2}$	$3.89 \cdot 10^{-2}$	$1.96 \cdot 10^{-3}$	$1.17 \cdot 10^{-3}$
Thalassiosira weissflogii	$2.06 \cdot 10^{3}$	$9.86 \cdot 10^{-11}$	$2.38 \cdot 10^{-10}$	$1.37 \cdot 10^{-2}$	$3.32 \cdot 10^{-2}$	$4.70 \cdot 10^{-4}$	$1.14 \cdot 10^{-3}$
Hyalodiscus sp.	$6.76 \cdot 10^{3}$	$4.17 \cdot 10^{-10}$	$5.67 \cdot 10^{-10}$	$3.51 \cdot 10^{-2}$	$4.78 \cdot 10^{-2}$	$1.01 \cdot 10^{-3}$	$1.37 \cdot 10^{-3}$
Planktoniella sol	$2.43 \cdot 10^{4}$	$1.41 \cdot 10^{-9}$	$1.69 \cdot 10^{-9}$	$8.33 \cdot 10^{-2}$	$9.94 \cdot 10^{-2}$	$5.07 \cdot 10^{-4}$	$6.05 \cdot 10^{-4}$
Coscinodiscus 312	$1.33 \cdot 10^{5}$	$3.08 \cdot 10^{-9}$	$2.01 \cdot 10^{-9}$	$2.54 \cdot 10^{-2}$	$1.66 \cdot 10^{-2}$	$4.15 \cdot 10^{-4}$	$2.71 \cdot 10^{-4}$
Coscinodiscus 1583	$2.37 \cdot 10^{5}$	$1.56 \cdot 10^{-8}$	$4.26 \cdot 10^{-9}$	$3.45 \cdot 10^{-2}$	$9.45 \cdot 10^{-3}$	$2.89 \cdot 10^{-4}$	$7.92 \cdot 10^{-5}$

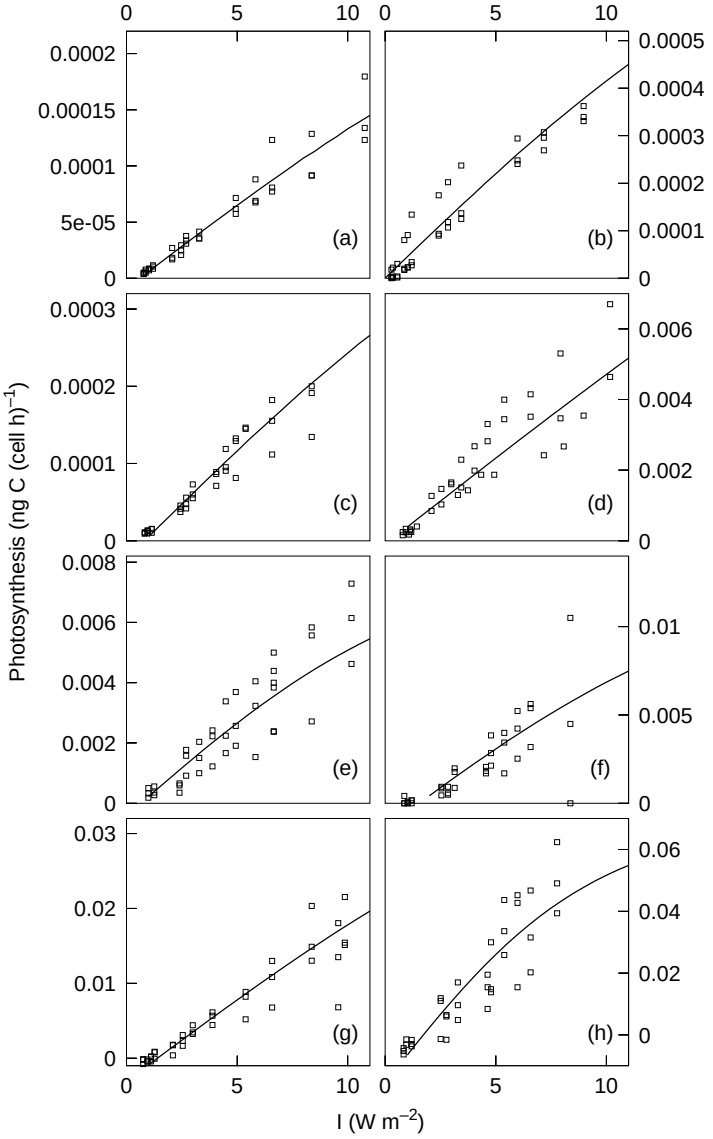

Figure 3.1: The indirect estimate of dark respiration from the photosynthesis-irradiance curve. The ^{14}C uptake in the dark bottles has been subtracted. Replicate photosynthesis-irradiance data from ^{14}C incubations are shown as open squares and fitted curves are solid lines. Plots are labeled with a small letter: (a) *Chaetoceros calcitrans* (b) *Cyclotella nana*, (c) *Chaetoceros* sp., (d) *Thalassiosira weissflogii*, (e) *Hyalodiscus* sp., (f) *Planktoniella sol*, (g) *Coscinodiscus 312*, and (h) *Coscinodiscus 1583*.

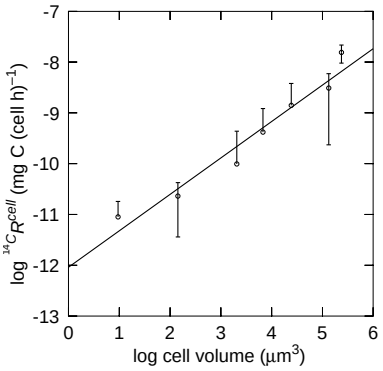

(a) Cell-specific

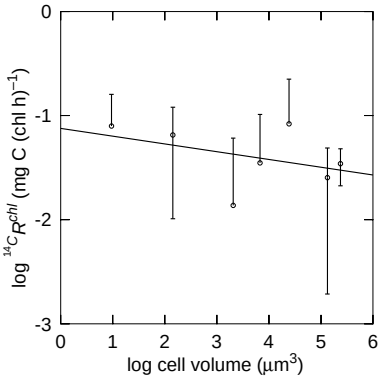

(b) Chlorophyll *a*-specific

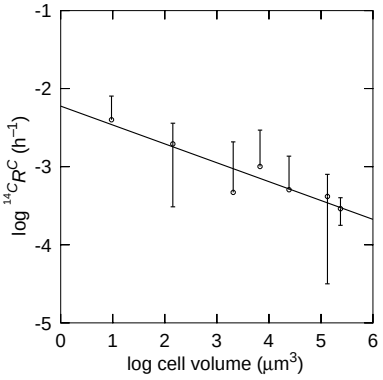

(c) Carbon-specific

Figure 3.2: The size-dependence of dark respiration determined from ^{14}C uptake. Missing error bars indicate that respiration is within one standard error of 0.

Table 3.2: Regression coefficients for the log of the catabolic rates versus the log of cell size.

Equation	n	Intercept	se	Slope	se	r^2
${}^{O(14)}R^C - V$	8	−1.780	0.523	−0.194	0.137	0.250
${}^{O(1)}R^C - V$	7	−0.941	0.483	−0.218	0.129	0.360
${}^{14C}R^C - V$	7	−2.220	0.159	−0.242	0.041	0.880
${}^{O(14)}R^{\text{chl}} - V$	8	−0.698	0.471	0.047	0.124	0.020
${}^{14C}R^{\text{chl}} - V$	7	−1.120	0.286	−0.075	0.074	0.170
${}^{O(14)}R^{\text{cell}} - V$	8	−11.440	0.370	0.726	0.097	0.820
${}^{14C}R^{\text{cell}} - V$	7	−12.040	0.199	0.717	0.051	0.950

(a) $\log R$ vs. $\log V$

Equation	n	Intercept	se	Slope	se	r^2
${}^{14C}R^{\text{cell}} - V$	15	−9.28		0.23	0.2	
${}^{14C}R^{\text{chl}} - V$	15	0.5532	0.6153	−0.4842	0.142	0.47
${}^{14C}R^C - V$	15	−0.5752	0.6044	−0.5403	0.1395	0.54

(b) $\log R$ vs. $\log V$ – Taguchi (1976).

Equation	n	Intercept	se	Slope	se	r^2
$E^{\text{cell}} - V$	8	−11.930	0.312	0.824	0.082	0.940
$E^{\text{chl}} - V$	8	1.187	0.175	0.145	0.046	0.628
$E^C - V$	8	−2.125	0.312	−0.126	0.082	0.284

(c) $\log E$ vs. $\log V$.

Equation	n	Intercept	se	Slope	se
${}^{14C}R - C$	7	−3.96	0.612	−0.255	0.056
${}^{O(14)}R - C$	7	−3.17	1.56	−0.205	0.144
${}^{0(1)}R - C$	8	−2.51	1.49	−0.23	0.138
$E^C - C$	8	−3.03	0.94	−0.13287	0.086983

(d) Log of the carbon-specific catabolic rates vs. $\log V$.

no significant differences between the respiratory rates of species for the chlorophyll *a*-specific respiratory rates of the diatom clones. Uncertainty in the size-dependence of respiration also exists in the literature. To obtain a better estimate of the energetic losses associated with dark respiration, oxygen consumption (^{O}R) was measured.

3.3.1.2 Dark respiratory rate – oxygen consumption

All of the respiratory rates determined from oxygen consumption are listed in Table 3.3. Respiratory rate determined by oxygen electrode is denoted by the incubation period: $^{O(1)}R$ refers to the average respiratory rate over the first hour of the electrode incubation, and $^{O(14)}R$ refers to the average respiratory rate determined from the last 14 hours of the day-long incubation. The following discussion refers primarily to $^{O(14)}R$, because there was less scatter associated with these respiratory rates. Cellular respiratory rates increase with cell volume, spanning three orders of magnitude, while chlorophyll *a* and carbon-specific respiration range 39- and 11-fold, respectively (Figure 3.3).

Regression analysis confirms a statistically significant relationship between cell size and the cell-specific respiratory rates (Table 3.2). In constrast, the relationship between $^{O(14)}R^{\mathrm{C}}$ and $^{O(14)}R^{\mathrm{chl}}$ and cell volume are not statistically significant, although the $^{O(14)}R^{\mathrm{C}}$ to V relationship is statistically significant at the 80% significance level. The size-scaling exponents for the $^{O(14)}R^{\mathrm{cell}}$ and $^{O(14)}R^{\mathrm{C}}$ to cell volume relationship are 0.725 ± 0.097 and -0.194 ± 0.137, respectively. The exponents are in agreement with the comparable ^{14C}R to V relationships. The exponent associated with the $^{O(14)}R^{\mathrm{C}}$ to C relationship, -0.205, also suggests a size-dependent relationship between the carbon-specific respiratory rate and cell size of diatoms similar to that found for other organisms (Ikeda and Mitchell, 1982). In constrast, the exponent of the chlorophyll *a*-specific ^{O}R to cell volume relationship, like the exponent of the $^{14C}R^{C}$ to cell volume relationship is not statistically significant, although larger cells tend to have slightly higher chlorophyll *a*-specific respiratory rates. Eppley and Sloan (1965) reported similar results for the chlorophyll *a*-specific respiratory rate to cell

Table 3.3: Dark respiratory rate estimated from oxygen consumption.

Taxa	Volume	R^{cell}	se	R^{chl}	se
	μm^3	mg C/cell hr		mg C/mg chl-a hr	
Chaetoceros calcitrans	$2.49 \cdot 10^{1}$	$4.64 \cdot 10^{-11}$	$1.04 \cdot 10^{-12}$	$2.16 \cdot 10^{-1}$	$4.82 \cdot 10^{-3}$
Cyclotella nana	$2.18 \cdot 10^{2}$	$3.04 \cdot 10^{-10}$	$1.37 \cdot 10^{-11}$	$5.82 \cdot 10^{-1}$	$2.61 \cdot 10^{-2}$
Chaetoceros sp.	$1.22 \cdot 10^{2}$	$6.56 \cdot 10^{-11}$	$1.28 \cdot 10^{-12}$	$1.39 \cdot 10^{-1}$	$2.71 \cdot 10^{-3}$
Thalassiosira weissflogii	$2.03 \cdot 10^{3}$	$1.15 \cdot 10^{-9}$	$2.40 \cdot 10^{-11}$	$2.47 \cdot 10^{-1}$	$5.17 \cdot 10^{-3}$
Hyalodiscus sp.	$8.97 \cdot 10^{3}$	$2.67 \cdot 10^{-10}$	$2.08 \cdot 10^{-11}$	$6.19 \cdot 10^{-2}$	$4.83 \cdot 10^{-3}$
Planktoniella sol	$1.80 \cdot 10^{4}$	$2.80 \cdot 10^{-8}$	$5.57 \cdot 10^{-10}$	$2.42 \cdot 10^{0}$	$4.82 \cdot 10^{-2}$
Coscinodiscus 312	$3.72 \cdot 10^{5}$	$2.56 \cdot 10^{-8}$	$6.43 \cdot 10^{-10}$	$2.24 \cdot 10^{-1}$	$5.61 \cdot 10^{-3}$
Coscinodiscus 1583	$2.47 \cdot 10^{5}$	$4.62 \cdot 10^{-8}$	$2.03 \cdot 10^{-9}$	$3.86 \cdot 10^{-1}$	$1.70 \cdot 10^{-2}$

Taxa	Volume	${}^{0(14)}R^{C}$	se	${}^{O(1)}R^{C}$	se
	μm^3	mg C/mg C hr		mg C/mg C hr	
Chaetoceros calcitrans	$2.49 \cdot 10^{1}$	$1.13 \cdot 10^{-2}$	$2.52 \cdot 10^{-4}$	$1.41 \cdot 10^{-1}$	$4.79 \cdot 10^{-2}$
Cyclotella nana	$2.18 \cdot 10^{2}$	$1.00 \cdot 10^{-2}$	$4.50 \cdot 10^{-4}$	$3.67 \cdot 10^{-2}$	$4.87 \cdot 10^{-2}$
Chaetoceros sp.	$1.22 \cdot 10^{2}$	$3.69 \cdot 10^{-3}$	$7.20 \cdot 10^{-5}$	$4.11 \cdot 10^{-2}$	$3.67 \cdot 10^{-3}$
Thalassiosira weissflogii	$2.03 \cdot 10^{3}$	$4.87 \cdot 10^{-3}$	$1.02 \cdot 10^{-4}$	$1.02 \cdot 10^{-2}$	$5.43 \cdot 10^{-3}$
Hyalodiscus sp.	$8.97 \cdot 10^{3}$	$2.88 \cdot 10^{-4}$	$2.25 \cdot 10^{-5}$	$3.19 \cdot 10^{-3}$	$3.53 \cdot 10^{-3}$
Planktoniella sol	$1.80 \cdot 10^{4}$	$1.59 \cdot 10^{-2}$	$3.16 \cdot 10^{-4}$	$-1.00 \cdot 10^{-1}$	$-2.89 \cdot 10^{-2}$
Coscinodiscus 312	$3.72 \cdot 10^{5}$	$8.99 \cdot 10^{-4}$	$2.25 \cdot 10^{-5}$	$5.09 \cdot 10^{-3}$	$1.78 \cdot 10^{-3}$
Coscinodiscus 1583	$2.47 \cdot 10^{5}$	$2.36 \cdot 10^{-3}$	$1.04 \cdot 10^{-4}$	$4.22 \cdot 10^{-2}$	$3.97 \cdot 10^{-2}$

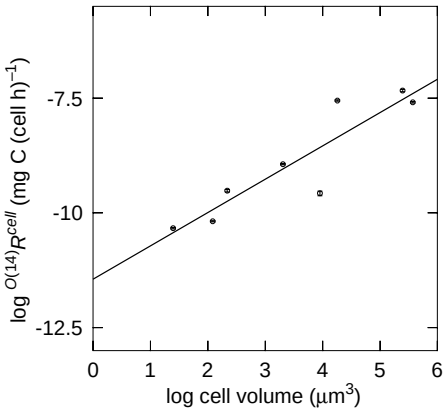

(a) Cell-specific respiratory rate

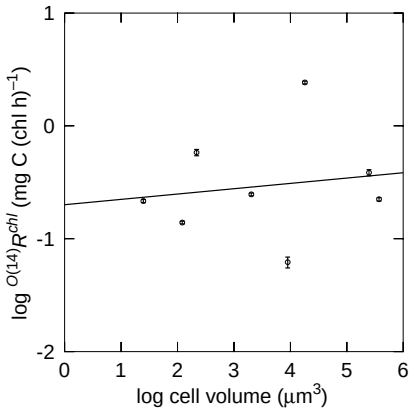

(b) Chlorophyll *a*-specific respiratory rate

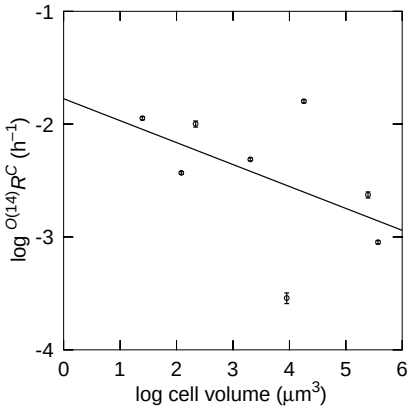

(c) Carbon-specific respiratory rate

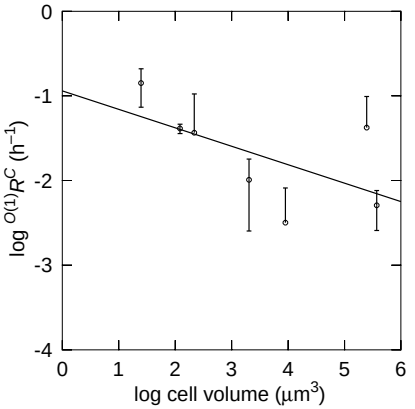

(d) Carbon-specific respiratory rate (1 hour incubation)

Figure 3.3: Size-dependence of oxygen consumption.

volume relationship.

Overall, the size-dependence of oxygen comsumption supports and reinforces the size-dependence of the PI derived estimates of respiratory loss. This complicated series of relationships is easier to understand if θ is included in the discussion.

3.3.2 Respiration and cellular composition

The size-dependence of θ has a significant impact on the relative size-dependence of the carbon and chlorophyll *a* normalized respiratory rates. The carbon oxidation and oxygen liberation rates of respiration both indicate that, per unit of chlorophyll *a*, there is an equivalent respiratory rate for large and small cells on the basis of cell volume. In contrast, per unit of C, smaller cells respire more than larger cells. The size-dependence of θ has repercussions on the relative chlorophyll *a*- and carbon-specific respiratory rates, specifically because the photosynthetically functional components (chlorophyll *a*) of the cell have a much higher metabolic cost than structural components (C) within the cell (Raven, 1984). The diatom light harvesting apparatus, of which chlorophyll *a* is a major component, exacts a metabolic cost that is approximately 305 times greater than the generation of an equivalent amount of carbohydrate (Raven, 1984). Since larger cells have higher θ than small cells, the carbon-specific respiratory rates will be negatively size-dependent. In contrast, the chlorophyll-specific respiratory rates will be size-independent because chlorophyll biomass represents one of the highest metabolic costs to the cell. The decrease in the fraction of functional to structural biomass with increasing cell size reduces the cost of cellular metabolism with increasing cell size, as reflected in the carbon-specific respiratory rate.

There appears to be a slight, statistically insignificant increase in the chlorophyll *a*-specific respiratory rates with increasing cell size. The increase in the package effect with increasing cell size may be the cause of this increase. As the package effect increases, each mole of chromophore captures fewer photons. Therefore, as the package effect increases, each unit of chlorophyll *a* captures less photons suggesting that in larger cells, each unit of chlorophyll *a* has a higher energetic cost. The higher

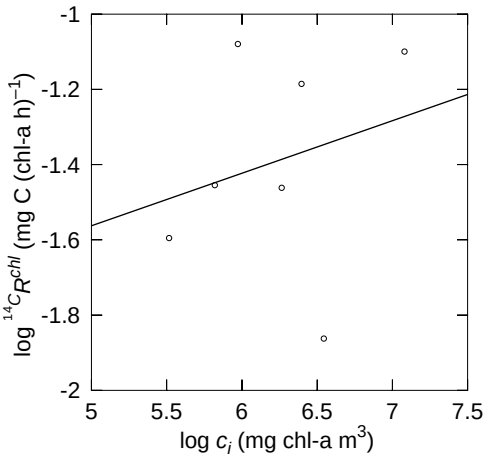

Figure 3.4: Respiratory rate as a function of intracellular chlorophyll concentration.

energetic cost associated with the chlorophyll *a* may be reflected as a higher respiratory rate, since respiratory rate is a reflection of the total metabolic costs associated with the maintenance of the cell. Figure 3.4 illustrates the decreasing efficiency of chlorophyll *a*-specific light absorption as reflected in an increasing respiratory cost with increasing intracellular chlorophyll concentration, note the relationship is not statistically significant.

In summary, the close agreement between the size scaling exponents calculated for the carbon and oxygen estimates of respiration suggest the cell- and carbon-specific respiratory rates are size-dependent but the chlorophyll *a*-specific rates of respiration are not (Table 3.2). The error associated with the size scaling exponents of the respiration to cell volume and cell carbon relationships make it impossible to determine if algal respiration is less size-dependent than that of other organisms as suggested by Banse (1976) and Tang and Peters (1995).

3.3.3 Relationship between carbon and oxygen based estimates of respiratory rate

Biomass-specific respiratory rates determined from the PI experiments were 10 times lower than the rates estimated from the oxygen electrodes. C-14 experiments provide

an estimate between net and gross photosynthesis and therefore, ^{14C}R estimates of respiratory loss will tend to be underestimates of true respiratory rates (Williams, 1993). Enhanced or suppressed respiration in response to light could also be responsible for a discrepancy in the two methods used to measure respiration. Oxygen measurements of respiration will be augmented by any heterotrophic activity in the vessel, therefore oxygenic measurements of respiration will tend to be overestimates of true phytoplankton respiratory rates. The cultures used in these studies were not axenic, but bacterial contribution to respiration is assumed negligible due to the application of aseptic techniques and the continual addition of bacteria-free nutrient media. In addition, oxygenic measurements had to be converted to carbon units for comparison with the ^{14C}R estimates of respiration. The respiratory quotient was not experimentally determined, and was assumed to be one (Geider and Osborne, 1989). Deviation of the respiratory quotient from unity could also be responsible for the systematic difference in the respiratory rates estimated by the two methods.

The incubation time has an important role in the difference between the respiratory rates. Short term respiration measurements are associated with transition stress and biosynthetic processes. Short term respiratory estimates are expected to be much higher than the longer term respiratory rates associated with maintenance metabolism (Geider and Osborne, 1989). Oxygen measurements of respiration from the first hour of the incubation were between two- to eighteen-fold higher than the comparative 14 hour incubation estimate (Figure 3.5). Remarkably, despite the large and systematic difference between the three different estimates of respiratory rate, there is a great deal of similarity in their relationship to cell size (Table 3.2), suggesting that the size-dependent relationships are reliable and robust.

3.3.4 Relationship between respiration and photosynthetic capacity

The second objective is to examine the relationship between respiration and photosynthesis. Based on the ^{14C}R data, the diatom clones respire $6.3 \pm 5.9\%$ of their

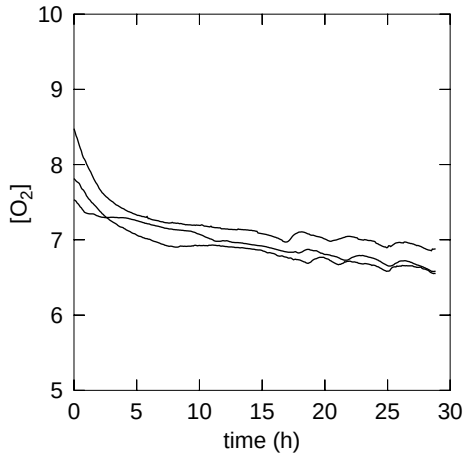

Figure 3.5: Change in oxygen concentration ([O_2] measured in mL O_2/L) over time as measured by three oxygen electrodes for *Chaetoceros* sp..

maximum photosynthetic rate. This is in good agreement with the values reported by other workers (Langdon, 1993; Geider and Osborne, 1989). Within its large standard error, the ${}^{O(14)}R/P$ ratio ratio is in agreement with the ${}^{14C}R/P$ ratio, and therefore similar to values reported in the literature.

Over the size range examined there is $\sim$ 7.2-fold variation in the respiration to photosynthesis (${}^{14C}R/P$) ratio. The following discussion on the R/P ratio and its correlation to cell volume and cellular composition refers to the ${}^{14C}R/P$ ratio because it is much less variable than the ${}^{O(14)}R/P$ ratio. Cell volume can explain 70% of the variation associated with the R/P ratio (Figure 3.6). Respiration increases relative to photosynthesis with increasing cell volume,

$$\log R/P = 0.162 \pm 0.092 \log V - 1.82, \tag{3.2}$$

indicating that the metabolic cost associated with photosynthetic gain increases with increasing cell size. The relative cost compared to benefit of light absorption can provide a mechanistic interpretation of the size-dependence of the R/P. As discussed in Section 2.3.3, efficient light absorption is a priority for light-limited cells. Each mole of chlorophyll has the same metabolic cost, but its benefit in terms of energy capture will decrease with increased cell size and pigment concentration (Raven, 1984). The

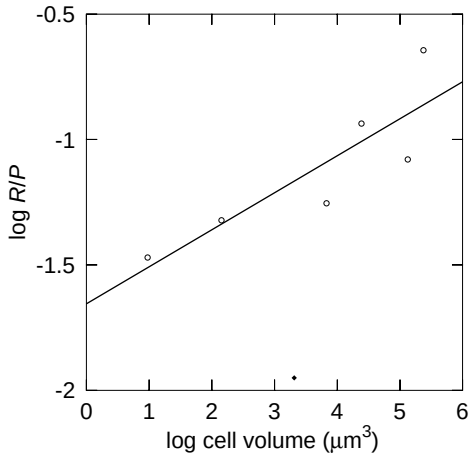

Figure 3.6: R/P as a function of the cell volume. *Thalassiosira weissflogii* is shown as a filled-in circle, and *Cyclotella nana* is not shown since its respiration is negative.

balance between the cost and benefit of increased chlorophyll content changes with cell size. As the pigment packaging effect increases with cell size (Kirk, 1994), the metabolic cost, reflected as respiratory rate, will increase relative to photosynthetic output. As the cellular chlorophyll content increases relative to carbon content the pigment packaging increases, accounting for the positive correlation between the R/P ratio and θ (Figure 3.7).

Thalassiosira weissflogii and *Cyclotella nana* were excluded from regression analysis between the R/P ratio and cell volume. *Cyclotella nana* was excluded from all the ^{14}C respiratory analysis because its respiratory rate was negative. *Thalassiosira weissflogii* was excluded due to its extremely low rate of respiration relative to photosynthesis. The R/P ratio of *Thalassiosira weissflogii* was less than one fifth of the next lowest value, suggesting that *Thalassiosira weissflogii* may be particularly well suited to the environmental conditions provided.

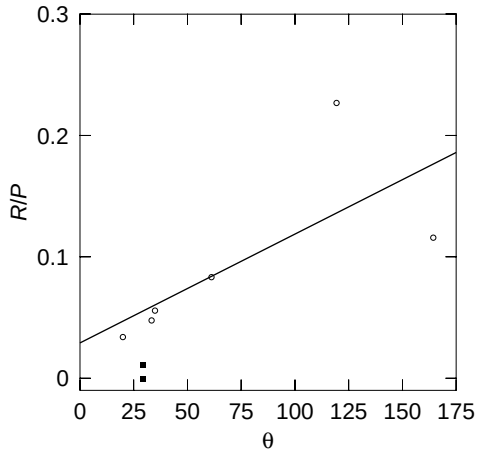

Figure 3.7: R/P as a function of θ. The outliers *Thalassiosira weissflogii* and *Cyclotella nana* are shown as filled-in squares.

3.3.5 Size-dependence of exudation

Malinsky-Rushansky and Legrand (1996) suggest small cells may exude a higher percentage of dissolved organic carbon than larger cells, but found no statistically significant size-dependent relationship for the rate of exudation for a variety of phytoplankton cultures representing a number of different classes. The size range examined was relatively small, with data from a variety of studies, which employed a variety of growth conditions and methodologies to determine the rate of exudation. The following data set examines exudation rates for a large size range of diatoms under identical light limited, nutrient replete conditions.

The exudation per cell spans over three orders of magnitude. Chlorophyll *a*- and carbon-specific rates of exudation exhibit 7.6-fold and 12-fold variation, respectively (Table 3.4). Exudation by the phytoplankton cultures demonstrated a number of size-dependent patterns, some similar to those found for respiration, and some unique to exudation (Figure 3.8). Excretion per cell increases with cell size with a size scaling exponent of 0.824 ± 0.082, similar to the comparable exponent for respiration (Table 3.2). Carbon-specific exudation decreases with increasing cell volume with an exponent of -0.126 ± 0.082. Although the exponent of the E^C to V relationship is not statistically significant at the 95% level, it is significant at the 80% level. The

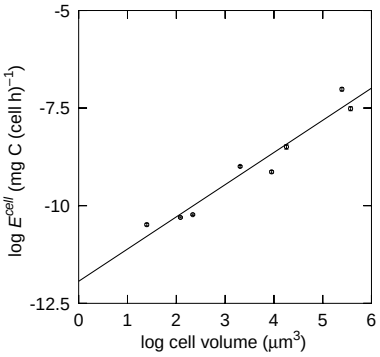

(a) Cell-specific

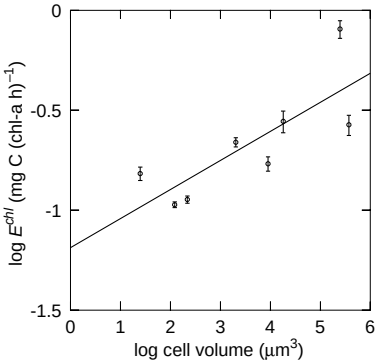

(b) Chlorophyll *a*-specific

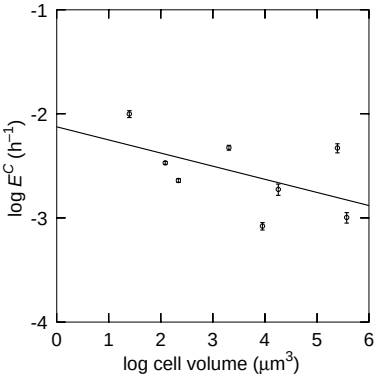

(c) Carbon-specific

Figure 3.8: Size-dependence of diatom exudation.

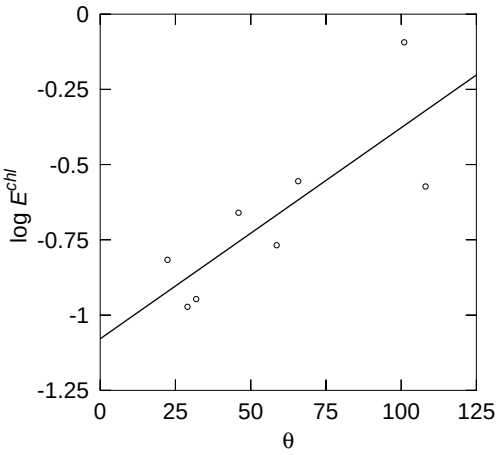

Figure 3.9: Relationship between the chlorophyll *a*-specific rates of exudation and θ.

exponent of the E^C to C relationship, -0.133, is also not statistically significant at the 95% significance level. In contrast to E^{cell} and E^{C}, the chlorophyll *a*-specific rates of exudation increase with cell volume, even though none of the other chlorophyll *a*-specific metabolic parameters in this study increased significantly with cell volume. This suggests that the mechanisms controlling the size-dependence of exudation may be different than those for the photosynthetic or respiratory processes.

3.3.6 Size-dependent exudation and cellular composition

The change in the carbon-to-chlorophyll *a* ratio can help explain the anomalous, positive size-dependence of the chlorophyll *a*-specific rates of exudation. The increase in the chlorophyll *a*-specific rates of exudation with cell volume indicates that exudation is a function of total cell biomass and not solely of photosynthetically functional biomass. As cell volume increases, chlorophyll *a* content decreases relative to carbon content. As a result, chlorophyll *a* represents a smaller fraction of total biomass with increasing cell size. This is illustrated by the correlation ($r = 0.84$) between θ and the chlorophyll *a*-specific rates of exudation (Figure 3.9).

Table 3.4: Exudation, photosynthesis, and percent extracellular release (PER) of dissolved organic carbon.

Taxa	Volume	E^{cell}	se	E^{chl}	se	E^{C}	se
	μm^3	mg C/cell h		mg C/mg chl-a h		mg C/mg C h	
Chaetoceros calcitrans	$2.49 \cdot 10^{1}$	$3.28 \cdot 10^{-11}$	$1.78 \cdot 10^{-12}$	$1.53 \cdot 10^{-1}$	$8.31 \cdot 10^{-3}$	$9.97 \cdot 10^{-3}$	$5.43 \cdot 10^{-4}$
Cyclotella nana	$2.18 \cdot 10^{2}$	$5.92 \cdot 10^{-11}$	$1.76 \cdot 10^{-12}$	$1.13 \cdot 10^{-1}$	$3.36 \cdot 10^{-3}$	$2.29 \cdot 10^{-3}$	$6.80 \cdot 10^{-5}$
Chaetoceros sp.	$1.22 \cdot 10^{2}$	$5.02 \cdot 10^{-11}$	$1.17 \cdot 10^{-12}$	$1.07 \cdot 10^{-1}$	$2.49 \cdot 10^{-3}$	$3.38 \cdot 10^{-3}$	$7.89 \cdot 10^{-5}$
Thalassiosira weissflogii	$2.03 \cdot 10^{3}$	$1.02 \cdot 10^{-9}$	$3.81 \cdot 10^{-11}$	$2.19 \cdot 10^{-1}$	$8.20 \cdot 10^{-3}$	$4.73 \cdot 10^{-3}$	$1.77 \cdot 10^{-4}$
Hyalodiscus sp.	$8.97 \cdot 10^{3}$	$7.36 \cdot 10^{-10}$	$4.26 \cdot 10^{-11}$	$1.71 \cdot 10^{-1}$	$9.90 \cdot 10^{-3}$	$8.35 \cdot 10^{-4}$	$4.84 \cdot 10^{-5}$
Planktoniella sol	$1.80 \cdot 10^{4}$	$3.22 \cdot 10^{-9}$	$2.82 \cdot 10^{-10}$	$2.79 \cdot 10^{-1}$	$2.44 \cdot 10^{-2}$	$1.88 \cdot 10^{-3}$	$1.65 \cdot 10^{-4}$
Coscinodiscus 312	$3.72 \cdot 10^{5}$	$3.07 \cdot 10^{-8}$	$2.52 \cdot 10^{-9}$	$2.67 \cdot 10^{-1}$	$2.19 \cdot 10^{-2}$	$1.01 \cdot 10^{-3}$	$8.29 \cdot 10^{-5}$
Coscinodiscus 1583	$2.47 \cdot 10^{5}$	$9.64 \cdot 10^{-8}$	$6.89 \cdot 10^{-9}$	$8.06 \cdot 10^{-1}$	$5.75 \cdot 10^{-2}$	$4.69 \cdot 10^{-3}$	$3.35 \cdot 10^{-4}$

Taxa	P_k^C	se	PER
	mg C / mg C h^{-1}		
Chaetoceros calcitrans	$1.18 \cdot 10^{-1}$	$3.58 \cdot 10^{-3}$	7.82
Cyclotella nana	$8.90 \cdot 10^{-2}$	$2.85 \cdot 10^{-3}$	2.51
Chaetoceros sp.	$4.11 \cdot 10^{-2}$	$1.39 \cdot 10^{-3}$	7.61
Thalassiosira weissflogii	$4.19 \cdot 10^{-2}$	$1.70 \cdot 10^{-3}$	10.14
Hyalodiscus sp.	$1.81 \cdot 10^{-2}$	$1.45 \cdot 10^{-3}$	4.42
Planktoniella sol	$4.38 \cdot 10^{-3}$	$6.71 \cdot 10^{-4}$	30.04
Coscinodiscus 312	$4.99 \cdot 10^{-3}$	$3.34 \cdot 10^{-4}$	16.84
Coscinodiscus 1583	$1.28 \cdot 10^{-3}$	$8.12 \cdot 10^{-5}$	78.62

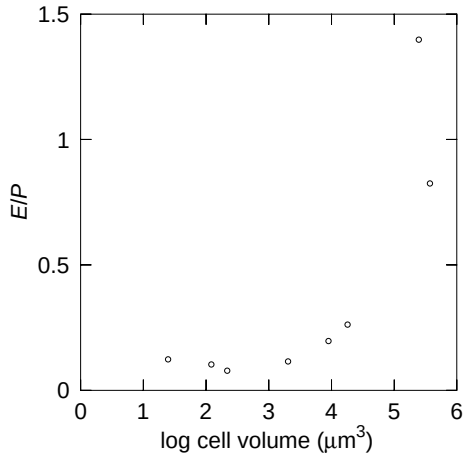

Figure 3.10: Size-dependence of the E/P ratio.

3.3.7 Relationship of exudation to photosynthetic capacity

The 18-fold range in the E/P ratio corresponds with the large variation reported in the literature (Hellebust, 1965; Fogg, 1977; Malinsky-Rushansky and Legrand, 1996). The E/P ratio tends to increase with cell volume (Figure 3.10). The increase in exudation compared with photosynthesis with cell size indicates a decrease in the growth efficiency with increased cell size. For comparison to values in the literature, algal exudation was also calculated as a percent of total production (Malinsky-Rushansky and Legrand, 1996),

$$\mathrm{PER} = \frac{100E^C}{E^C + P_k^C}, \tag{3.3}$$

where PER refers to percent extracellular production, and P_k^C refers to the photosynthetic rate at the growth irradiance computed from the PI parameters (Figure 3.11 and Table 3.4). The percent extracellular release has a 31-fold range, with an average of 20±25%. The percent extracellular release for the small and medium size cells for this study are in good agreement with the small and medium sized cells from other studies (Hellebust, 1965; Fogg, 1977; Malinsky-Rushansky and Legrand, 1996).

It is possible that the high rates of exudation associated with *Coscinodiscus 312* and *Coscinodiscus 1583* are species-specific, not size-dependent. The percent extracellular release of *Coscinodiscus 1583* is over two times higher than the next highest

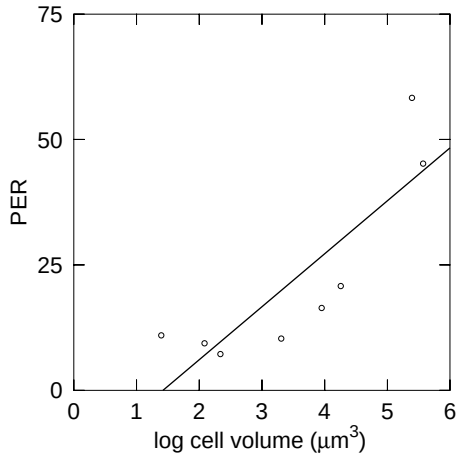

Figure 3.11: Size-dependence of the percent extracellular release (PER) of dissolved organic carbon.

value. If the percent extracellular release of *Coscinodiscus 1583* is excluded from the analysis, there is an 11-fold range in values with an average of 11±9%. There were large amounts of mucilaginous material associated with the three largest clones, *Coscinodiscus 312*, *Coscinodiscus 1583* and *Planktoniella sol*. Some of this material may have been considered in the exudation rate, but some may have been captured on the filter and not included in the estimate of exudation. Mucilaginous material may reduce sinking rates, keeping cells surrounded by mucilage up in the photic zone for longer periods of time. More data are required on the photosynthetic and exudation rates of large phytoplankton cells to clarify the size-dependence of exudation and its relationship to photosynthetic production.

3.4 Summary – Size as a scaling factor for catabolic processes

3.4.1 Respiration

The first objective of this chapter was to quantify the rates of respiration over a large size range of diatoms grown under identical environmental conditions. The PI derived estimates of respiration were, on average, 10-fold lower than the oxygen estimates of respiration (Tables 3.1 and 3.3). Oxygen estimates of respiration in the dark are considered better estimates of phytoplankton respiration because they are not subject to variable rates of light respiration or the other errors associated with the ^{14}C method. There was much less variation in the PI derived estimates than in the oxygen electrode derived esimates of dark respiration.

The size scaling exponent of carbon-specific respiration as a function of cell carbon is somewhat lower than the exponent found in a recent literature review of algal respiratory rates (Tang and Peters, 1995). In contrast to the carbon- and cell-specific rates of respiration, the chlorophyll-specific rates of respiration demonstrate no size-dependence. Eppley and Sloan (1965) also found that chlorophyll *a*-specific rates of respiration are independent of cell size. Due to the large error associated with the respiratory estimates for each clone, it is difficult to determine if the size-independence of the chlorophyll-specific respiratory rates is a reflection of algal physiology or a statistical artifact due to the large variation in values and a relatively small sample size. However, given these limitations, it can still be suggested that chlorophyll *a*-specific respiration should be size-independent because chlorophyll *a* represents one of the highest metabolic costs to the cell.

In contrast, carbon-specific respiratory rates have a size scaling exponent similar to reported literature values for a variety of organisms (Ikeda and Mitchell, 1982), but lower than reported by a number of studies on marine diatoms (Blasco et al., 1982; Lewis, 1989; Tang and Peters, 1995). Although the size scaling exponent of the ^{14C}R to cell volume relationship is significant, the size scaling exponent of the

$^{O(14)}R$ to cell volume relationship was not statistically significant (Table 3.2). More data are required to determine if the magnitude of the diatom respiratory size-scaling exponent is significantly different from that of other classes of organisms, especially under conditions that limit growth.

3.4.2 Exudation

There is a large amount of variation within and between the exudation rates of the diatom cultures (Table 3.4). The carbon-specific rates of exudation decreased with cell volume (Figure 3.8). In contrast, the chlorophyll *a*-specific rates of exudation had a positive size scaling exponent with cell volume. The size scaling exponents for the cell- and carbon-specific rates of exudation were smaller than expected by the 3/4 allometric rule. The size-dependent variations of E^{cell}, E^{chl}, and E^{C} suggest that the mechanisms controlling the size-dependence of exudation may be different than those for the photosynthetic or respiratory processes measured in this study (Table 3.2).

Exudation appears to be a function of total volume. Normalization to chlorophyll content results in a division of the exudation rate by a progressively smaller fraction of the total biomass with increasing cell volume. This results in an increase in the rate of chlorophyll-specific exudation with increasing cell volume. In contrast, carbon-specific exudation rates decrease with cell volume because carbon provides a proxy for total cell biomass, revealing the true size-dependence of the exudation process.

There is a great deal of variation within the estimates of exudation for the diatom clones, and previous studies do not support a size-dependent relationship. The only conclusion that seems well established is that certain species exude much more dissolved organic carbon than others of similar size or genetic relationship (Sakshaug, 1993). This generally accepted conclusion may be more a function of a general lack of knowledge and experiemntal control. More information is required to assess the size-dependence of exudation in diatoms to determine the value of size-scaling for the quantification of exudation in studies of phytoplankton physiological ecology.

Chapter 4

Size-dependence of phytoplankton growth

4.1 Introduction

4.1.1 The size-dependence of phytoplankton growth

Measurements of photosynthesis in the absence of respiration, exudation, and growth do not provide a complete picture of carbon metabolism in the phytoplankton cell. This is because high rates of photosynthesis may be accompanied by variable rates of respiration and exudation. Measurements of growth provide an unequivocal estimate of the net increase in biomass with time. Patterns of growth with biological, chemical, and physical factors may be more straightforward than comparable patterns of gross photosynthesis. Unfortunately direct measurements of growth are difficult in a field setting, but laboratory studies can provide direct information about growth and its relationship to component anabolic and catabolic processes.

Eppley and Sloan (1966) were among the first to report size-dependence in the growth of marine phytoplankton (Chisholm, 1992). Growth rates of phytoplankton are extremely variable, with doubling times ranging from a few hours to weeks (Goldman et al., 1979). Some of the variability in algal growth rates can be attributed to cell size. Diatoms have an extremely large size range, spanning approximately eight orders of magnitude in weight (Banse, 1976). Over this size range the allometric equation, with an exponent of 3/4, predicts approximately 100-fold variability in the specific growth rates of the diatom cells.

The relationship between cell size and growth rate is a useful concept in algal ecology (Peters, 1983), and several models of energy transfer through the food web rely on the allometric relationship between size and growth (Silvert and Platt, 1978; Peters, 1983; Platt, 1985; Tang, 1995). Unfortunately the size scaling exponents reported for algal growth are highly variable (Tang, 1995). Variability in the size scaling exponent for growth may be a function of phyletic differences, the type of measurement employed, or environmental forcing (Fenchel, 1974; Chan, 1980; Blasco et al., 1982; Langdon, 1988; Chisholm, 1992; Tang, 1995).

Some studies have suggested that the size-dependence of unialgal growth is weak (Sommer, 1989; Banse, 1982). Banse (1976), Sommer (1989) and Peters (1983) suggest that environmental conditions may further modify the size-dependence of phytoplankton growth. Specifically there is some doubt about the existence and magnitude of the size scaling exponent of growth under environmental conditions that limit growth (Sommer, 1989; Tang, 1995). Light is one of the primary growth limiting factors for phytoplankton in the ocean. The maximum quantum yield of growth and photosynthesis must be examined under low light. This chapter examines the size-dependence of growth in marine diatoms under light-limiting conditions.

It would be useful to correlate growth with commonly measured anabolic and catabolic parameters, since growth is so difficult to measure in nature. Growth can be calculated from the balanced growth equation as the difference between anabolic and catabolic processes,

$$k = P_g^C - R^C - E^C, \tag{4.1}$$

where k is the growth rate per hour, P_k^C is used as an approximation of P_g^C, P_g^C is the carbon-specific gross photosynthetic rate at the growth irradiance per hour, R^C is the carbon-specific dark respiratory rate per hour, and E^C is the carbon-specific rate of exudation per hour. Equation 4.1 suggests that growth can be estimated from measurements of P_g^C, if we understand the relationship of k, R^C, and E^C to P_g^C. Understanding the interaction of the size-dependence of anabolic and catabolic processes is essential to understanding the size-dependence of growth. It has been

established in Chapters 2 and 3 that absorption, photosynthesis, and respiration are size-dependent. The interaction of the absorptive properties, photosynthetic parameters, and the catabolic rates of respiration and exudation are examined in context of growth to determine if there is any strong correlation to permit the estimation of growth from absorptive properties, and anabolic and catabolic processes.

4.2 Materials and methods

4.2.1 Growth rate

Cells were counted with a Levy Improved Neubauer or American Optical Brightline haemacytometer (both 0.2 mm deep), or a Sedwick-Rafter chamber, depending on the size of the cells. The haemacytometers were used to determine the growth rates for the five smallest diatom cultures. The Sedwick-Rafter chamber was used to determine the growth rates of the three largest diatom clones. When practically possible, enough cells were counted to keep the coefficient of variation of the mean population estimate below twenty percent. Samples for the growth rate determinations were taken after manual agitation but before each dilution. Aseptic techniques were used to take a one to five milliliter aliquot. Subsamples from the aliquot were used for the growth rate determinations. In general, four slides, or eight fields of view were measured for the five smallest diatoms. The Sedwick-Rafter chamber was divided into 11 fields of view. Two to four slides were employed, and approximately 20–40 fields of view were examined. The log base two specific growth rate (k) was determined from the following equation as described by Guillard (1973):

$$\frac{\log_2(X_1/X_0)}{t_1 - t_0}, \tag{4.2}$$

where X refers to cell number or concentration and t refers to time in hours. The log base two estimate of specific growth (k) had to be converted to the log base e specific growth rate (k_e) using a multiplicative factor of 0.6931 to properly compare the specific growth rate to the estimates of photosynthesis, respiration, and exudation.

Exponential growth was determined by the response of the growth rate over a series of dilution rates with axenic culture media. The exponential growth rate and the optimum standing stock was obtained once the growth rate no longer increased with an increase in the influx of new culture media. The sampling time was specific to each culture, depending on the dilution required to maintain exponential growth.

4.2.2 Quantum yield of growth

The quantum yield of growth (ϕ_{k_e}), was calculated using a simplified form of the equation described by Sosik and Mitchell (1991):

$$\phi_k = 12000 \frac{k_s \theta}{a^* I_g} \tag{4.3}$$

where k_s is the specific growth rate (natural log) in seconds, θ is the C to chlorophyll a ratio (mg:mg), a^* is the chlorophyll a-specific absorption coefficient in m^2 mg chl-a^{-1}, I_g is the irradiance in the growth incubator in μE m^{-2} s^{-1}, and 12000 is a constant that converts mg C into moles C. A correction factor was calculated for the spectral quality of the fluorescent lights in the growth chamber as described in Chapter 2. Spectral irradiance values were provided by Sylvania Ltd. for the F30T12 and F15T12D fluorescent tubes.

4.3 Results and discussion

4.3.1 Size-dependence of growth

4.3.1.1 Specific growth

The specific growth rates span an approximate 8-fold range, with doubling times ($1/k$) from 23 hours for the smallest clone, to 179 hours for the largest clone (Table 4.1).

The reconstructed growth curves demonstrate that over a long time interval the cells were growing at a constant rate (Figure 4.1). The growth rates calculated are estimates of the maximum growth rate for a dilute culture at the growth irradiance in the growth medium at 20°C. Extra dilutions were made periodically as a check that the cells would not grow faster at a lower cell density. The reconstructed growth curves were computed by scaling the cell density determinations by the dilution rate. The curves show unrealistically high cell concentrations due to the omission of the dilution factor in the calculation of cell concentration. These cell concentrations did not occur in the actual culture vessels because of the periodic dilutions. These curves can be imagined to correspond to the growth of a dilute culture in an infinitely large culture vessel. (Approximate dilution rates are shown in Table 4.2.) One to three days before experiments were performed, the cultures were diluted again to ensure that cells remained growing exponentially and that the experimental cell concentrations were below those shown in Table 4.2.

The growth rate of the phytoplankton cells has a strong relationship with cell volume (Figure 4.2). The size-dependent relationship between k_e and V is

$$\log k_e = -0.219 \pm 0.032 \log V - 1.189 \pm 0.119 \qquad r^2 = 0.88. \tag{4.4}$$

This relationship predicts an approximate 80% decrease in specific growth rate for every thousand-fold increase in volume. This exponent is slightly higher than the slopes derived from a number of similar studies on marine diatom growth (Blasco et al., 1982; Banse, 1982; Mizuno, 1991; Tang, 1995). Differences in the size-dependence of cellular components such as C and chlorophyll a under low versus high light conditions may

Table 4.1: Growth parameters.

Taxa	$\log V$ (μm^3)	k_2 (h^{-1})	se	k_e (h^{-1})	se	ϕ_{k_e} (mol C/E)	se
Chaetoceros calcitrans	$9.75 \cdot 10^{-1}$	$4.39 \cdot 10^{-2}$	$2.73 \cdot 10^{-3}$	$3.04 \cdot 10^{-2}$	$1.90 \cdot 10^{-3}$	$3.11 \cdot 10^{-2}$	$5.54 \cdot 10^{-3}$
Cyclotella nana	$1.79 \cdot 10^{0}$	$3.62 \cdot 10^{-2}$	$3.77 \cdot 10^{-3}$	$2.51 \cdot 10^{-2}$	$2.62 \cdot 10^{-3}$	$4.67 \cdot 10^{-2}$	$9.01 \cdot 10^{-3}$
Chaetoceros sp.	$2.15 \cdot 10^{0}$	$3.33 \cdot 10^{-2}$	$2.02 \cdot 10^{-3}$	$2.31 \cdot 10^{-2}$	$1.40 \cdot 10^{-3}$	$4.35 \cdot 10^{-2}$	$7.62 \cdot 10^{-3}$
Thalassiosira weissflogii	$3.31 \cdot 10^{0}$	$3.26 \cdot 10^{-2}$	$1.49 \cdot 10^{-3}$	$2.26 \cdot 10^{-2}$	$1.03 \cdot 10^{-3}$	$6.26 \cdot 10^{-2}$	$1.59 \cdot 10^{-2}$
Hyalodiscus sp.	$3.83 \cdot 10^{0}$	$1.54 \cdot 10^{-2}$	$2.38 \cdot 10^{-3}$	$1.07 \cdot 10^{-2}$	$1.65 \cdot 10^{-3}$	$2.67 \cdot 10^{-2}$	$4.16 \cdot 10^{-3}$
Planktoniella sol	$4.39 \cdot 10^{0}$	$7.76 \cdot 10^{-3}$	$1.75 \cdot 10^{-3}$	$5.38 \cdot 10^{-3}$	$1.21 \cdot 10^{-3}$	$4.33 \cdot 10^{-2}$	$9.01 \cdot 10^{-3}$
Coscinodiscus 312	$5.12 \cdot 10^{0}$	$5.60 \cdot 10^{-3}$	$5.13 \cdot 10^{-4}$	$3.88 \cdot 10^{-3}$	$3.56 \cdot 10^{-4}$	$2.74 \cdot 10^{-2}$	$3.47 \cdot 10^{-3}$
Coscinodiscus 1583	$5.38 \cdot 10^{0}$	$6.33 \cdot 10^{-3}$	$9.06 \cdot 10^{-4}$	$4.39 \cdot 10^{-3}$	$6.28 \cdot 10^{-4}$	$1.40 \cdot 10^{-2}$	$4.16 \cdot 10^{-3}$

Taxa	F ($^{O(14)}R$)	se	F (^{14}C)	se	P_n ($^{O(14)}R$) mg C (mg C h)$^{-1}$	se	P_n (^{14}C)	se
Chaetoceros calcitrans	$5.89 \cdot 10^{-1}$	$6.73 \cdot 10^{-2}$	$6.86 \cdot 10^{-1}$	$1.24 \cdot 10^{-1}$	$9.64 \cdot 10^{-2}$	$4.37 \cdot 10^{-3}$	$1.04 \cdot 10^{-1}$	$6.97 \cdot 10^{-3}$
Cyclotella nana	$6.71 \cdot 10^{-1}$	$1.26 \cdot 10^{-1}$	$9.16 \cdot 10^{-1}$	$2.62 \cdot 10^{-1}$	$7.67 \cdot 10^{-2}$	$3.37 \cdot 10^{-3}$	$8.68 \cdot 10^{-2}$	$5.20 \cdot 10^{-3}$
Chaetoceros sp.	$7.65 \cdot 10^{-1}$	$8.56 \cdot 10^{-2}$	$8.12 \cdot 10^{-1}$	$1.25 \cdot 10^{-1}$	$3.40 \cdot 10^{-2}$	$1.54 \cdot 10^{-3}$	$3.57 \cdot 10^{-2}$	$2.64 \cdot 10^{-3}$
Thalassiosira weissflogii	$7.02 \cdot 10^{-1}$	$6.06 \cdot 10^{-2}$	$8.13 \cdot 10^{-1}$	$1.06 \cdot 10^{-1}$	$3.23 \cdot 10^{-2}$	$1.98 \cdot 10^{-3}$	$3.67 \cdot 10^{-2}$	$3.01 \cdot 10^{-3}$
Hyalodiscus sp.	$9.05 \cdot 10^{-1}$	$2.72 \cdot 10^{-1}$	$8.53 \cdot 10^{-1}$	$3.41 \cdot 10^{-1}$	$1.69 \cdot 10^{-2}$	$1.52 \cdot 10^{-3}$	$1.62 \cdot 10^{-2}$	$2.87 \cdot 10^{-3}$
Planktoniella sol	$2.32 \cdot 10^{-1}$	$6.93 \cdot 10^{-2}$	$6.92 \cdot 10^{-1}$	$3.33 \cdot 10^{-1}$	$-1.34 \cdot 10^{-2}$	$1.15 \cdot 10^{-3}$	$1.99 \cdot 10^{-3}$	$1.44 \cdot 10^{-3}$
Coscinodiscus 312	$6.70 \cdot 10^{-1}$	$1.15 \cdot 10^{-1}$	$7.32 \cdot 10^{-1}$	$1.65 \cdot 10^{-1}$	$3.08 \cdot 10^{-3}$	$4.39 \cdot 10^{-4}$	$3.56 \cdot 10^{-3}$	$6.88 \cdot 10^{-4}$
Coscinodiscus 1583	$3.83 \cdot 10^{-1}$	$9.07 \cdot 10^{-2}$	$4.68 \cdot 10^{-1}$	$1.19 \cdot 10^{-1}$	$-5.78 \cdot 10^{-3}$	$5.20 \cdot 10^{-4}$	$-3.71 \cdot 10^{-3}$	$4.96 \cdot 10^{-4}$

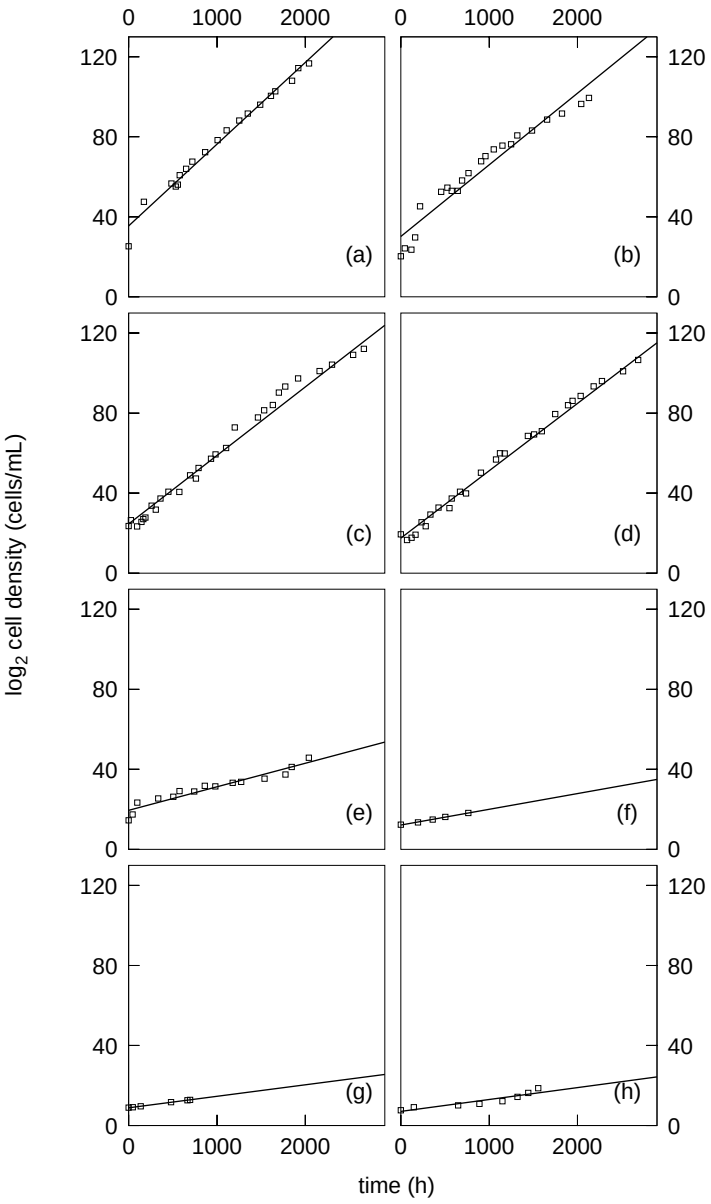

Figure 4.1: Growth curves for the eight diatom clones. Plots are labeled with a small letter: (a) *Chaetoceros calcitrans* (b) *Cyclotella nana*, (c) *Chaetoceros* sp., (d) *Thalassiosira weissflogii*, (e) *Hyalodiscus* sp., (f) *Planktoniella sol*, (g) *Coscinodiscus 312*, and (h) *Coscinodiscus 1583*.

Table 4.2: Cell concentrations and dilution intervals associated with the semi-continuous culture technique used for the specific growth determinations. Cell concentrations were determined from cell counts. The average cell concentration refers to the concentration at which the cultures were typically diluted. Cell concentrations never exceeded the maximum cell concentration. Cultures were diluted by the dilution factor, e.g. a 2-fold dilution means the new culture was 1 part fresh media and 1 part transfered culture. The dilution interval refers to the time interval between dilutions.

Taxa	Average cell concentration cell/ml	Maximum cell concentration cell/ml	Average dilution factor	Average dilution interval days
Chaetoceros calcitrans	$1.2 \cdot 10^6$	$2 \cdot 10^6$	16-fold	3-4
Cyclotella nana	$3.4 \cdot 10^5$	$6.0 \cdot 10^5$	16-fold	4-5
Chaetoceros sp.	$3.0 \cdot 10^5$	$6.5 \cdot 10^5$	16-fold	5
Thalassiosira weissflogii	$3.0 \cdot 10^4$	$6.2 \cdot 10^4$	16-fold	5
Hyalodiscus sp.	$2.3 \cdot 10^4$	$3.4 \cdot 10^4$	2-fold	2-3
Planktoniella sol	800	1 400	2-fold	5-6
Coscinodiscus 312	500	650	2-3-fold	7-10
Coscinodiscus 1583	100	200	2-fold	7-10

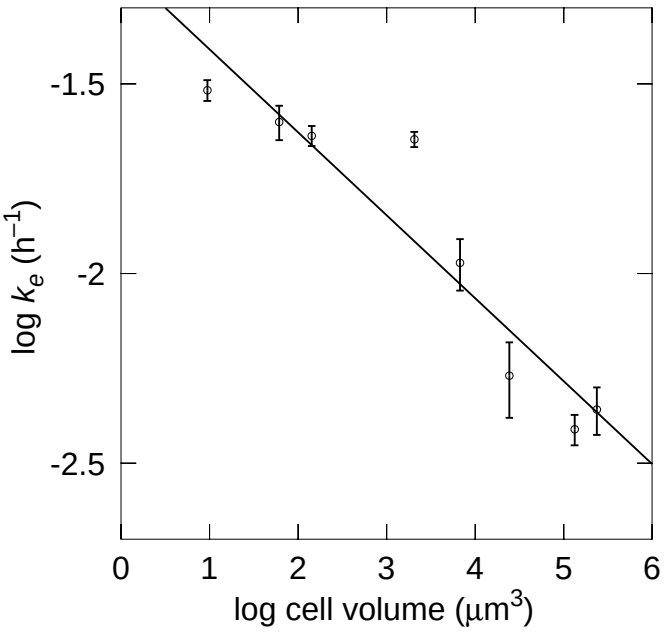

Figure 4.2: Size-dependence of growth.

account for the higher size scaling exponent associated with the present growth to volume relationship.

The exponent of the size-scaling relationship between k_e and cell size estimated from carbon content,

$$\log k_e = -0.230 \pm 0.034 \log C - 2.76 \pm 0.132, \tag{4.5}$$

is lower than the comparable k_e to V exponent. There is no statistical difference between the size scaling exponents for the growth to volume and the growth to cell carbon relationships. The present scaling exponents of diatom growth are in agreement with the values found for other algal taxa and other organisms in general (Schlesinger et al., 1981; Tang, 1995).

4.3.1.2 Efficiency of growth

The quantum yield of growth (ϕ_{k_e}) provides an estimate of the efficiency of light energy conversion into net carbon products. The quantum yield of growth has a 4.5-fold range, from 0.014 to 0.063, with an average value of 0.04 mole C/E (Table 4.1).

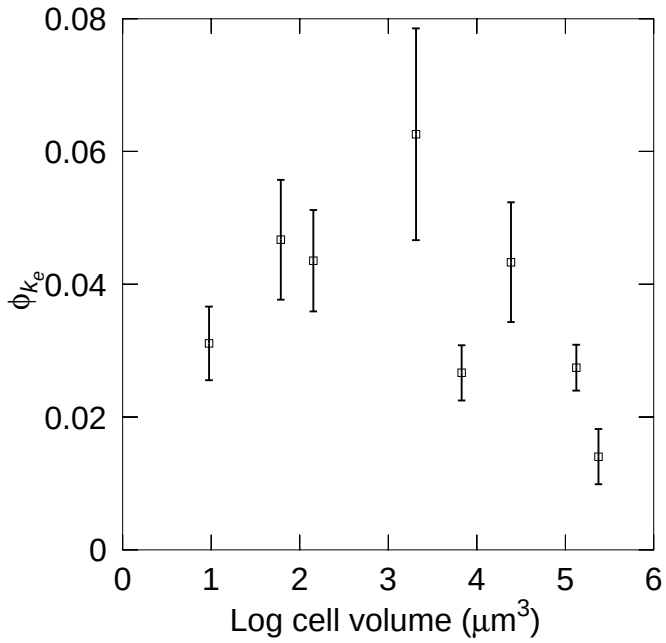

Figure 4.3: The quantum efficiency of growth as a function of the log of cell volume.

There is a curvilinear relationship between the logarithm of ϕ_{k_e} and cell volume, where cells with intermediate cell volumes have the highest growth efficiencies (Figure 4.3). The magnitude of the size scaling exponent associated with the ϕ_{k_e} to V relationship is in good agreement with the exponent associated with the quantum yield of carbon assimilation (ϕ_c) to V relationship. In a few cases ϕ_{k_e} was higher than ϕ_c. This is surprising since ϕ_{k_e} provides an estimate of the efficiency of light energy conversion into net biomass, and ϕ_c provides an estimate of light energy conversion into carbon.

Raven (1984) suggested that some of the energy collected from the initial and intermediate photochemical reactions of photosynthesis may go to biosynthetic requirements other than carbon fixation. The funneling of ATP and reductant to reactions other than carbon fixation will reduce the apparent quantum yield of carbon assimilation (ϕ_c), but this will eventually contribute to growth processes (Raven, 1984). Therefore the quantum yield of growth (ϕ_k) could in some cases be larger than the quantum yield of carbon fixation. The funneling of ATP and reductant from the quantum yield of carbon assimilation will increase the fraction of net compared to

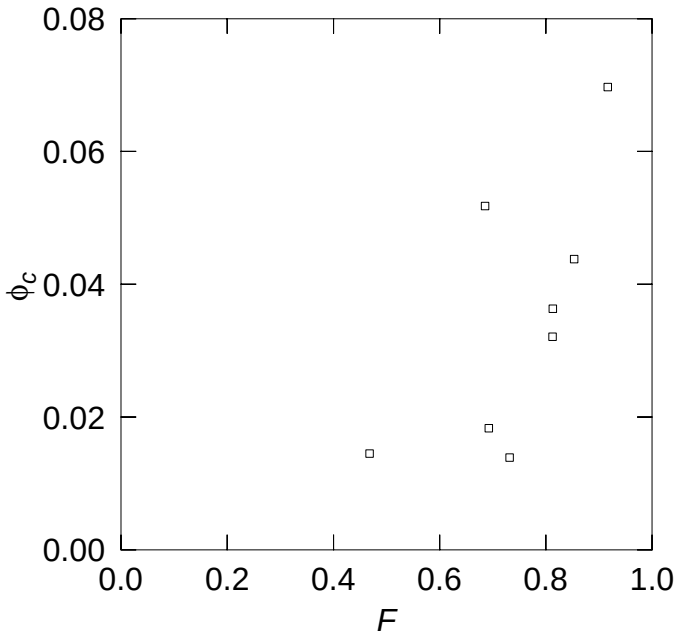

Figure 4.4: Quantum yield of carbon assimilation as a function of the ratio of net to gross photosynthetic rate. F was calculated using the PI derived estimate of carbon-specific respiration.

gross production (F). Banse (1976) defines the net growth efficiency (F) as:

$$F = \frac{k}{k + R^C + E^C}, \tag{4.6}$$

the fraction of gross photosynthate that is transformed into net growth. Figure 4.4 shows ϕ_c as a function of F, and demonstrates the correlation between ϕ_c and the fraction of gross photosynthesis which is incorporated into cellular material. Although the relationship between ϕ_c and F is not statistically significant, it appears that some of the larger cells, which convert less of their gross photosynthate to net growth, have lower apparent values of the quantum yield of carbon assimilation. The size-dependence of ϕ_c may be a result of the increased funneling of photoreductant to biosynthetic requirements, and not truly a reflection of a decrease in the quantum yield of photosynthesis.

Laws (1975) concluded that the size spectrum of phytoplankton cells in nature is controlled by the size-dependence of the net growth efficiency. Banse (1976) found

that net growth efficiency was independent of cell size, but did not include exudation as a loss term in the calculation. Net growth efficiency was calculated including exudation as a loss term in the equation. *Coscinodiscus 1583* had an extremely low value of F, suggesting that its growth rate may have been underestimated. When *Coscinodiscus 1583* is excluded from the analysis there is clearly no size-dependence in the net growth efficiency of the diatom clones, in agreement with Banse (1976) and Peters (1983). The hourly net growth efficiency ranges from 26 to 92% when the ^{14}C estimate of respiration is used in the calculation of F (Table 4.1).

The correlation between low values of F and low values of ϕ_c strongly suggest that the size-dependence of ϕ_c may be a result of the increased funneling of photoreductant to biosynthetic requirements, and not truly a reflection of a decrease in the quantum yield of photosynthesis. The size independence of k_e and ϕ_k, and perhaps ϕ_c confirm the conclusions of Kleiber (1961) and Peters (1983) that the efficiencies of metabolic processes are not size-dependent, and are not the cause of the size-dependence of metabolic rates. The metabolic requirements for a given amount of production is identical for small and large cells. It is the rate of production and the rate of metabolic requirments for the production that are size-dependent.

4.3.2 Correlation of growth to absorptive properties, and to anabolic and catabolic processes

4.3.2.1 Specific growth and absorptive properties

Eight diatom cultures were grown under identical conditions of light, temperature, and nutrients. Despite the similarity in environmental conditions, the specific growth rate varied by a factor of 24 (Table 4.1). The chlorophyll *a*- and carbon-specific absorption coefficients describe 75% and 65% of the variability in the growth rate of the diatoms cells, respectively (Figure 4.5). Large values of k_e are associated with high values of specific absorption because, for any one pigment concentration, large cells have lower values of specific absorption due to an increase in the package effect

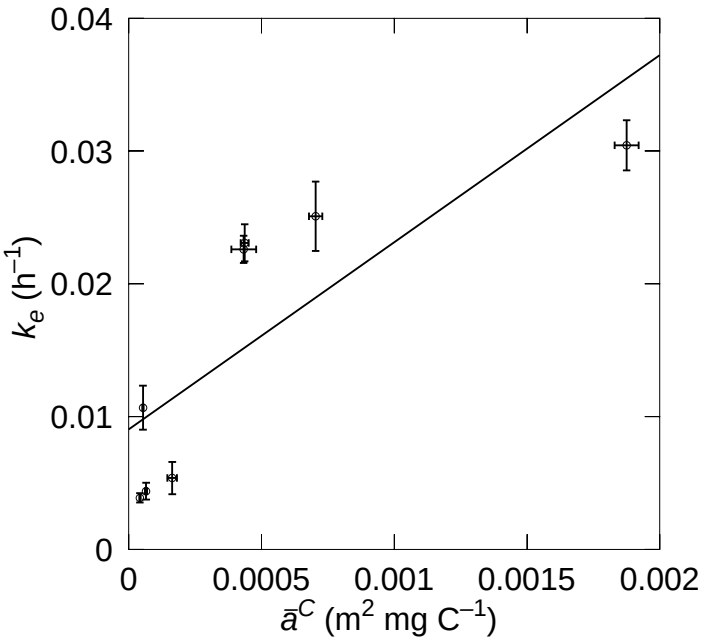

(a) Carbon-specific absorption

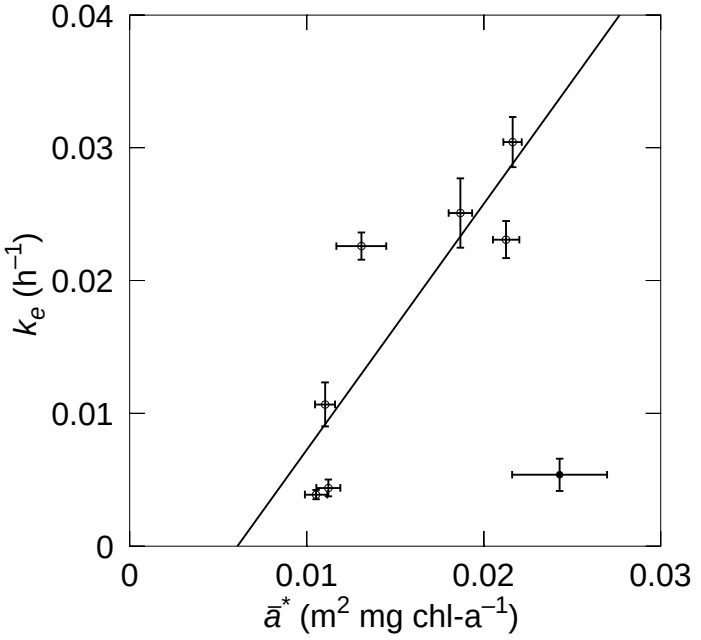

(b) Chlorophyll *a*-specific absorption

Figure 4.5: Growth rate as a function of the absorption coefficient. (b) *Planktoniella sol* was excluded from the regression analysis and is represented by a filled circle.

(Morel and Bricaud, 1981; Kirk, 1994). There is a higher energetic cost for light absorption in larger cells.

To offset the inefficiencies of the package effect, the diatom cells decrease their pigment concentration with increasing cell size (Agustí, 1991). As θ increases with cell volume, there is a lower concentration of photosynthetic pigment to support the anabolic requirements of the cell. This results in a decrease in the magnitude of anabolic processes relative to the catabolic as cell size increases. The associated decrease between intracellular pigment content and cell size appears to be related to an optimization of energy harvesting, suggesting that every cell size has an optimum pigment concentration to optimize light harvesting. The smaller cells tend to have higher, and the larger cells lower, intracellular pigment concentrations. Increases in intracellular pigment content are progressively less effective at harvesting light due to the package effect.

4.3.2.2 Relationship of growth and anabolic processes

There is 12-fold variability in the ratio of growth to photosynthetic rate (P_k^C). The variability in the k_e/P_k^C ratio appears to be related to cell volume (Figure 4.6). The growth rate of the smaller cells is several times smaller than P_k^C, the medium sized cells have a growth rate similar to P_k^C, and the largest cells have a growth rate that is much higher than P_k^C. The size-dependence of the k_e/P_k^C ratio suggests P_k^C may be closer to gross photosynthesis in the smaller cells and closer to net photosynthesis in the bigger cells.

C-14 measurements of photosynthesis with short incubation times are considered estimates of gross photosynthesis because there is less time for the radioisotope to come into equilibrium with the cell's internal carbon pool. As the incubation time increases, the radioisotope approaches equilibrium with the internal carbon pool of the cell, and the measurement approaches net photosynthesis (Banse, 1993). Since the smaller cells have a faster growth rate they should be closer to an equilibrium state than the larger cells. The opposite pattern was observed in this case. Li and

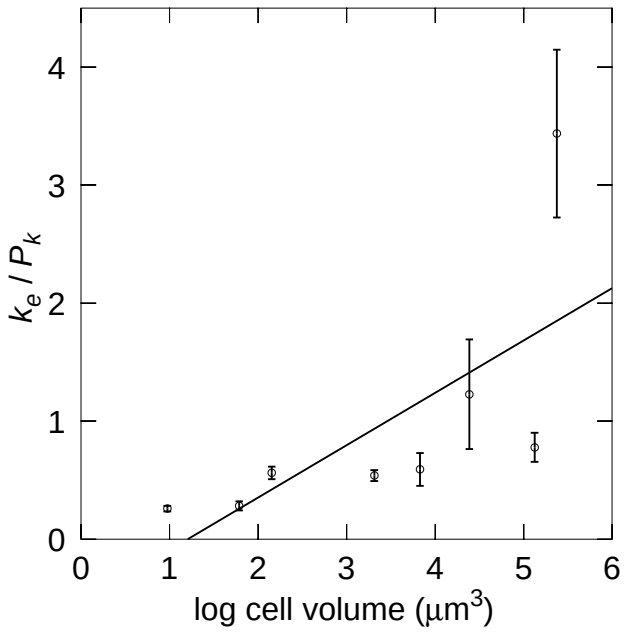

Figure 4.6: The growth rate to photosynthesis ratio as a function of volume.

Goldman (1981) found that the ^{14}C method can both underestimate and overestimate phytoplankton growth rates. They suggest that the ^{14}C method has serious weaknesses that need to be considered for further progress in the estimation of growth rates from ^{14}C estimates of photosynthesis. The results reported here support this observation.

4.3.2.3 Relationship of growth and catabolic processes

4.3.2.3.1 Growth and respiration

A linear relationship between respiration and growth has been demonstrated for a number of species (Laws and Caperon, 1976; Verity, 1982), where the growth rate of single clones were manipulated by nutrient supply or light availability, and corresponding respiratory rates were measured. Implicit in this work is the assumption that the change in environmental conditions will not alter the respiratory rate (Geider and Osborne, 1989). To test this assumption, the growth-respiration relationship was examined for a number of diatom species of different sizes grown under the same

environmental conditions.

The maintenance respiratory rate (r_0) and the growth-specific respiratory rate (r_k) can be determined from the growth-respiration relationship:

$$R_t = r_0 + kr_k, \tag{4.7}$$

where R_t is the total biomass-specific respiratory rate per hour, r_0 is the maintenance respiratory rate per hour, k is the growth rate per hour, and r_k is the respiratory cost associated with growth, which is dimensionless. The ${}^{14C}R^C$ and ${}^{O(14)}R^C$ rates were correlated with k (Table 4.1). The ^{14}C estimate of r_k was approximately 3-fold lower than the oxygen estimate, but considering the large standard errors, the two estimates are in agreement (Figure 4.7). Note that the ^{14}C estimates of respiration of by *Cyclotella nana* and *Thalassiosira weissflogii* and the oxygen estimate of respiration by *Planktoniella sol* were omitted from the data analysis due to their anomalously low or high respiratory rates. The anomalously low respiratory rates of *Cyclotella nana* and *Thalassiosira weissflogii* are discussed in Chapter 3, *Planktoniella sol* had a respiratory rate more than two-fold higher than cells with similar growth rates. The diatoms have an average r_k of 0.061 and 0.108 for the ^{14}C and oxygen electrode estimate of respiration, respectively. The oxygen electrode estimate of r_k is in agreement with the average (0.20 ± 0.08) calculated by Langdon (1988).

Langdon (1993) suggests that for modeling primary production, the photosynthesis-respiration relationship is more useful than the growth-respiration relationship. The photosynthesis-respiration relationship is more strongly correlated than the comparable growth-respiration relationship (Figure 4.8). This may be because growth can be rate-limited by the supply of reductant and carbon skeletons provided by respiratory processes. Deviations of the growth-respiration relationship from linearity could be due to input of reductant and other cofactors from the light reactions (Geider and Osborne, 1989). Another way to examine the relationship of respiration to photosynthesis is to examine the ratio of respiration to photosynthesis. The ^{14}C estimate of P_k/r_k is 0.019 ± 0.001, and the oxygen estimate is 0.054 ± 0.049, more than two times higher than the ^{14}C estimate. The oxygen estimate of P_k/r_k is in

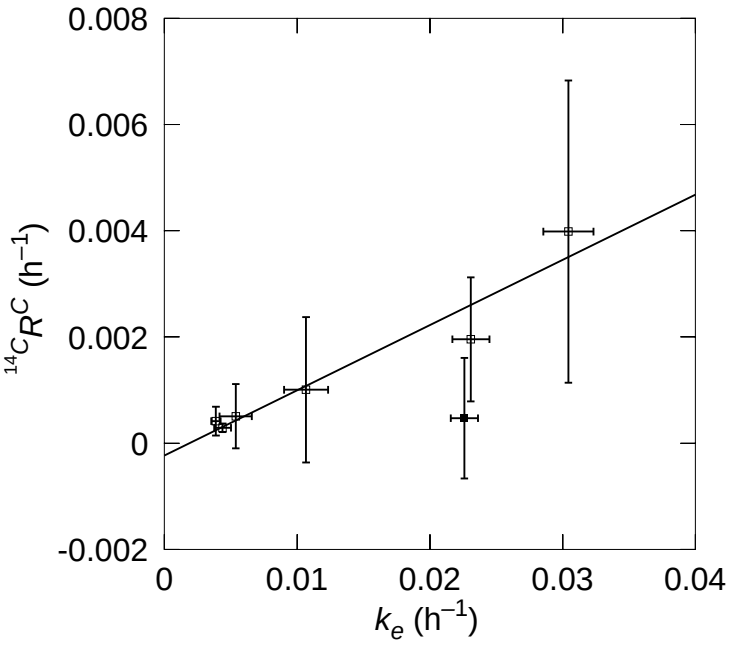

(a) Respiration estimated from ^{14}C

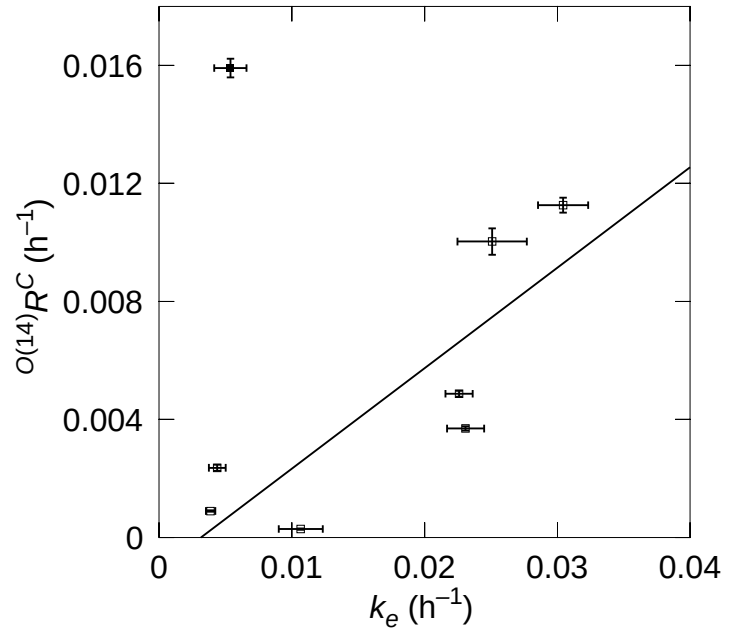

(b) Respiration estimated from oxygen.

Figure 4.7: Respiration as a function of growth rate.

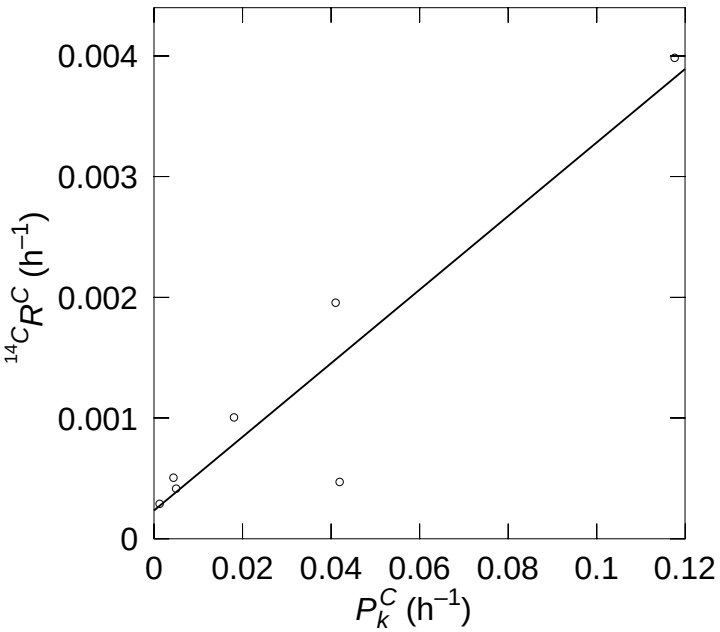

(a) Respiration estimated from ^{14}C

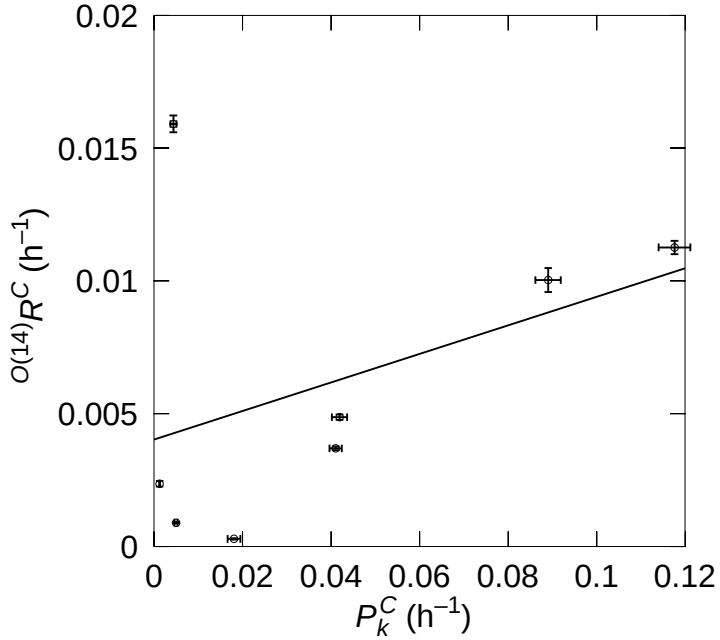

(b) Respiration estimated from oxygen.

Figure 4.8: Respiration as a function of photosynthesis.

excellent agreement with values reported in the literature (Langdon, 1988). Oxygen estimates of respiration are generally considered better estimates of diatom respiratory loss than ^{14}C estimates because they are direct measurements of respiration and are not clouded by issues of isotopic equilibrium.

The maintenance metabolic rate was estimated using equation 4.1, but can also be estimated as the respiratory rate associated with long-term incubations in the dark (Geider and Osborne, 1989; Geider, 1992). The maintenance metabolic rate was calculated from two types of respiratory estimates, respiration derived from the short term extrapolation of the PI curve to zero irradiance, and a long term estimate of oxygen consumption using oxygen electrodes. When these respiratory rates were regressed against the corresponding growth rate, two different maintenance metabolic rates were derived. The ^{14}C estimate of r_0 is many times lower than the oxygen estimate of respiration. The error in the two measurements is approximately as big as, or bigger than r_0, but the two methods are in agreement when the standard errors are considered (Table 4.2). On average, the diatoms have a maintenance metabolic rate of between -0.00023 ± 0.00027 and 0.0011 ± 0.0019 h^{-1} for the ^{14}C and oxygen electrode estimates, respectively. The oxygen estimate of r_0 is in excellent agreement with the average r_0 (0.003 ± 0.001) calculated by Langdon (1993) in a literature review of algal respiratory rates.

In summary, ^{14}C estimates of r_0, r_k, and the ratio of r_k/P_k are lower than oxygen electrode estimates. On average, total respiratory costs represent between four to twenty percent of growth using the ${}^{14C}R^C$ and ${}^{O(14)}R^C$ estimates, respectively. In general the ${}^{14C}R^C$ is considered an underestimate of respiratory loss, especially for short incubation times. Therefore, ${}^{O(14)}R^C$, which accounts for approximately 20% of growth, is considered a better estimate of true respiratory loss.

The respiratory rates associated with biosynthetic activities, r_k, and the maintenance of cellular integrity, r_0, are in agreement with literature values. Within the large error associated with the respiratory parameters derived from the respiration-growth relationship, different species with different intrinsic growth rates grown under

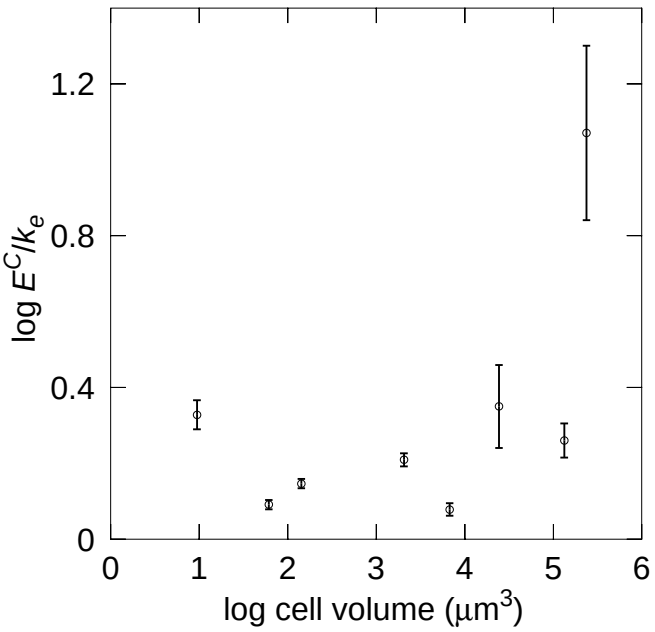

Figure 4.9: Carbon-specific exudation to growth ratio as a function of log cell volume.

the same environmental conditions have similar biosynthetic and maintenance respiratory costs compared with the parameters from the respiration-growth relationship derived from the same clone grown under a gradient of environmental conditions.

4.3.2.3.2 Growth and exudation

The relationship between the carbon-specific rates of exudation and the specific growth rate is not statistically significant. The carbon-specific rate of exudation was examined as a function of the specific growth rate. There was an over 12-fold variation in the E^C/k ratio. The relationship between the E^C/k ratio and V is not statistically significant, only 27% of the variation in the E^C/k ratio can be attributed to cell size (Figure 4.9). The weak correlation between E^C and k_e, and the lack of statistical significance for the growth-exudation relationship indicates it would be difficult to predict exudation from the specific growth rate.

4.3.3 Growth as a function of anabolic and catabolic processes – a cautionary note

Estimates of net and gross photosynthesis were calculated in an attempt to reconcile estimates of net photosynthesis and growth. Specific growth, as calculated from cell counts over time, was considered to be an estimate of net photosynthesis. As a first approximation, photosynthesis at the growth irradiance, P_k^C, was used as an estimate of gross photosynthesis. There is a size-dependent trend between P_k^C and k_e. Gross photosynthetic rate is 3-4-fold higher than growth rate for the 2 smallest clones, 70-85% higher for the three intermediate sized diatoms, and 28% higher to 70% lower for the 3 largest clones. The data clearly demonstrate that the photosynthetic rates derived from the PI curve cannot be considered a simple reflection of either gross or net photosynthetic rates.

Net photosynthetic rate was calculated from the balanced growth equation:

$$P_n = P_g^C - R^C - E^C, \tag{4.8}$$

where P_n is the difference between P_g^C and the sum of the carbon-specific respiratory and exudatory rates. The net photosynthetic rate was compared to the measured growth rate (Figure 4.10). Two different respiratory rates were used to calculate two different net photosynthetic rates, ${}^{14_C R}P_n$ and ${}^{O(14)R}P_n$. The net photosynthetic rates calculated with ${}^{O(14)}R^C$ were lower than the comparable photosynthetic rates calculated using ${}^{14C}R^C$. There was a positive and statistically significant ($p < 0.05$) correlation between both estimates of net photosynthesis and the measured growth rate. Net photosynthesis overestimated k_e for the small cells, was in good agreement for the medium sized cells, and underestimated k_e for the largest cells.

If the photosynthetic rate derived from the PI curve is not gross photosynthesis but somewhere between net and gross photosynthesis, it is impossible to derive a good estimate of net photosynthetic gain. Subtraction of respiration and exudation from the photosynthetic estimate will tend to underestimate net photosynthesis in the larger cells but overestimate net photosynthesis in the smaller cells. The over-estimation of

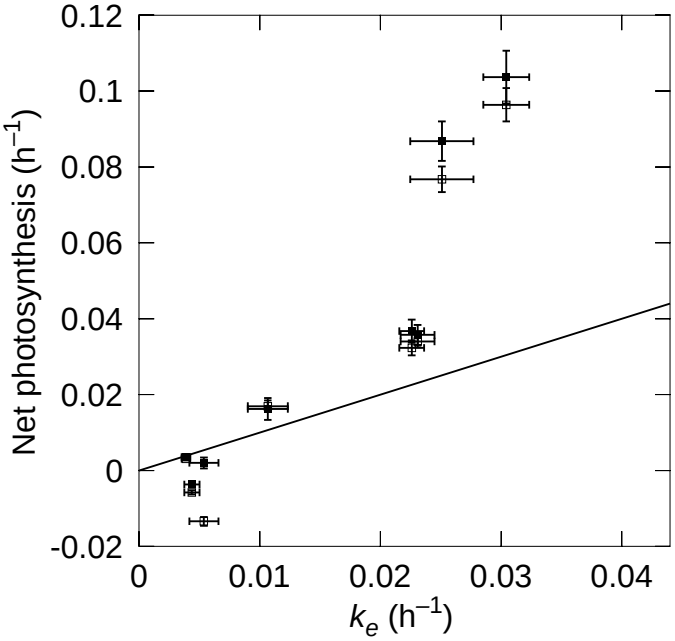

Figure 4.10: The comparison of the measured growth rate to calculated rates of net photosynthsis. The open boxes represent P_n calculated using ${}^{O(14)}R$, and the filled boxes represent P_n calculated using ${}^{14C}R$. The line represents a 1:1 relationship between the x and y variables.

k_e from photosynthetic measurements could be due to an underestimation of catabolic losses or inappropriate comparisons of measurements made on different time-scales.

Photosynthesis and absorption were measured over seconds to hours, respiration and excretion were measured over hours to days, and growth rate was measured over days to weeks. The different time scales of measurement may have an important impact on the relevance of these rates to one another. Extrapolation of measurements beyond the time period of measurement is speculative. Growth rate and exudation measurements were made *in situ* (cultures were in incubated in the growth chamber), while photosynthetic and respiratory estimates were made *in vitro*. Stress associated with experimental manipulations may have caused increases in some metabolic rates and decreases in others. Li and Goldman (1981) suggest that some species are sensitive to physical manipulation and may experience physiological stress that may affect photosynthetic ^{14}C uptake. In addition, respiration was measured in the dark, but growth, photosynthesis, and exudation were measured in the light. It is possible that respiration in the light was much higher than in the dark and may account for the discrepancy between the calculated rates of net photosynthesis and measured rates of growth.

4.4 Summary – Size as a scaling factor in phytoplankton growth

There is some suggestion in the literature that the size-dependence of diatom growth is weaker than in other organisms (Banse, 1976; Blasco et al., 1982). In addition, other workers have suggested that environmental conditions may modify the size-dependence of algal growth (Peters, 1983; Sommer, 1989). A recent literature review has examined the size-dependence of growth under light-saturating conditions (Tang, 1995). Diatom growth was examined under light-limiting conditions to complement these and other previous studies.

The specific growth rate of the eight diatom clones has a statistically significant relationship with both cell carbon and cell volume. The use of C or V as representations of cell size did not make a significant difference to the size scaling exponent of the growth to cell size relationship because the exponent of the relationship of C to V was close to one (Figure 2.3). As the relationship between the two representations of biomass, C and V, changes, the representation of cell size becomes more important. The size-scaling exponent of diatom growth in this case adheres to the 3/4 allometric rule. This indicates that the size-dependence of growth can be an important source of variation in diatom growth rates.

Growth rates are extremely hard to measure in nature (Cullen, 1990). However, Equation 4.1 suggests that growth can be estimated from measurements of P_k^C. Therefore, if we understand the relationship of P_g^C, R^C and E^C to P_k^C, we should be able to estimate growth rates. The interaction of the absorptive properties, photosynthetic parameters, and the catabolic rates of respiration and exudation were examined in the context of growth to determine if there was any strong correlation to permit the estimation of growth from absorptive properties, and anabolic and catabolic processes.

The carbon- and chlorophyll a-specific absorption coefficients, P_k, $\alpha^C$and R^C are

Table 4.3: Regression coefficients associated with relationships discussed in Chapter 4.

Equation	n	Intercept	se	Slope	se	r^2
$\log k_e$ - $\log V$	8	-1.19	$1.19 \cdot 10^{-1}$	-0.219	$3.24 \cdot 10^{-2}$	0.88
$\log k_e$ - $\log C$	8	-2.76	$1.32 \cdot 10^{-1}$	-0.230	$3.40 \cdot 10^{-2}$	0.88
k_e - a^C	8	$9.00 \cdot 10^{-3}$	$2.13 \cdot 10^{-3}$	14.090	$2.99 \cdot 10^{0}$	0.65
k_e - a^*	7	$-1.13 \cdot 10^{-2}$	$5.40 \cdot 10^{-3}$	1.854	$3.40 \cdot 10^{-1}$	0.75
k_e vs P_k^C	7	$6.66 \cdot 10^{-2}$	$1.63 \cdot 10^{-3}$	0.229	$2.91 \cdot 10^{-2}$	0.85
k_e/P_k^C - $\log V$	7	$-5.34 \cdot 10^{-1}$	$5.09 \cdot 10^{-1}$	0.443	$1.38 \cdot 10^{-1}$	0.46
${}^{14C}R^C$ - k_e	6	$-2.30 \cdot 10^{-4}$	$1.91 \cdot 10^{-4}$	0.123	$1.18 \cdot 10^{-2}$	0.93
${}^{O(14)}R^C$ - k_e	7	$-1.07 \cdot 10^{-3}$	$1.37 \cdot 10^{-3}$	0.341	$6.90 \cdot 10^{-2}$	0.71
${}^{14C}P^C$ - k_e	7	$2.35 \cdot 10^{-4}$	$2.64 \cdot 10^{-4}$	0.031	$5.26 \cdot 10^{-3}$	0.87
${}^{O(14)}P^C$ - k_e	8	$4.03 \cdot 10^{-3}$	$2.75 \cdot 10^{-3}$	0.054	$4.86 \cdot 10^{-2}$	0.17
$\log E_k^C$ - $\log V$	8	$-3.37 \cdot 10^{-2}$	$1.82 \cdot 10^{-1}$	0.104	$4.92 \cdot 10^{-2}$	0.27

all significantly related to the growth rate. Of all the parameters, P_k and the absorptive properties are among the most highly correlated with k_e (Table 4.3). In contrast, the carbon-specific rates of E are not significantly related to the growth rate of the diatoms cells. The relationship of the absorptive properties and anabolic and catabolic rates of the marine diatom clones tends to be better with cell volume than growth, indicating that the size scaling of metabolic rates is a useful model in diatom physiological ecology.

The respiratory parameters r_k and r_0 were derived from the respiration-growth relationship. The respiratory rates associated with biosynthetic processes (r_k) and maintenance respiratory requirements (r_0) are in good agreement with literature values. This suggests that the manipulation of growth rate by light or nutrient limitation does not produce significantly different respiratory rates from those derived from different species grown under the same environmental conditions.

According to equation 4.1 if we know R^C, E^C and P_g^C, growth can be calculated. Calculations of growth from equation 4.1 were compared with measurements

of growth. The ^{14}C estimate of P_k both underestimated and overestimated phytoplankton growth rates. Growth was overestimated for the small cells, approximately correct for the medium sized cells, and underestimated for the large cells. These results suggest that the ^{14}C method has serious weaknesses that need to be addressed before growth rates can be determined from ^{14}C estimates of photosynthesis. Problems associated with stress from the experimental manipulations and with the different time scales associated with the different metabolic rate measurements may have contributed to the discrepancies between the calculated and measured rates of diatom growth.

Chapter 5

Conclusions – The size-dependence of diatom metabolism

5.1 Introduction

According to Kleiber (1961), the size-dependence of metabolic rates for heterotrophs has been recognized for well over a century. Metabolic rates for many organisms can be related to body mass by a power function with a common exponent of 3/4 (Kleiber, 1961; Peters, 1983). Diatoms cells cover an extremely large size range, with diameters from several microns to over a millimeter, suggesting they would be particularly well-suited for the prediction of metabolic rates from cell size. If cell size is a significant factor contributing to variation in the measured metabolic rates of diatoms, ignoring the role of cell size could make it difficult to resolve patterns in metabolic rates with other biological and environmental covariables.

There is still controversy over the causative factors behind the size-dependence of metabolic rates (Kleiber, 1961; Peters, 1983). Kleiber (1961) suggests several hypotheses for the size-dependence of metabolic rates, all involving morphological features and physiological processes unavailable to unicellular photoautotrophs. Such

hypotheses cannot account for the size-dependence of metabolic rates in phytoplankton. In contrast, the size-dependence of light absorption due to the increased intracellular shading of photosynthetic pigments may play an important role in the size-dependence of phytoplankton metabolic rates (Kirk, 1994). If the processes underlying size-dependence in heterotrophs also occur in autotrophs, the size-dependence of phytoplankton photosynthetic processes and growth may differ from those of heterotrophs, given the additional size-dependence of light absorption. Therefore, the theories and the equations describing allometric relationships in animals are not sufficient to describe the size-dependence of anabolic processes in algae. The interaction between the size-dependence of light absorption and the size-dependence of the metabolic parameters in the balanced growth equation has not been previously examined, despite some reports of anomalous size scaling exponents associated with the metabolic rates of some algae (Banse, 1976; Taguchi, 1976; Blasco et al., 1982; Lewis, 1989; Tang and Peters, 1995).

The present study provides information on cell size and light limited metabolic rates for 8 species of marine centric diatoms: *Chaetoceros calcitrans*, *Cyclotella nana*, *Chaetoceros* sp., *Thalassiosira weissflogii* (Grunow), *Hyalodiscus* sp., *Planktoniella sol*, *Coscinodiscus* sp. (CCMP312) and *Coscinodiscus* sp. (CCMP1583). This study provides novel information on the metabolic rates and their dependence on size for these organisms. There are reviews on the size-dependence of algal absorption (Agustí, 1991), photosynthesis (Banse, 1976), respiration (Tang and Peters, 1995), and growth (Tang, 1995). Anomalous size scaling exponents have been reported for the metabolic rates of algae, and diatoms in particular (Banse, 1976; Taguchi, 1976; Blasco et al., 1982; Lewis, 1989). Although previous studies have examined the size-dependence of absorption, photosynthesis, respiration and growth of phytoplankton, never have all these parameters been measured for a single set of phyletically-related phytoplankton under the same environmental conditions. In addition, physiological parameters, light absorption and quantum yield were quantified. The size-dependence

of light absorption and the affect of light absorption on the quantum yield of photosynthesis and growth provides the information required to propose a mechanism for the anomalous size-scaling of metabolic processes in unicellular algae. In this study, the error associated with pooling different data sets was avoided. All the metabolic rates were measured under the same set of conditions. Unlike the field study of Sommer (1989), and the reviews of Tang (1995) and Tang and Peters (1995), this study was conducted under high nutrient, low light conditions, providing an evaluation of the size-dependence of all the metabolic variables in the balanced growth equation under conditions that limit growth.

5.2 Summary

5.2.1 Photosynthetic parameters

Taguchi (1976) found that photosynthetic capacity had a size scaling exponent less than $-1/4$. In Chapter 2, it was shown that $P^{\mathrm{C}}_{\mathrm{max}}$ and P^{C}_{k} decreased with increasing cell size with size scaling exponents less than $-1/4$. The results are in good agreement with the work of Taguchi (1976), indicating that the highly negative size scaling exponent of $P^{\mathrm{C}}_{\mathrm{max}}$ and P^{C}_{k} is a general physiological characteristic of marine diatoms.

A number of photosynthetic parameters were examined that, unlike P_{max} and P_k, are not metabolic rates. Carbon-specific photosynthetic efficiency, like photosynthetic capacity, had a size scaling exponent somewhat lower than expected by the 3/4 allometric rule. In conjunction with the absorption coefficient, photosynthetic efficiency was used to examine the size-dependence of the quantum yield of photosynthesis. There is no previous laboratory study indicating size-dependence in the quantum yield of ϕ_c or ϕ_D. This study found a negative, statistically significant size scaling exponent for the ϕ_c to cell volume relationship of -0.141 ± 0.021. In contrast, ϕ_D demonstrated no size-dependent properties. The lack of size-dependence in ϕ_D indicates the size-dependence of ϕ_c is linked to biochemical reactions that occur after photophosphorylation, and correlation of ϕ_c with the net growth efficiency suggests

that the size-dependence of ϕ_c may be an artifact of the ^{14}C method.

The size scaling exponents associated with all the biomass normalized photosynthetic parameters deviate from the commonly reported size scaling exponent reported for heterotrophic organisms. In Chapter 1 it was suggested that the size scaling exponents established for the metabolic rates of heterotrophic organisms may not apply to unicellular algae due to the additional size-dependence of light absorption. The chlorophyll *a* and carbon-specific absorption coefficients were correlated with cell volume. The size scaling exponents of the photosynthetic parameters and absorptive properties were generally lower than 3/4. This supports the assertion that the size-dependence of anabolic processes in photosynthetic unicells will differ from the size-dependence of metabolic rates in heterotrophs. Although the size scaling exponents often differ from 3/4, the anabolic rates and absorptive properties measured have a robust relationship with cell size, indicating that the allometric power law is a good model for the quantitative prediction of photosynthesis, but that the 3/4 rule does not adequately describe the size-dependence of photosynthetic rates.

5.2.2 Respiration

The rate of respiration represents the summed energy expenditure for all the metabolic processes occurring in the cell (Peters, 1983). A recent review by Tang (1995) with 178 compiled observations of respiratory rate and cell size concluded that the size scaling exponent of algal respiratory rate was statistically different from 3/4. In Chapter 3, the size-dependence of respiratory loss was re-examined using two different methods to determine respiratory rates. The carbon-specific respiratory rates are size-dependent with size scaling exponents of -0.242 ± 0.056 and -0.194 ± 0.137, for the ^{14}C and oxygen estimate of respiration, respectively. In contrast, there is no relationship between the chlorophyll *a*-specific respiratory rates and cell size, which agrees with previously reported results (Eppley and Sloan, 1965). When the magnitude of the errors was considered, the size scaling exponents found for the carbon-specific oxygen estimate of respiration in this study were in agreement with that found by Tang

and Peters (1995) and the 3/4 rule. This indicates that more data is required to conclude that respiratory rates associated with light limited growth deviate from the 3/4 allometric rule.

5.2.3 Exudation

Exudation of dissolved organic carbon represents a loss of organic carbon from the phytoplankton cell. Carbon-specific rates of exudation tend to be larger for larger cells, but the exponent for the E^C to V relationship, -0.126 ± 0.082, is not significantly different from zero. In contrast, the exponent for the E^{chl} to V relationship is positive and statistically significant. No other chlorophyll *a*-specific metabolic rate measured in this study had a statistically significant positive size scaling exponent with cell size. In Chapter 3, it was suggested that the mechanisms controlling exudation may be different from those controlling photosynthetic or respiratory processes. Data in the literature indicate that there is strong species-specific variation in the exudation of dissolved organic carbon (Sakshaug, 1993). More data are required to substantiate any conclusion of definitive size-dependence in the exudation of dissolved organic carbon in marine diatoms.

5.2.4 Growth

In Chapter 4, the size-dependence of diatom growth under light-limiting conditions was examined to evaluate the size scaling exponent of a single phyletic group under growth-limiting conditions. The specific growth rate of the diatom clones have a slope of -0.22 ± 0.03 and -0.23 ± 0.03 for the k to V and the k to C relationships, respectively. Both slopes are in agreement with slopes found by a number of other workers (Banse, 1976; Schlesinger et al., 1981; Langdon, 1988), and are similar to that expected from the usual metabolic exponent of 3/4. This study found that size scaling exponent associated with light limited growth rates is indistinguishable from $-1/4$, and confirmed that the growth efficiency of diatoms is not size-dependent. In addition, the data indicate that the calculation of diatom growth from the variables in

the balanced growth equation can under- and over-estimate the measured growth rate. Variables measured at different time scales, and sensitivity to physical manipulation may have contributed to the discrepancies between the two estimates of growth. Other forms of environmental modification of the growth rate were not examined. Further work is required to determine the effect of other environmental factors on the size-dependence of phytoplankton growth.

5.3 Concluding remarks and recommendations for future work

Large and small cells often coexist in the aquatic environment, yet the negative size scaling exponent associated with the biomass specific metabolic rates indicates that small cells would tend to out-compete larger cells. This is because many relevant biological and environmental factors are not considered in the allometric model. Vertical mixing, sinking rates, boundary layers, luxury consumption, and non-scalable components will all have considerable impact on the metabolic rates of large and small cells in nature. More research is required to examine the relative advantages and disadvantages of large and small size in a variety of environmental conditions.

This study confirms that the allometric power law is a good model for the predication of diatom light limited metabolic processes. However, the 3/4 rule does not adequately describe the size-dependence of light limited anabolic rates. The size-dependence of light absorption provides a mechanism to describe the anomalous size scaling exponents associated with light limited diatom photosynthesis. If the allometric model is to be used to predict growth rates and primary production in aquatic ecosystems more work is required to quantify the effect of different environmental conditions on different taxonomic groups of phytoplankton.

Appendix A

Description of diatom clones

Table A.1: Detailed taxanomic information about each diatom clone.

Taxa:	*Chaetoceros calcitrans*	*Cyclotella nana*	*Chaetoceros* sp.	*Thalassiosira weissflogii*	*Hyalodiscus* sp.	*Planktoniella sol*	*Coscinodiscus 312*	*Coscinodiscus 1583*
Strain Number:	CCMP1315	CCMP1335	n/a	CCMP1336	CCMP1679	CCMP1608	CCMP312	CCMP1583
Name Authority:	Paulsen	(Hustedt) Hasle et Heimdal		(Grunow) Fryxell et Hasle			Ehr. 1839	
Identified by:							Medlin, L	Hargraves, P
Collected by:	Umebayashi, O	Guillard, R	Martin, J	Guillard, R	Hill, DRA	Goldman, J	Sakin-Jacoff	Adnan, Q via Anderson, DM
Collection Year:	1960	1958		1956			1973	1992
Collection Site:		Moriches Bay, Forge River, Long Island, NY		Gardiners Island, Long Island, NY		Sargasso Sea	Baja California, Mexico	Jakarta Harbor, Indonesia
Ocean:		North Atlantic	North Atlantic	North Atlantic		North Atlantic	North Pacific	South Pacific
Sea:				Long Island Sound		Sargasso Sea		Java Sea
Other Information:	from a culture of Porphyra							
Isolated by:	Umebayashi, O	Guilllard, R		Guillard, R	Andersen, RA		Sakin-Jacoff	Hargraves, P
Deposited by:	Booth, B	Guillard, R		Guillard, R	Hill, DRA	Hargraves, P		Hargraves, P
Deposit Date:	17-Feb-83	8-Sep-58			29-Apr-95	1-Apr-93		1-Apr-93
Culture medium:	f/2:AlgaGro	f/2:WC, Aquil, AlgaGro, ASM4	f/2	f/2:Aquil, AlgaGro	f/2:	f/2:K+si	f/2:	f/2
Low Temperature:	17°C	4°C	10°C	11°C	17°C	17°C	11°C	17°C
High Temperature:	26°C	25°C	20°C	22°C	22°C	22°C	16°C	22°C
Cell length:	3–7μm	4–6μm	9μm	12–22μm	8–10μm	8–10μm	50–115μm	60–85μm
Cell width:	3–5μm	4–5μm	4.5μm	10–12μm	14–18μm	45–50μm	40–45μm	60–85μm
Strain Synonyms:	CCAL, NEPCC590	3H:NEPCC58		ACTIN		42G	C38B	JA92Z
Name Synonyms:		*Thalassiosira pseudonna*		*Thalassiosira fluviatilis* Hustedt				
Axenic:	Yes	Yes	No	Yes	No	No	No	No

Bibliography

Agustí, S. (1991) Allometric scaling of light absorption and scattering by phytoplankton cells. *Canadian Journal of Fisheries and Aquatic Sciences*, **48**: 763–767.

Amon, R. M. W. and R. Benner (1996) Bacterial utilization of different size classes of organic matter. *Limnology and Oceanography*, **41**(1): 41–51.

Banse, K. (1976) Rates of growth, respiration and photosynthesis of unicellular algae as related to cell size – A review. *Journal of Phycology*, **12**: 135–140.

Banse, K. (1982) Cell volumes, maximal growth rates of unicellular algae and ciliates, and the role of ciliates in the marine pelagial. *Limnology and Oceanography*, **27**(6): 1059–1071.

Banse, K. (1993) On the dark bottle in the ^{14}C method for measuring marine phytoplankton production. *International Council for the Exploration of the Sea. Marine Science Symposia*, **197**: 132–140.

Blasco, D., T. T. Packard, and P. C. Garfield (1982) Size dependence of growth rate, respiratory electron transport system activity, and chemical composition in marine diatoms in the laboratory. *Journal of Phycology*, **18**: 58–63.

Chan, A. T. (1980) Comparative physiological study of marine diatoms and dinoflagellates in relation to irradiance and cell size. II. Relationship between photosynthesis, growth, and carbon/chlorophyll *a* ratio. *Journal of Phycology*, **16**: 428–432.

Chen, W. and P. J. Wangersky (1996) Production of dissolved organic carbon in phytoplankton cultures as measured by high-temperature catalytic oxidation and ultraviolet photo-oxidation methods. *Journal of Plankton Research*, **18**(7): 1201–1211.

Chisholm, S. W. (1992) Phytoplankton size. In P. G. Falkowski and A. D. Woodhead, editors, *Primary productivity and Biogeochemical cycles in the sea*, pp. 213–237. Plenum Press.

Cleveland, J. S. and A. D. Weidemann (1993) Quantifying absorption by aquatic particles: A multiple scattering correction for glass-fiber filters. *Limnology and Oceanography*, **38**(6): 1321–1327.

Côté, B. and T. Platt (1983) Day-to-day variations in the spring-summer photosynthetic parameters of coastal marine phytoplankton. *Limnology and Oceanography*, **28**(2): 320–344.

Cullen, J. J. (1990) On models of growth and photosynthesis in phytoplankton. *Deep-Sea Research 1*, **37**(4): 667–683.

Cullen, J. J., X. Yang, and H. L. MacIntyre (1992) Nutrient limitation of marine photosynthesis. In P. G. Falkowski and A. D. Woodhead, editors, *Primary Productivity and Biogeochemical Cycles in the Sea*, pp. 69–88. Plenum Press.

Davison, I. R. (1991) Environmental effects on algal photosynthesis: temperature. *Journal of Phycology*, **27**: 2–8.

Dubinsky, Z., P. G. Falkowski, and K. Wyman (1986) Light harvesting and utilization by phytoplankton. *Plant Cell Physiology*, **27**: 1335–1349.

Duysens, L. N. M. (1956) The flattening of the absorption spectrum of suspensions, as compared to that of solutions. *Biochimica et Biophysica Acta*, **19**: 1–12.

Eppley, R. W. and P. R. Sloan (1966) Growth rates of marine phytoplankton: correlation with light absorption by cell chlorophyll *a*. *Physiologia Plantarum*, **19**: 47–59.

Eppley, R.W. and P.R. Sloan (1965) Carbon balance experiments with marine phytoplankton. *Journal of the Fisheries Research Board of Canada*, **22**(4): 1083–1097.

Falkowski, P. G. and J. LaRoche (1991) Acclimation to spectral irradiance in algae. *Journal of Phycology*, **27**: 8–14.

Fenchel, T. (1974) Intrinsic rate of natural increase: the relationship with body size. *Oecologia (Berl.)*, **14**: 317–326.

Fogg, G. E. (1977) Excretion of organic matter by phytoplankton. *Limnology and Oceanography*, **22**: 576–577.

Geider, R. J. (1992) Respiration: Taxation without representation? In P. G. Falkowski and A. D. Woodhead, editors, *Primary Productivity and Biogeochemical Cycles in the Sea*, pp. 333–360. Plenum Peess.

Geider, R. J. and B. A. Osborne (1989) Respiration and microalgal growth: a review of the quantitative relationship between dark respiration and growth. *New Phytologist*, **112**: 327–341.

Geider, R. J. and B. A. Osborne (1992) *Algal photosynthesis*. Chapman and Hall.

Geider, R. J., T. Platt, and J. A. Raven (1986) Size dependence of growth and photosynthesis in diatoms: A synthesis. *Marine Ecology Progress Series*, **30**: 93–104.

Gerath, M.W. and S.W. Chisholm (1989) Change in photosynthetic capacity over the cell cycle in light/dark cycle is due solely to the photocycle. *Plant Physiology*, **91**: 999–1005.

Goldman, J.C., J.J. McCarthy, and D.G. Peavey (1979) Growth rate influence on the chemical composition of phytoplankton in oceanic waters. *Nature*, **279**: 210–215.

Greene, R. M., Z. S. Kolber, D. G. Swift, N. W. Tindale, and P. G. Falkowski (1994) Physiological limitation of phytoplankton photosynthesis in the eastern equatorial Pacific determined from variability in the quantum yield of fluorescence. *Limnology and Oceanography*, **39**(5): 1061–1074.

Guillard, R. R. L. and J. H. Ryther (1962) Studies of marine planktonic diatoms. I. *Cyclotella nana* Hustedt and *Detonula confervacea* Cleve. *Canadian Journal of Microbiology*, **8**: 229–239.

Guillard, R.R.L. (1973) Division rates. In J.R. Stein, editor, *Handbook of phycological methods: culture methods and growth measurements*, pp. 289–312. Cambridge University Press.

Head, E. J. H. and E. P. W. Horne (1993) Pigment transformation and vertical flux in an area of convergence in the North Atlantic. *Deep-Sea Research II*, **40**: 329–346.

Hellebust, J. A. (1965) Excretion of some organic compounds by marine phytoplankton. *Limnology and Oceanography*, **10**(2): 192–206.

Hoepffner, N. and S. Sathyendranath (1993) Determination of the major groups of phytoplankton pigments from the absorption spectra of total particulate matter. *Journal of Geophysical Research*, **98**(C12): 22,789–22,803.

Holm-Hansen, O., C. J. Lorenzen, R. W. Holmes, and J. D. H. Strickland (1965) Fluorometric determination of chlorophyll. *Journal du Conseil (Conseil Permanent International pour l'Exploration de la Mer)*, **30**: 3–15.

Ikeda, T. and A. W. Mitchell (1982) Oxygen uptake, ammonia excretion and phosphate excretion by krill and other Antarctic zooplankton in relation to their body size and chemical composition. *Marine Biology*, **71**: 283–298.

Irwin, B., C. Caverhill, P. Dickie, E. Horne, and T. Platt (1986) Primary productivity on the Labrador Shelf during June and July 1984. *Canadian Data Report of Fisheries and Aquatic Sciences*, **577**.

Jassby, A. D. and T. Platt (1976) Mathematical formulation of the relationship between photosynthesis and light for phytoplankton. *Limnology and Oceanography*, **21**(4): 540–547.

Johnsen, Geir (1994) *Light harvesting and utilization in marine phytoplankton.* Ph.D. thesis, University of Trondheim.

Joint, I. (1991) The allometric determination of pelagic production rates. *Journal of Plankton Research*, **13**: 69–81.

Joint, I.R. and A.J. Pomroy (1988) Allometric estimation of the productivity of phytoplankton assemblages. *Marine Ecology Progress Series*, **47**: 161–168.

Kepkay, P. E., J. F. Jellett, and S. E. H. Niven (1997*a*) Respiration and the carbon-to-nitrogen ratio of a phytoplankton bloom. *Marine Ecology Progress Series*, **150**: 249–261.

Kepkay, P. E., S. E. H. Niven, and J. F. Jellett (1997*b*) Colloidal organic carbon and phytoplankton speciation during a coastal bloom. *Journal of Plankton Research*, **19**(3): 369–389.

Kiefer, D. A. and J. B. SooHoo (1982) Spectral absorption by marine particles of coastal waters of Baja California. *Limnology and Oceanography*, **27**(3): 492–499.

Kirk, J. T. O. (1976) A theoretical analysis of the contribution of algal cells to the attenuation of light within natural waters. III. Cylindrical and spheroidal cells. *New Phytologist*, **77**: 341–358.

Kirk, John T. O. (1994) *Light and Photosynthesis in Aquatic Ecosystems*. Cambridge University Press, 2nd edition.

Kleiber, M. (1947) Body size and metabolic rate. *Physiological Reviews*, **27**: 511–541.

Kleiber, M. (1961) *The fire of life: an introduction to animal energetics*. John Wiley and Sons.

Kolber, Z. and P. G. Falkowski (1993) Use of active fluorescence to estimate phytoplankton photosynthesis in situ. *Limnology and Oceanography*, **38**(8): 1646–1665.

Kroon, B., B. B. Prézelin, and O. Schofield (1993) Chromatic regulation of quantum yields for photosystem II charge separation, oxygen evolution, and carbon fixation in *Heterocapsa Pygmaea* (Pyrrophyta). *Journal of Phycology*, **29**: 453–462.

Kyewalyanga, M.N. (1997) *Spectral-dependence of photosynthesis in marine phytoplankton*. Ph.D. thesis, Dalhousie University.

LaBarbera, Michael (1989) Analyzing body size as a factor in ecology and evolution. *Annual Review of Ecological Systems*, **20**: 97–117.

Langdon, C. (1988) On the causes of interspecific differences in the growth-irradiance relationship for phytoplankton. II. A general review. *Journal of Plankton Research*, **10**: 1291–1312.

Langdon, C. (1993) The significance of respiration in production measurements based on oxygen. *International Council for the Exploration of the Sea. Marine Science Symposia*, **197**: 69–78.

Laws, E. and J. Caperon (1976) Carbon and nitrogen metabolism by Monochrysis lutheri: measurement of growth-rate-dependent respiration rates. *Marine Biology*, **36**: 85–97.

Laws, E. A. (1975) The importance of respiration losses in controlling the size distribution of marine phytoplankton. *Ecology*, **56**: 419–426.

Levy, E. M., C. C. Cunningham, C. D. W. Conrad, and J. D. Moffatt (1977) The determination of dissolved oxygen in seawater. *Bedford Institute of Oceanography Report Series*, **BI-R-77-9**: 16.

Lewis, W. M., Jr. (1989) Further evidence for anomalous size scaling of respiration in phytoplankton. *Journal of Phycology*, **25**: 395–397.

Li, W.K.W. and J.C. Goldman (1981) Problems in estimating growth rates of marine phytoplankton from short-term assays. *Microbial Ecology*, **7**: 113–121.

Mague, T. H., F. Friberg, D. J. Hughes, and I. Morris (1980) Extracellular release of carbon by marine phytoplankton: a physiological approach. *Limnology and Oceanography*, **25**: 262–279.

Malinsky-Rushansky, N. Z. and C. Legrand (1996) Excretion of dissolved organic carbon by phytoplankton of different sizes and subsequent bacterial uptake. *Marine Ecology Progress Series*, **132**: 249–255.

Mitchell, B. G. (1990) Algorithms for determining the absorption coefficient of aquatic particulates using the quantitative filter technique (QFT). *Proceedings of the Society of Photo-Optical Instrumentation Engineers. Ocean Optics X.*, **1302**: 137–148.

Mizuno, M. (1991) Influence of cell volume on the growth and size reduction of marine and estuarine diatoms. *Journal of Phycology*, **27**: 473–478.

Morel, A. and A. Bricaud (1981) Theoretical results concerning light absorption in a discrete medium, and application to specific absorption of phytoplankton. *Deep-Sea Research 1*, **28A**(11): 1375–1393.

Olson, R. J., A. M. Chekalyuk, and H. M. Sosik (1996) Phytoplankton photosynthetic characteristics from fluorescence induction assays of individual cells. *Limnology and Oceanography*, **41**(6): 1253–1263.

Parsons, T. R., K. Stephens, and J. D. H. Strickland (1961) On the chemical composition of eleven species of marine phytoplankters. *Journal of the Fisheries Research Board of Canada*, **18**(6): 1001–1016.

Parsons, T. R. and M. Takahashi (1973) *Biological Oceanographic Processes*. Pergamon Press.

Peters, R. H. (1983) *The ecological implications of body size*. Cambridge University Press.

Platt, T. (1985) Structure of the marine ecosystem: Its allometric basis. In R. E. Ulanowicz and T. Platt, editors, *Ecosystem Theory for Biological Oceanography*, volume 213, pp. 55–64. Can. Bull. Fish. Aquat. Sci.

Platt, T. and A. D. Jassby (1976) The relationship between photosynthesis and light for natural assemblages of coastal marine phytoplankton. *Journal of Phycology*, **12**: 421–430.

Pomeroy, L. R. (1974) The ocean's food web, a changing paradigm. *Bioscience*, **24**: 499–504.

Raven, J. A. (1984) A cost-benefit analysis of photon absorption by photosynthetic unicells. *New Phytologist*, **98**: 593–625.

Ricker, W. E. (1973) Linear regressions in fisheries research. *Journal of the Fisheries Research Board of Canada.*, **30**: 409–434.

Sakshaug, E. (1993) The relationship between phytoplankton growth rate and production with emphasis on respiration and excretion. *International Council for the Exploration of the Sea. Marine Science Symposia*, **197**: 63–68.

Sathyendranath, S., A. Longhurst, C. M. Caverhill, and T. Platt (1995) Regionally and seasonally differentiated primary production in the North Atlantic. *Deep-Sea Research*, **42**(10): 1773–1802.

Sathyendranath, S., T. Platt, V. Stuart, B. D. Irwin, M. J. W. Veldhuis, G. W. Kraay, and W. G. Harrison (1996) Some bio-optical characteristics of phytoplankton in the NW Indian Ocean. *Marine Ecology Progress Series*, **132**: 299–311.

Schlesinger, D. A., L. A. Molot, and B. G. Shuter (1981) Specific growth rates of freshwater algae in relation to cell size and light intensity. *Canadian Journal of Fisheries and Aquatic Sciences*, **38**: 1052–1058.

Senger, H. and N. I. Bishop (1967) Quantum yield of photosynthesis in synchronous *Scenedesmus* cultures. *Nature*, **214**: 140–142.

Sharp, J. H. (1977) Excretion of organic matter by marine phytoplankton: Do healthy cells do it? *Limnology and Oceanography*, **22**: 381–399.

Silvert, W. and T. Platt (1978) Energy flux in the pelagic ecosystem: A time-dependent equation. *Limnology and Oceanography*, **23**(4): 813–816.

Sommer, U. (1989) Maximal growth rates of Antarctic phytoplankton: Only weak dependence on cell size. *Limnology and Oceanography*, **34**(6): 1109–1112.

Sosik, H. M. and B. G. Mitchell (1991) Absorption, fluorescence, and quantum yield for growth in nitrogen-limited *Dunaliella tertiolecta*. *Limnology and Oceanography*, **36**(5): 910–921.

Sosik, H. M. and B. G. Mitchell (1994) Effects of temperature on growth, light absorption, and quantum yield in *Dunaliella Tertiolecta* (Chlorophyceae). *Journal of Phycology.*, **30**: 833–840.

Steemann Nielsen, E. and V. K. Hansen (1959) Light adaptation in marine phytoplankton populations and its interrelation with temperature. *Physiologia Plantarium*, **12**: 353–370.

Strathmann, R. R. (1967) Estimating the organic carbon content of phytoplankton from cell volume or plasma volume. *Limnology Oceangraphy*, **12**: 411–418.

Stuart, V., S. Sathyendranath, T. Platt, H. Maass, and B. D. Irwin (1997) Pigments and species composition of natural phytoplankton populations: Effect on the absorption spectra. *Journal of Plankton Research*, in press.

Taguchi, S. (1976) Relationship between photosynthesis and cell size of marine diatoms. *Journal of Phycology*, **12**: 185–189.

Tang, E. P. Y. (1995) The allometry of algal growth rates. *Journal of Plankton Research*, **17**(6): 1325–1335.

Tang, E. P. Y. and R. H. Peters (1995) The allometry of algal respiration. *Journal of Plankton Research.*, **17**(2): 303–315.

Verity, P.G. (1982) Effects of temperature, irradiance and day length on the marine diatom *Skeletonema costatum (Grev.) Cleve. IV Growth. Journal of Experimental Marine Biological Ecology*, **60**: 209.

von Bertalanffy, Ludwig and W. J. Pirozynski (1952) Ontogenetic and evolutionary allometry. *Evolution*, **6**: 387–392.

Williams, P.J. LeB. (1993) Chemical and tracer methods of measuring plankton production. *International Council for the Exploration of the Sea. Marine Science Symposia*, **197**: 20–36.

Zlotnik, I. and Z. Dubinsky (1989) The effect of light and temperature on DOC excretion by phytoplankton. *Limnology and Oceanography*, **34**(5): 831–839.